

# 9

# MOLECULAR INTEGRAL EVALUATION

We consider in this chapter techniques for the evaluation of the one- and two-electron molecular integrals needed for the calculation of the standard *ab initio* wave functions and energies. Only integrals over GTOs will be considered, since these are the only basis functions widely used for multi-centre molecular calculations. Having introduced the GTOs in Sections 9.1 and 9.2, we discuss simple one-electron integrals in Sections 9.3–9.6 and Coulomb integrals in Sections 9.7–9.11. After a discussion of the scaling properties of integrals in Section 9.12, we consider the multipole method for the evaluation of two-electron Coulomb integrals in Section 9.13. We conclude with a discussion of the fast multipole method for the evaluation of Coulomb interactions in large systems in Section 9.14. Although the integrals needed for the evaluation of a few basic molecular properties are considered in this chapter, a comprehensive account of property integrals is not given.

## 9.1 Contracted spherical-harmonic Gaussians

The *one- and two-electron integrals* considered in this chapter may all be written in the form

$$O_{\mu\nu} = \langle \chi_\mu | \hat{O}_1 | \chi_\nu \rangle = \int \chi_\mu(\mathbf{r}) \hat{O}(\mathbf{r}) \chi_\nu(\mathbf{r}) \, d\mathbf{r} \quad (9.1.1)$$

$$\begin{aligned} O_{\mu\nu\lambda\sigma} &= \langle \chi_\mu(1) \chi_\nu(1) | \hat{O}_{12} | \chi_\lambda(2) \chi_\sigma(2) \rangle \\ &= \int \int \chi_\mu(\mathbf{r}_1) \chi_\nu(\mathbf{r}_1) \hat{O}(\mathbf{r}_1, \mathbf{r}_2) \chi_\lambda(\mathbf{r}_2) \chi_\sigma(\mathbf{r}_2) \, d\mathbf{r}_1 \, d\mathbf{r}_2 \end{aligned} \quad (9.1.2)$$

where the integrations are over the full space of Cartesian coordinates of one and two electrons, respectively. We shall return to the operators that appear in these integrals later. In the present section, we shall discuss the form of the AOs  $\chi_\mu(\mathbf{r})$  over which the integrals (9.1.1) and (9.1.2) are calculated.

### 9.1.1 PRIMITIVE CARTESIAN GTOs

The functional form of the AOs was discussed in Chapters 6 and 8. In nearly all calculations on polyatomic systems, the AOs are taken as fixed linear combinations of real-valued *primitive Cartesian GTOs* of the form [1,2]

$$G_{ijk}(\mathbf{r}, a, \mathbf{A}) = x_A^i y_A^j z_A^k \exp(-ar_A^2) \quad (9.1.3)$$

centred on the atomic nuclei of the molecular system. In (9.1.3), the position of the electron is defined relative to a nucleus at position  $\mathbf{A}$ :

$$\mathbf{r}_A = \mathbf{r} - \mathbf{A} \quad (9.1.4)$$

The vector  $\mathbf{r}_A$  has the three Cartesian components  $x_A$ ,  $y_A$  and  $z_A$  and the norm  $r_A$ . The *Gaussian exponent*  $a$  is a real number greater than zero, the numerical value of which is determined in calculations on atomic systems as discussed in Chapter 8. The *Cartesian quantum numbers*  $i$ ,  $j$  and  $k$  are integers greater than or equal to zero. The full set of GTOs of a given *total angular-momentum quantum number*

$$l = i + j + k \quad (9.1.5)$$

and of the same exponent  $a$  are said to constitute a *shell*. Gaussians with the angular-momentum quantum number  $l = i + j + k = 0$  are referred to as *spherical Gaussians* (not to be confused with the *spherical-harmonic Gaussians* discussed in Section 9.1.2). The number of Cartesian GTOs in a shell of total angular-momentum quantum number  $l$  is given by the expression

$$N_l^c = \frac{(l+1)(l+2)}{2} \quad (9.1.6)$$

In molecular calculations, we always employ full shells of GTOs – that is, the individual Cartesian components of a given shell are never used alone. As we shall see in the present chapter, the simple analytical form of the primitive Cartesian GTOs (9.1.3) allows for an efficient evaluation of the polyatomic integrals entering the standard Hamiltonian operator (2.2.18).

As discussed in Chapter 8, the primitive Cartesian GTOs (9.1.3) are mostly used in fixed linear combinations  $\chi_\mu(\mathbf{r})$ . A typical AO thus consists of a linear combination of primitive Cartesian GTOs of the same angular-momentum quantum number  $l$  but of different Cartesian quantum numbers  $i$ ,  $j$  and  $k$  and of different exponents  $a$ . In Section 9.1.2, we shall discuss how Cartesian GTOs of the same  $l$  but different  $i$ ,  $j$  and  $k$  are combined to yield the real-valued spherical-harmonic GTOs; next, in Section 9.1.3, we shall see how the GTOs of different exponents are combined to yield the final AOs as contracted spherical-harmonic GTOs.

### 9.1.2 SPHERICAL-HARMONIC GTOs

A real-valued *spherical-harmonic GTO* of quantum numbers  $l$  and  $m$ , with exponent  $a$  and centred on  $\mathbf{A}$  is given by the expression

$$G_{lm}(\mathbf{r}, a, \mathbf{A}) = S_{lm}(x_A, y_A, z_A) \exp(-ar_A^2) \quad (9.1.7)$$

where  $S_{lm}(\mathbf{r}_A)$  is one of the real solid harmonics introduced in Section 6.4.2 – see in particular equations (6.4.19)–(6.4.21). A shell of spherical-harmonic GTOs contains all GTOs of the same  $a$  and  $l$  but different  $|m| \leq l$ . The number of spherical-harmonic GTOs that constitute a complete shell is therefore given by the expression

$$N_l^s = 2l + 1 \quad (9.1.8)$$

In a given shell, the number of spherical-harmonic GTOs (1,3,5,7,9, ...) is always less than or equal to the number of Cartesian GTOs (1,3,6,10,15, ...).

As discussed in Section 6.4, the relationship between the spherical-harmonic and Cartesian GTOs is given by the expression

$$G_{lm}(\mathbf{r}, a, \mathbf{A}) = N_{lm}^s \sum_{t=0}^{[(l-|m|)/2]} \sum_{u=0}^t \sum_{v=v_m}^{[|m|/2-v_m]+v_m} C_{tuv}^{lm} G_{2t+|m|-2(u+v), 2(u+v), l-2t-|m|}(\mathbf{r}, a, \mathbf{A}) \quad (9.1.9)$$

where

$$N_{lm}^S = \frac{1}{2^{|m|} l!} \sqrt{\frac{2(l+|m|)!(l-|m|)!}{2^{\delta_{0m}}}} \quad (9.1.10)$$

$$C_{tuv}^{lm} = (-1)^{t+v-v_m} \left(\frac{1}{4}\right)^t \binom{l}{t} \binom{l-t}{|m|+t} \binom{t}{u} \binom{|m|}{2v} \quad (9.1.11)$$

$$v_m = \begin{cases} 0 & m \geq 0 \\ \frac{1}{2} & m < 0 \end{cases} \quad (9.1.12)$$

The analytical form of the spherical-harmonic GTOs is thus more complicated than that of the Cartesian GTOs – see Table 6.3, which contains the lowest-order real-valued solid harmonics. In particular, the angular part of the spherical-harmonic GTOs is not separable in the Cartesian directions, making the integration over spherical-harmonic GTOs more complicated than the integration over Cartesian GTOs.

The integration techniques discussed in this chapter involve most directly the Cartesian GTOs. The integrals over Cartesian GTOs may subsequently be transformed to integrals over spherical-harmonic GTOs. However, since a relatively large number of Cartesian GTOs contribute to a smaller number of spherical-harmonic GTOs, it is advantageous to carry out the transformation (9.1.9) as early as possible in the evaluation of the molecular integrals. We shall return to this point later in this chapter, in our discussion of two-electron integrals.

### 9.1.3 CONTRACTED GTOs

The primitive Cartesian Gaussians are combined not only in their angular parts, but also in their radial parts. The final *contracted GTOs* may be written as linear combinations of primitive spherical-harmonic GTOs of different exponents  $a_v$

$$G_{\mu lm}(\mathbf{r}, \mathbf{a}, \mathbf{A}) = \sum_v G_{lm}(\mathbf{r}, a_v, \mathbf{A}) d_{v\mu} \quad (9.1.13)$$

where the *contraction coefficients*  $d_{v\mu}$  are the same for all the angular components. The number of contracted GTOs is often considerably smaller than the number of primitive GTOs. To reduce the computational cost, the contraction should therefore (like the transformation to solid harmonics) be carried out as early as possible in the integration over contracted GTOs.

As discussed in Section 8.2.4, contractions of primitive GTOs come in two varieties: segmented and general contractions. In *segmented contractions*, each primitive GTO contributes to only one contracted GTO. The contraction (9.1.13) can then be carried out as a simple addition process, in which primitive integrals premultiplied by the appropriate contraction coefficients are added together. In *general contractions*, each primitive GTO contributes to several contracted GTOs. The contraction must then be carried out as a matrix multiplication involving the contraction coefficients and the integrals over primitive GTOs.

### 9.1.4 COMPUTATIONAL CONSIDERATIONS

As should be apparent from our discussion so far, a large number of integrals over *primitive Cartesian GTOs* (9.1.3) contribute to a smaller number of integrals over *contracted spherical-harmonic GTOs* (9.1.13). This is especially true for the two-electron integrals (9.1.2), since the

number of such integrals grows as the fourth power of the number of GTOs. Therefore, although the algorithms discussed in this chapter are mostly presented in terms of primitive Cartesian GTOs, we should as early as possible carry out the transformations (9.1.9) and (9.1.13) so as to reduce the number of quantities to be manipulated further in the integration. Note that the Cartesian-to-spherical-harmonic and primitive-to-contracted transformations (9.1.9) and (9.1.13) are independent of each other and may be carried out in the order that suits the integration best.

Another important observation is that each primitive Cartesian GTO may contribute to several contracted spherical-harmonic GTOs. First, for  $l \geq 2$ , each Cartesian GTO may contribute to several spherical-harmonic GTOs; second, in the general contraction scheme, each primitive GTO may contribute to several contracted GTOs. To avoid any recalculation of integrals over primitive Cartesian GTOs, all contracted integrals made up from the same primitive integrals should be evaluated simultaneously. In fact, even if the different Cartesian components of the same shell are not combined in the generation of the spherical-harmonic components, it will still be advantageous to generate simultaneously the full shell of GTOs since (as we shall see later) integrals over the individual components share the same intermediates. Clearly, the calculation of integrals over contracted spherical-harmonic GTOs is a challenging organizational problem, where the number of floating-point operations should be kept as small as possible while keeping memory usage as low as possible.

## 9.2 Cartesian Gaussians

Cartesian Gaussians and products of two such Gaussians (i.e. the Cartesian overlap distributions) play an important role in the evaluation of molecular integrals. In the present section, we prepare ourselves for the study of integration techniques by examining the analytical properties of single Gaussians and their overlap distributions.

### 9.2.1 CARTESIAN GAUSSIANS

The primitive Cartesian Gaussians to be considered in this chapter may all be written in the form [1]

$$G_{ijk}(\mathbf{r}, a, \mathbf{A}) = x_A^i y_A^j z_A^k \exp(-ar_A^2) \quad (9.2.1)$$

An important property of the Cartesian Gaussians is that they may be factorized in the three Cartesian directions

$$G_{ijk}(\mathbf{r}, a, \mathbf{A}) = G_i(x, a, A_x) G_j(y, a, A_y) G_k(z, a, A_z) \quad (9.2.2)$$

where, for example,

$$G_i(x, a, A_x) = x_A^i \exp(-ax_A^2) \quad (9.2.3)$$

As we shall see, this factorization simplifies the calculation of integrals over Cartesian Gaussians significantly.

The first few Cartesian Gaussians of unit exponent are illustrated in Figure 9.1. All functions except the spherical Gaussian ( $i = 0$ ) have one node at the origin. The Cartesian Gaussians are either symmetric or antisymmetric with respect to inversion through the origin.

We shall always work with Cartesian GTOs in the unnormalized form (9.2.1). Still, it is of some interest to consider the self-overlap of these fundamental functions. The self-overlap of the

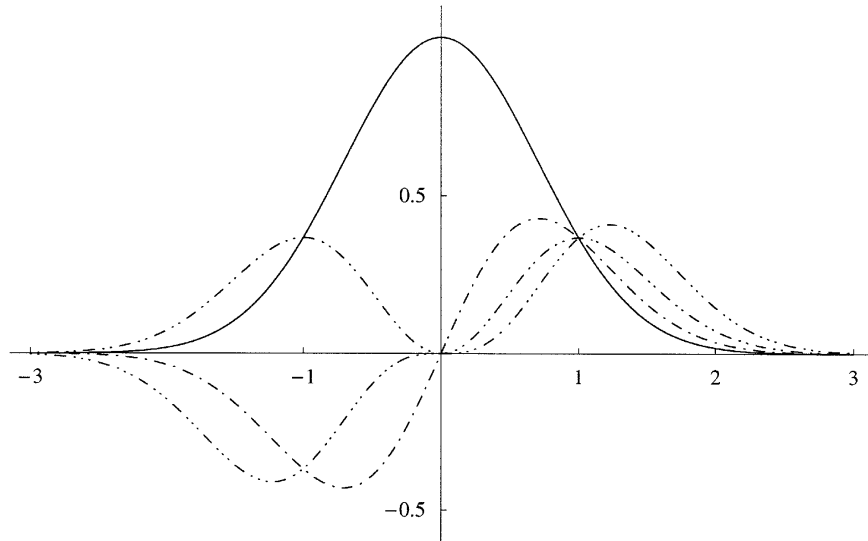


**Fig. 9.1.** The Cartesian Gaussians  $G_i(x, 1, 0)$  for quantum numbers 0, 1, 2 and 3. The number of consecutive dots in the lines corresponds to the quantum number  $i$  of the Cartesian Gaussian.

$x$  component of the unnormalized GTO (9.2.3) is given by (see Exercise 6.9)

$$\langle G_i | G_i \rangle = \frac{(2i-1)!!}{(4a)^i} \sqrt{\frac{\pi}{2a}} \quad (9.2.4)$$

The double factorial is given in (6.5.10).

### 9.2.2 RECURRENCE RELATIONS FOR CARTESIAN GAUSSIANS

For a number of purposes, we shall need the differentiation property of the Gaussians. The first derivative is given by (omitting arguments for clarity)

$$\frac{\partial G_i}{\partial A_x} = -\frac{\partial G_i}{\partial x} = 2aG_{i+1} - iG_{i-1} \quad (9.2.5)$$

The derivative depends on the exponent and is a linear combination of two undifferentiated Gaussians with incremented and decremented quantum numbers. We may obtain higher derivatives by further differentiation, but recursion is often more useful. From (9.2.5), we obtain

$$\frac{\partial^{q+1} G_i}{\partial A_x^{q+1}} = \left( \frac{\partial}{\partial A_x} \right)^q (2aG_{i+1} - iG_{i-1}) = 2a \frac{\partial^q G_{i+1}}{\partial A_x^q} - i \frac{\partial^q G_{i-1}}{\partial A_x^q} \quad (9.2.6)$$

In the notation

$$G_i^q = \frac{\partial^q G_i}{\partial A_x^q} \quad (9.2.7)$$

we therefore have the following recurrence relation

$$G_i^{q+1} = 2aG_{i+1}^q - iG_{i-1}^q \quad (9.2.8)$$

In this way, we may construct higher derivatives from those of lower orders. This is useful since we normally need all derivatives up to a given order. We also note the trivial recurrence

$$x_A G_i = G_{i+1} \quad (9.2.9)$$

which is used on several occasions later.

### 9.2.3 THE GAUSSIAN PRODUCT RULE

The product of two spherical Gaussians centred on **A** and **B** may be written in terms of a single spherical Gaussian located on the line segment connecting the two centres. Using (6.2.6)–(6.2.10), we obtain the *Gaussian product rule* [1]

$$\exp(-ax_A^2) \exp(-bx_B^2) = \exp(-\mu X_{AB}^2) \exp(-px_p^2) \quad (9.2.10)$$

Here the *total exponent*  $p$  and the *reduced exponent*  $\mu$  are defined as

$$p = a + b \quad (9.2.11)$$

$$\mu = \frac{ab}{a + b} \quad (9.2.12)$$

while the *centre-of-charge coordinate*  $P_x$  and the *relative coordinate* or *Gaussian separation*  $X_{AB}$  are given by

$$P_x = \frac{aA_x + bB_x}{p} \quad (9.2.13)$$

$$X_{AB} = A_x - B_x \quad (9.2.14)$$

Note that only the last factor on the right-hand side of (9.2.10) depends on the electronic coordinate  $x$ . The first factor

$$K_{ab}^x = \exp(-\mu X_{AB}^2) \quad (9.2.15)$$

is constant and is sometimes referred to as the *pre-exponential factor*. This factor is small when the separation between the centres is large.

The Gaussian product rule greatly simplifies the calculation of integrals. It is illustrated in Figure 9.2 for products of Gaussians of different exponents and separations. We note the dependence on the Gaussian separation (upper plots) and also the tendency of the product Gaussian to resemble most closely the Gaussian with the largest exponent (lower plots).

### 9.2.4 GAUSSIAN OVERLAP DISTRIBUTIONS

In the following short-hand notation for the Gaussians

$$G_a(\mathbf{r}) = G_{ikm}(\mathbf{r}, a, \mathbf{A}) \quad (9.2.16)$$

$$G_b(\mathbf{r}) = G_{jlm}(\mathbf{r}, b, \mathbf{B}) \quad (9.2.17)$$

we define the *Gaussian overlap distribution* of  $G_a(\mathbf{r})$  and  $G_b(\mathbf{r})$ :

$$\Omega_{ab}(\mathbf{r}) = G_a(\mathbf{r})G_b(\mathbf{r}) \quad (9.2.18)$$

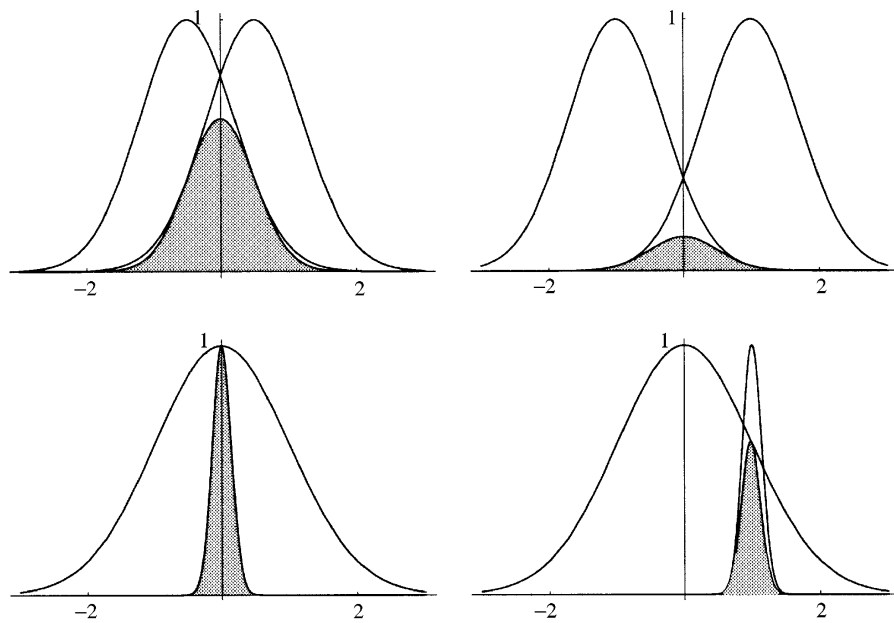


**Fig. 9.2.** The Gaussian product rule. The shaded areas represent the product of the two individual Gaussians. In the upper plots, the exponents are equal to 1 and the two Gaussians are centred at  $\pm\frac{1}{2}$  and  $\pm 1$ ; in the lower plots, the exponents are  $\frac{1}{2}$  (for the Gaussian at the origin in both plots) and 25 (for the Gaussian centred at 0 and 1).

Since the two Gaussians factorize into the three Cartesian directions, we may factorize the overlap distribution in the same way

$$\Omega_{ab}(\mathbf{r}) = \Omega_{ij}^x(x, a, b, A_x, B_x) \Omega_{kl}^y(y, a, b, A_y, B_y) \Omega_{mn}^z(z, a, b, A_z, B_z) \quad (9.2.19)$$

where the  $x$  component is given by

$$\Omega_{ij}^x(x, a, b, A_x, B_x) = G_i(x, a, A_x) G_j(x, b, B_x) \quad (9.2.20)$$

and likewise for the  $y$  and  $z$  components.

According to the Gaussian product rule (9.2.10), the overlap distribution (9.2.20) may be written as a single Gaussian positioned at the centre of charge  $P_x$ :

$$\Omega_{ij}^x = K_{ab}^x x_A^i x_B^j \exp(-p x_P^2) \quad (9.2.21)$$

Noting that we may rewrite  $x_A$  and  $x_B$  as

$$x_A = x_P + X_{PA} = x_P - \frac{b}{p} X_{AB} \quad (9.2.22)$$

$$x_B = x_P + X_{PB} = x_P + \frac{a}{p} X_{AB} \quad (9.2.23)$$

we find that the overlap distribution (9.2.21) may be expanded in Cartesian Gaussians of orders  $0 \leq k \leq i + j$  centred at  $\mathbf{P}$

$$\Omega_{ij}^x = K_{ab}^x \sum_{k=0}^{i+j} C_k^{ij} x_{\mathbf{P}}^k \exp(-px_{\mathbf{P}}^2) \quad (9.2.24)$$

where the expansion coefficients may be obtained by application of the binomial theorem. Using the expansion (9.2.24), we may, for example, reduce all four-centre two-electron integrals over Cartesian Gaussians to a linear combination of two-centre integrals. This approach has indeed been taken in some schemes developed for the evaluation of two-electron integrals [3]. In Section 9.5, we shall take a similar but slightly different approach, expanding the Gaussian overlap distributions in Hermite rather than Cartesian Gaussians. Integrals over  $\Omega_{ij}^x$  may, however, be obtained also without constructing such expansions explicitly, as will be shown in Section 9.3.

### 9.2.5 PROPERTIES OF GAUSSIAN OVERLAP DISTRIBUTIONS

The properties of Gaussian overlap distributions are easily inferred from those of the constituent Gaussians. We note in particular the trivial relationships

$$x_A \Omega_{ij}^x = \Omega_{i+1,j}^x \quad (9.2.25)$$

$$x_B \Omega_{ij}^x = \Omega_{i,j+1}^x \quad (9.2.26)$$

which follow from (9.2.9) and the recurrence

$$\Omega_{i,j+1}^x - \Omega_{i+1,j}^x = X_{AB} \Omega_{ij}^x \quad (9.2.27)$$

which follows by subtracting (9.2.25) from (9.2.26). Differentiating the overlap distributions, we obtain the relations

$$\frac{\partial \Omega_{ij}^x}{\partial A_x} = 2a \Omega_{i+1,j}^x - i \Omega_{i-1,j}^x \quad (9.2.28)$$

$$\frac{\partial \Omega_{ij}^x}{\partial B_x} = 2b \Omega_{i,j+1}^x - j \Omega_{i,j-1}^x \quad (9.2.29)$$

which follow directly from the derivative expression (9.2.5).

When working with overlap distributions, it is sometimes more convenient to use the coordinates  $P_x$  and  $X_{AB}$  rather than  $A_x$  and  $B_x$ , for example when derivatives are calculated [4]. From (9.2.13) and (9.2.14), we obtain

$$A_x = P_x + \frac{b}{p} X_{AB} \quad (9.2.30)$$

$$B_x = P_x - \frac{a}{p} X_{AB} \quad (9.2.31)$$

which give us the following expressions for the partial derivatives with respect to  $P_x$  and  $X_{AB}$ :

$$\frac{\partial}{\partial P_x} = \frac{\partial}{\partial A_x} + \frac{\partial}{\partial B_x} \quad (9.2.32)$$

$$\frac{\partial}{\partial X_{AB}} = \frac{b}{p} \frac{\partial}{\partial A_x} - \frac{a}{p} \frac{\partial}{\partial B_x} \quad (9.2.33)$$

The inverse relations are obtained directly from (9.2.13) and (9.2.14) by using the chain rule

$$\frac{\partial}{\partial A_x} = \frac{a}{p} \frac{\partial}{\partial P_x} + \frac{\partial}{\partial X_{AB}} \quad (9.2.34)$$

$$\frac{\partial}{\partial B_x} = \frac{b}{p} \frac{\partial}{\partial P_x} - \frac{\partial}{\partial X_{AB}} \quad (9.2.35)$$

From these expressions, we may establish the following relations

$$\frac{\partial \Omega_{ij}^x}{\partial P_x} = 2a\Omega_{i+1,j}^x + 2b\Omega_{i,j+1}^x - i\Omega_{i-1,j}^x - j\Omega_{i,j-1}^x \quad (9.2.36)$$

$$\frac{\partial \Omega_{ij}^x}{\partial X_{AB}} = 2\mu(\Omega_{i+1,j}^x - \Omega_{i,j+1}^x) + \frac{1}{2p}(2aj\Omega_{i,j-1}^x - 2bi\Omega_{i-1,j}^x) \quad (9.2.37)$$

for differentiation with respect to  $P_x$  and  $X_{AB}$ .

#### 9.2.6 INTEGRALS OVER SPHERICAL OVERLAP DISTRIBUTIONS

As an introduction to the integration over GTOs, let us consider the simplest of all multicentre molecular integrals – namely, the integral over a spherical Gaussian charge distribution

$$\int_{-\infty}^{\infty} \Omega_{00}^x dx = \exp(-\mu X_{AB}^2) \int_{-\infty}^{\infty} \exp(-px_p^2) dx \quad (9.2.38)$$

Using the expression

$$\int_{-\infty}^{\infty} \exp(-px_p^2) dx = \sqrt{\frac{\pi}{p}} \quad (9.2.39)$$

we obtain

$$\int_{-\infty}^{\infty} \Omega_{00}^x dx = \sqrt{\frac{\pi}{p}} \exp(-\mu X_{AB}^2) \quad (9.2.40)$$

for the  $x$  component. Combing this expression with those for the  $y$  and  $z$  components, we arrive at the following simple expression for the overlap between two  $s$  orbitals separated by a distance  $R_{AB}$ :

$$\int \Omega_{ss} dr = \left(\frac{\pi}{p}\right)^{3/2} \exp(-\mu R_{AB}^2) \quad (9.2.41)$$

Note that the overlap integral behaves like a Gaussian with respect to variations in the separation between the Gaussian centres.

### 9.3 The Obara–Saika scheme for simple integrals

Having discussed the Cartesian Gaussian functions and their overlap distributions, we are now ready to consider the evaluation of the *simple* one-electron integrals. By *simple*, we here mean the standard molecular integrals that do not involve the Coulomb interaction. In the present section, we thus discuss the evaluation of overlap integrals and multipole-moment integrals by the *Obara–Saika scheme* [5], based on the translational invariance of the integrals. We also

consider the evaluation of one-electron integrals over differential operators and, in particular, the momentum and kinetic-energy integrals. A different approach to the calculation of integrals (the McMurchie–Davidson scheme), based on the expansion of the overlap distributions in Hermite Gaussians [6], is discussed in Section 9.5.

### 9.3.1 OVERLAP INTEGRALS

Let us first consider the simple overlap integrals

$$S_{ab} = \langle G_a | G_b \rangle \quad (9.3.1)$$

which, according to (9.2.19), may be factorized in the three Cartesian directions

$$S_{ab} = S_{ij} S_{kl} S_{mn} \quad (9.3.2)$$

where, for example

$$S_{ij} = \int_{-\infty}^{\infty} \Omega_{ij}^x dx \quad (9.3.3)$$

We begin by noting that this integral is invariant to an overall translation of the coordinate system along the  $x$  axis. Since the overlap integral depends only on the coordinates  $\mathbf{A}$  and  $\mathbf{B}$  of the two centres  $A$  and  $B$ , this invariance implies that the overlap integral should be unaffected by identical translations of these two centres in the  $x$  direction. The sum of the derivatives of the overlap integral with respect to  $A_x$  and  $B_x$  must therefore be equal to zero:

$$\frac{\partial S_{ij}}{\partial A_x} + \frac{\partial S_{ij}}{\partial B_x} = 0 \quad (9.3.4)$$

We now insert (9.3.3) and take the differential operators inside the integration sign (which is allowed since the integration limits are independent of  $A_x$  and  $B_x$ ):

$$\int_{-\infty}^{\infty} \frac{\partial \Omega_{ij}^x}{\partial A_x} dx + \int_{-\infty}^{\infty} \frac{\partial \Omega_{ij}^x}{\partial B_x} dx = 0 \quad (9.3.5)$$

Applying (9.2.28) and (9.2.29), we obtain the *translational recurrence relation*

$$2aS_{i+1,j} - iS_{i-1,j} + 2bS_{i,j+1} - jS_{i,j-1} = 0 \quad (9.3.6)$$

which relates overlap integrals of different Cartesian quantum numbers. The total quantum number is  $i + j + 1$  for the first and third terms and  $i + j - 1$  for the other two terms. To arrive at a useful recurrence, we must eliminate one of the terms of order  $i + j + 1$ . For this purpose, we invoke the *horizontal recurrence relation*

$$S_{i,j+1} - S_{i+1,j} = X_{AB} S_{ij} \quad (9.3.7)$$

which follows directly by integration over (9.2.27). Combining the translational and horizontal recurrences to eliminate either  $S_{i,j+1}$  or  $S_{i+1,j}$ , we arrive at the *Obara-Saika recurrence relations* for the Cartesian overlap integrals [5]:

$$S_{i+1,j} = X_{PA} S_{ij} + \frac{1}{2p} (iS_{i-1,j} + jS_{i,j-1}) \quad (9.3.8)$$

$$S_{i,j+1} = X_{PB} S_{ij} + \frac{1}{2p} (iS_{i-1,j} + jS_{i,j-1}) \quad (9.3.9)$$

Starting from the overlap integral for the spherical Gaussians (9.2.40)

$$S_{00} = \sqrt{\frac{\pi}{p}} \exp(-\mu X_{AB}^2) \quad (9.3.10)$$

we may use the Obara–Saika recurrences to generate the  $x$  overlap integrals over primitive Cartesian GTOs for arbitrary quantum numbers. With obvious modifications, the same recurrence relations may be used to generate the  $y$  and  $z$  overlap integrals. The primitive Cartesian integrals (9.3.2) are then obtained by taking the products of the three factors. To generate the final overlap integrals over contracted spherical-harmonic GTOs, the integrals (9.3.2) must be transformed first to the contracted basis using (9.1.13) and next to the spherical-harmonic representation using (9.1.9).

As with any recursion involving more than one index, the target integrals  $S_{ij}$  may be generated from the initial integral  $S_{00}$  in many different ways. We may not only apply the Obara–Saika recurrences (9.3.8) and (9.3.9) in different ways, we may also combine these recurrences with the horizontal relation (9.3.7). We may, for example, first generate a set of integrals of the form  $S_{i0}$  and then apply the horizontal recurrence to generate the final integrals  $S_{ij}$ . Since the generation of the overlap integrals is in any case a trivial matter, we shall not compare and investigate these different schemes in any detail here.

### 9.3.2 MULTIPOLE-MOMENT INTEGRALS

Having considered the simple overlap integrals in Section 9.3.1, let us now consider the slightly more complicated multipole-moment integrals of the form

$$S_{ab}^{efg} = \langle G_a | x_C^e y_C^f z_C^g | G_b \rangle \quad (9.3.11)$$

where  $\mathbf{C}$  is the origin of the Cartesian multipole moments. Special cases of the multipole integrals are the overlap, dipole and quadrupole integrals. Since the operator and the orbitals in (9.3.11) are separable, the integral may be calculated as

$$S_{ab}^{efg} = S_{ij}^e S_{kl}^f S_{mn}^g \quad (9.3.12)$$

where, for instance, the  $x$  component

$$S_{ij}^e = \langle G_i | x_C^e | G_j \rangle = \int_{-\infty}^{\infty} \Omega_{ij}^x x_C^e \, dx \quad (9.3.13)$$

may be treated by a simple extension to the scheme for the overlap integrals.

Like the overlap integrals, the multipole-moment integrals are invariant to an overall translation of the coordinate system. The sum of the derivatives of the integral (9.3.13) with respect to  $A_x$ ,  $B_x$  and  $C_x$  must therefore be zero:

$$\frac{\partial S_{ij}^e}{\partial A_x} + \frac{\partial S_{ij}^e}{\partial B_x} + \frac{\partial S_{ij}^e}{\partial C_x} = 0 \quad (9.3.14)$$

Taking the differential operators inside the integration, we obtain the following translational recurrence relation analogous to (9.3.6):

$$2aS_{i+1,j}^e - iS_{i-1,j}^e + 2bS_{i,j+1}^e - jS_{i,j-1}^e - eS_{ij}^{e-1} = 0 \quad (9.3.15)$$

Also, in addition to the horizontal recurrence for the orbital quantum numbers (9.3.7), we have the following horizontal recurrences involving the order of the multipole operator:

$$S_{ij}^{e+1} = S_{i+1,j}^e + X_{\text{AC}} S_{ij}^e = S_{i,j+1}^e + X_{\text{BC}} S_{ij}^e \quad (9.3.16)$$

as is easily verified. Combining the translational recurrences (9.3.15) with the horizontal recurrences (9.3.7) and (9.3.16), we obtain the Obara–Saika recurrence relations [5]

$$S_{i+1,j}^e = X_{\text{PA}} S_{ij}^e + \frac{1}{2p} (iS_{i-1,j}^e + jS_{i,j-1}^e + eS_{ij}^{e-1}) \quad (9.3.17)$$

$$S_{i,j+1}^e = X_{\text{PB}} S_{ij}^e + \frac{1}{2p} (iS_{i-1,j}^e + jS_{i,j-1}^e + eS_{ij}^{e-1}) \quad (9.3.18)$$

$$S_{ij}^{e+1} = X_{\text{PC}} S_{ij}^e + \frac{1}{2p} (iS_{i-1,j}^e + jS_{i,j-1}^e + eS_{ij}^{e-1}) \quad (9.3.19)$$

from which the full set of Cartesian multipole-moment integrals may be generated. As for the overlap integrals, the Obara–Saika recurrences may be used in conjunction with the horizontal recurrences (9.3.7) and (9.3.16). The final integrals are obtained by multiplying the Cartesian factors according to (9.3.12), followed by a transformation to the contracted spherical-harmonic basis. A transformation of the Cartesian multipole-moment components to spherical-harmonic components may sometimes also be required.

### 9.3.3 INTEGRALS OVER DIFFERENTIAL OPERATORS

As the next example of the Obara–Saika scheme for simple one-electron integrals, we consider the integrals over the differential operators

$$D_{ab}^{efg} = \langle G_a | \frac{\partial^e}{\partial x^e} \frac{\partial^f}{\partial y^f} \frac{\partial^g}{\partial z^g} | G_b \rangle \quad (9.3.20)$$

where the superscripts indicate the order of the differentiation with respect to the electronic coordinates. These integrals may again be factorized into three Cartesian components

$$D_{ab}^{efg} = D_{ij}^e D_{kl}^f D_{mn}^g \quad (9.3.21)$$

where the  $x$  component, for example, is now given by

$$D_{ij}^e = \langle G_i | \frac{\partial^e}{\partial x^e} | G_j \rangle \quad (9.3.22)$$

We first note that this integral may be written in the form of a differentiated overlap integral

$$D_{ij}^e = (-1)^e \frac{\partial^e S_{ij}^0}{\partial B_x^e} = \frac{\partial^e S_{ij}^0}{\partial A_x^e} \quad (9.3.23)$$

where the first relation comes from the first part of (9.2.5) and the second from translational invariance. To arrive at recurrence relations for these integrals, we simply differentiate the Obara–Saika recurrences for the overlaps (9.3.8) and (9.3.9) with respect to  $A_x$ . Noting that the only nonvanishing

derivatives of  $X_{\text{PA}}$  and  $X_{\text{PB}}$  are given by

$$\frac{\partial X_{\text{PA}}}{\partial A_x} = -\frac{b}{p} \quad (9.3.24)$$

$$\frac{\partial X_{\text{PB}}}{\partial A_x} = \frac{a}{p} \quad (9.3.25)$$

we obtain the following Obara–Saika recurrence relations [5]:

$$D_{i+1,j}^e = X_{\text{PA}} D_{ij}^e + \frac{1}{2p} (i D_{i-1,j}^e + j D_{i,j-1}^e - 2be D_{ij}^{e-1}) \quad (9.3.26)$$

$$D_{i,j+1}^e = X_{\text{PB}} D_{ij}^e + \frac{1}{2p} (i D_{i-1,j}^e + j D_{i,j-1}^e + 2ae D_{ij}^{e-1}) \quad (9.3.27)$$

$$D_{ij}^{e+1} = 2a D_{i+1,j}^e - i D_{i-1,j}^e \quad (9.3.28)$$

where the derivative recurrence (9.3.28) has been obtain from (9.2.28). Because of the presence of the differential operator, the horizontal recursion is slightly more complicated than for the overlap and multipole-moment integrals. Multiple differentiation of (9.3.7) with respect to  $A_x$  gives

$$D_{i,j+1}^e - D_{i+1,j}^e = X_{\text{AB}} D_{ij}^e + e D_{ij}^{e-1} \quad (9.3.29)$$

as the horizontal recurrence relation for the  $D_{ij}^e$  integrals. In passing, we note that these integrals may be expressed also directly in terms of the undifferentiated overlap integrals. To the lowest orders, we have

$$D_{ij}^1 = 2a S_{i+1,j} - i S_{i-1,j} \quad (9.3.30)$$

$$D_{ij}^2 = 4a^2 S_{i+2,j} - 2a(2i+1) S_{ij} + i(i-1) S_{i-2,j} \quad (9.3.31)$$

as may easily be verified.

### 9.3.4 MOMENTUM AND KINETIC-ENERGY INTEGRALS

In the previous two subsections, we have seen how the Obara–Saika scheme may be used to set up simple recurrence relations for the generation of the  $x$ ,  $y$  and  $z$  components of the one-electron integrals over multipole-moment and differential operators. These one-dimensional integrals may also be combined to yield other important integrals – namely, the integrals for linear and angular momentum as well as the kinetic-energy integrals:

$$\mathbf{P}_{ab} = -i \langle G_a | \nabla | G_b \rangle \quad (9.3.32)$$

$$\mathbf{L}_{ab} = -i \langle G_a | \mathbf{r} \times \nabla | G_b \rangle \quad (9.3.33)$$

$$T_{ab} = -\frac{1}{2} \langle G_a | \nabla^2 | G_b \rangle \quad (9.3.34)$$

Expanding the operators appearing in these integrals and factorizing in the Cartesian directions, we arrive at the following expressions for the  $z$  components of the momentum integrals

$$P_{ab}^z = -i S_{ij}^0 S_{kl}^0 D_{mn}^1 \quad (9.3.35)$$

$$L_{ab}^z = -i (S_{ij}^1 D_{kl}^1 S_{mn}^0 - D_{ij}^1 S_{kl}^1 S_{mn}^0) \quad (9.3.36)$$

and for the kinetic-energy integral

$$T_{ab} = -\frac{1}{2}(D_{ij}^2 S_{kl}^0 S_{mn}^0 + S_{ij}^0 D_{kl}^2 S_{mn}^0 + S_{ij}^0 S_{kl}^0 D_{mn}^2) \quad (9.3.37)$$

in terms of the basic one-dimensional integrals  $S_{ij}^e$  and  $D_{ij}^e$ .

Obviously, a large number of integrals may be generated by application of the basic Obara–Saika recurrence relations. Again, with the different integral types, there are often a number of possible approaches. We may thus write the kinetic-energy integrals also in the form

$$T_{ab} = T_{ij} S_{kl} S_{mn} + S_{ij} T_{kl} S_{mn} + S_{ij} S_{kl} T_{mn} \quad (9.3.38)$$

where, for example

$$T_{ij} = -\frac{1}{2} \langle G_i | \frac{\partial^2}{\partial x^2} | G_j \rangle \quad (9.3.39)$$

The Obara–Saika recurrence relations for these one-dimensional kinetic-energy integrals may be obtained from (9.3.26)–(9.3.28) as [5]

$$T_{i+1,j} = X_{\text{PA}} T_{ij} + \frac{1}{2p} (iT_{i-1,j} + jT_{i,j-1}) + \frac{b}{p} (2aS_{i+1,j} - iS_{i-1,j}) \quad (9.3.40)$$

$$T_{i,j+1} = X_{\text{PB}} T_{ij} + \frac{1}{2p} (iT_{i-1,j} + jT_{i,j-1}) + \frac{a}{p} (2bS_{i,j+1} - jS_{i,j-1}) \quad (9.3.41)$$

$$T_{00} = \left[ a - 2a^2 \left( X_{\text{PA}}^2 + \frac{1}{2p} \right) \right] S_{00} \quad (9.3.42)$$

In this way, we may generate the kinetic-energy integrals by a simple modification of the recurrences for the overlap integrals.

## 9.4 Hermite Gaussians

In the previous section, we explored one particular approach to the evaluation of molecular integrals – the Obara–Saika scheme, which makes use of recurrence relations based on the translational invariance of the integrals. In the present section, we introduce a new set of Gaussians, the *Hermite Gaussians*, thereby preparing ourselves for an alternative approach to integral evaluation – the McMurchie–Davidson scheme [6], based on the expansion of Gaussian overlap distributions in one-centre Hermite Gaussians as discussed in Section 9.5.

### 9.4.1 HERMITE GAUSSIANS

The Hermite Gaussians of exponent  $p$  and centred on  $\mathbf{P}$  are defined by

$$\Lambda_{tuv}(\mathbf{r}, p, \mathbf{P}) = (\partial/\partial P_x)^t (\partial/\partial P_y)^u (\partial/\partial P_z)^v \exp(-pr_{\mathbf{P}}^2) \quad (9.4.1)$$

where

$$\mathbf{r}_{\mathbf{P}} = \mathbf{r} - \mathbf{P} \quad (9.4.2)$$

Like the Cartesian Gaussians, these functions are separable

$$\Lambda_{tuv}(\mathbf{r}, p, \mathbf{P}) = \Lambda_t(x, p, P_x) \Lambda_u(y, p, P_y) \Lambda_v(z, p, P_z) \quad (9.4.3)$$

where, for example,

$$\Lambda_t(x, p, P_x) = (\partial/\partial P_x)^t \exp(-px_p^2) \quad (9.4.4)$$

The Hermite Gaussians differ from the Cartesian Gaussians (9.2.3) only in the polynomial factors, which for the Hermite Gaussians are generated by differentiation.

The first four Hermite Gaussians with unit exponents are plotted in Figure 9.3. Like the Cartesian Gaussians, the Hermite Gaussians are symmetric ( $t$  even) or antisymmetric ( $t$  odd) with respect to inversion through the origin but their nodal structure is quite different. Whereas the number of nodes for the Cartesian Gaussians is one for all  $i > 0$ , the number of nodes in the Hermite Gaussian  $\Lambda_t$  is  $t$ . This follows from their definition by differentiation:  $\Lambda_{t+1}$  has nodes where  $\Lambda_t$  has extrema because the gradient vanishes at the extrema. Since  $\Lambda_0$  has one extremum only and no nodes, we conclude that  $\Lambda_1$  has one node and therefore two extrema, that  $\Lambda_2$  has two nodes and therefore three extrema and so on.

It is possible to consider the use of Hermite Gaussians themselves as basis functions (in place of the Cartesian Gaussians) [7]. Here, we shall consider the use of Hermite Gaussians only as intermediates in the calculation of integrals over Cartesian Gaussians [6]. Their usefulness stems from the fact that they are defined by differentiation, which leads to many simplifications when calculating molecular one- and two-electron integrals, as will become apparent in Section 9.5 (for the one-electron integrals) and, in particular, in Section 9.9 (for the two-electron integrals).

#### 9.4.2 DERIVATIVE AND RECURRENCE RELATIONS FOR HERMITE GAUSSIANS

From the definition of Hermite Gaussians (9.4.4), we obtain the simple differentiation formula

$$\frac{\partial \Lambda_t}{\partial P_x} = -\frac{\partial \Lambda_t}{\partial x} = \Lambda_{t+1} \quad (9.4.5)$$

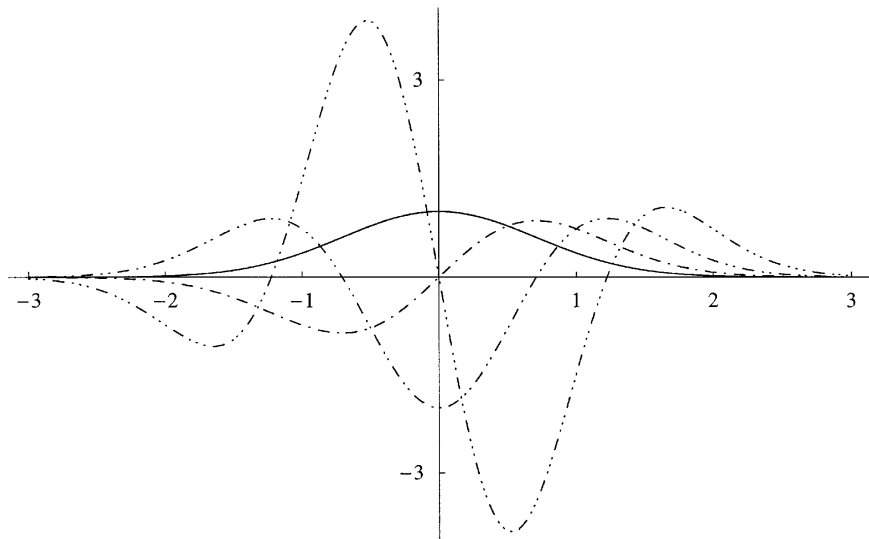


**Fig. 9.3.** The Hermite Gaussians  $\Lambda_t(x, 1, 0)$  for quantum numbers 0, 1, 2 and 3. The number of consecutive dots in the lines corresponds to the quantum number  $t$  of the Hermite Gaussian.

which should be compared with the slightly more complicated formula for the Cartesian Gaussians (9.2.5). We also need to know what happens when the Hermite Gaussians are multiplied by  $x_P$ . We note that

$$\Lambda_{t+1} = (\partial/\partial P_x)^t \frac{\partial \Lambda_0}{\partial P_x} = 2p(\partial/\partial P_x)^t x_P \Lambda_0 \quad (9.4.6)$$

To move  $x_P$  to the left of the differential operators, we use the commutator

$$[(\partial/\partial P_x)^t, x_P] = -t(\partial/\partial P_x)^{t-1} \quad (9.4.7)$$

which may be demonstrated by induction. Inserting (9.4.7) into (9.4.6), we obtain

$$\Lambda_{t+1} = 2p(x_P \Lambda_t - t \Lambda_{t-1}) \quad (9.4.8)$$

where we put

$$\Lambda_t = 0, \quad t < 0 \quad (9.4.9)$$

Equation (9.4.8) gives us the following basic recurrence relation for the Hermite Gaussians

$$x_P \Lambda_t = \frac{1}{2p} \Lambda_{t+1} + t \Lambda_{t-1} \quad (9.4.10)$$

Note that the corresponding formula for Cartesian Gaussians (9.2.9) is even simpler.

#### 9.4.3 INTEGRALS OVER HERMITE GAUSSIANS

Since the Hermite Gaussians are to be used as one-centre basis functions for the expansion of Cartesian overlap distributions (over which the integration will eventually be carried out), it is important to determine the integrals over these Gaussians. The integral over the  $x$  component of the Hermite Gaussians is given by

$$\int_{-\infty}^{+\infty} \Lambda_t(x) dx = \int_{-\infty}^{+\infty} (\partial/\partial P_x)^t \exp(-px_P^2) dx = (\partial/\partial P_x)^t \int_{-\infty}^{+\infty} \exp(-px_P^2) dx \quad (9.4.11)$$

According to (9.2.39), the integral on the right-hand side is independent of  $P_x$ . It therefore vanishes when differentiated and we obtain the following simple result:

$$\int_{-\infty}^{+\infty} \Lambda_t(x) dx = \delta_{t0} \sqrt{\frac{\pi}{p}} \quad (9.4.12)$$

which should be contrasted with the somewhat more complicated expression for the Cartesian Gaussians

$$\int_{-\infty}^{+\infty} G_i(x) dx = \begin{cases} (i-1)!!(2a)^{-i/2} \sqrt{\frac{\pi}{a}} & \text{for even } i \\ 0 & \text{for odd } i \end{cases} \quad (9.4.13)$$

obtained using (6E.9.2) and the fact that  $G_i(x)$  is antisymmetric for odd values of  $i$ .

Equation (9.4.11) illustrates an important technique, which will be used on several occasions. Since the Hermite Gaussians are defined as derivatives, we may take their differential operators

outside the integration sign. In this way, we may turn integrals over Hermite Gaussians into differentiated integrals over spherical Gaussians. No such simple scheme is possible for the Cartesian Gaussians, which is the main reason for preferring the Hermite rather than Cartesian Gaussians for expanding the overlap distributions.

#### 9.4.4 HERMITE GAUSSIANS AND HO FUNCTIONS COMPARED

Before we go on to consider the use of Hermite Gaussians as basis functions for overlap distributions, let us establish the relationship between Hermite Gaussians and Hermite polynomials. From Section 6.6.6, we recall that the Hermite polynomials may be generated from the Rodrigues expression (6.6.29)

$$H_n(x) = (-1)^n \exp(x^2) \frac{d^n}{dx^n} \exp(-x^2) \quad (9.4.14)$$

which, upon substitution of  $\sqrt{p} x_p$  for  $x$  in the argument, may be written in the form

$$H_t(\sqrt{p} x_p) = p^{-t/2} \exp(px_p^2) \left( \frac{d}{dp} \right)^t \exp(-px_p^2) \quad (9.4.15)$$

Inserting the definition of the Hermite Gaussians (9.4.4) on the right-hand side and rearranging, we obtain

$$\Lambda_t(\sqrt{p} x_p) = p^{t/2} H_t(\sqrt{p} x_p) \exp(-px_p^2) \quad (9.4.16)$$

Hence, apart from a constant, the Hermite Gaussians consist of a Hermite polynomial multiplied by a Gaussian. It is therefore of some interest to compare with the HO functions (6.6.25)

$$\chi_i^{\text{HO}}(x) = \left( \frac{2\alpha}{\pi} \right)^{1/4} \frac{1}{\sqrt{2^i i!}} H_i(\sqrt{2\alpha} x) \exp(-\alpha x^2) \quad (9.4.17)$$

of HO theory; see Section 6.6.6. Clearly, the Hermite Gaussians and HO functions differ by a factor of  $\sqrt{2}$  in the argument of the polynomials. Since the HO functions satisfy the orthonormality relations

$$\int_{-\infty}^{+\infty} \chi_i^{\text{HO}}(x) \chi_j^{\text{HO}}(x) dx = \delta_{ij} \quad (9.4.18)$$

we may conclude that the Hermite Gaussians are not orthogonal.

### 9.5 The McMurchie–Davidson scheme for simple integrals

Having introduced the Hermite Gaussians in the previous section, we shall now explore the McMurchie–Davidson scheme for the evaluation of molecular integrals over Cartesian Gaussians [6]. In this scheme, we proceed by expanding the Cartesian overlap distributions in one-centre Hermite Gaussians, thereby reducing the integration over two-centre functions to the evaluation over a set of one-centre functions whose analytical properties make them particularly well suited to integration – for the simple one-electron integrals studied in this section and for the more complicated Coulomb integrals to be studied in Section 9.9.

### 9.5.1 OVERLAP DISTRIBUTIONS EXPANDED IN HERMITE GAUSSIANS

Let us consider the expansion of two-centre Cartesian overlap distributions in Hermite Gaussians. Since the overlap distribution  $\Omega_{ij}$  is a polynomial of degree  $i + j$  in  $x_P$  (9.2.24), it may be expanded exactly in the Hermite polynomials of degree  $t \leq i + j$ . We therefore write

$$\Omega_{ij} = \sum_{t=0}^{i+j} E_t^{ij} \Lambda_t \quad (9.5.1)$$

where the expansion coefficients  $E_t^{ij}$  are constant – that is, independent of the electronic coordinates. It is possible to derive explicit expressions for these coefficients, but in practice it is easier to work with recurrence relations. Several such relations may be derived, based on the properties of the Cartesian overlap distributions and the Hermite Gaussians.

We begin by considering the incremented distribution

$$\Omega_{i+1,j} = \sum_{t=0}^{i+j+1} E_t^{i+1,j} \Lambda_t \quad (9.5.2)$$

To relate this expansion to that of  $\Omega_{ij}$ , we apply first (9.2.25) and then (9.2.22):

$$\Omega_{i+1,j} = x_A \Omega_{ij} = x_P \Omega_{ij} + X_{PA} \Omega_{ij} \quad (9.5.3)$$

We now expand the first term on the right-hand side of (9.5.3) in Hermite Gaussians and eliminate  $x_P$  using the Hermite recurrence relation (9.4.10):

$$x_P \Omega_{ij} = \sum_{t=0}^{i+j} E_t^{ij} \left( t \Lambda_{t-1} + \frac{1}{2p} \Lambda_{t+1} \right) = \sum_{t=0}^{i+j+1} \left[ (t+1) E_{t+1}^{ij} + \frac{1}{2p} E_{t-1}^{ij} \right] \Lambda_t \quad (9.5.4)$$

where the expansion coefficients are taken to satisfy the relations

$$E_t^{ij} = 0, \quad t < 0 \text{ or } t > i + j \quad (9.5.5)$$

The second term in (9.5.3) is expanded straightforwardly. Inserting these expansions into (9.5.3) and identifying the terms to same order in  $t$ , we arrive at the McMurchie–Davidson recurrence relations for the expansion coefficients [6]

$$E_t^{i+1,j} = \frac{1}{2p} E_{t-1}^{ij} + X_{PA} E_t^{ij} + (t+1) E_{t+1}^{ij} \quad (9.5.6)$$

$$E_t^{i,j+1} = \frac{1}{2p} E_{t-1}^{ij} + X_{PB} E_t^{ij} + (t+1) E_{t+1}^{ij} \quad (9.5.7)$$

where the second expression has been obtained by expanding  $\Omega_{i,j+1}$  by analogy with (9.5.2)–(9.5.5). The starting coefficient for the recursion is given by the factor (9.2.15)

$$E_0^{00} = K_{ab}^x \quad (9.5.8)$$

From these expressions, the full set of Hermite-to-Cartesian expansion coefficients may be generated and the overlap distribution may then be expanded in Hermite Gaussians according to (9.5.1).

Combining (9.5.6) and (9.5.7), we arrive at the trivial recurrence relation

$$E_t^{i,j+1} = E_t^{i+1,j} + X_{AB}E_t^{ij} \quad (9.5.9)$$

which also follows directly from the corresponding relation for the overlap distributions (9.2.27).

The Hermite-to-Cartesian coefficients  $E_t^{ij}$  are independent of  $P_x$ , depending only on the relative separation of the Gaussians  $X_{AB}$ :

$$\frac{\partial E_t^{ij}}{\partial P_x} = 0 \quad (9.5.10)$$

The independence of the coefficients of  $P_x$  is perhaps not immediately apparent from the recurrence relations (9.5.6) and (9.5.7). However, we note that, according to (9.2.15), the starting coefficients of the recursion (9.5.8) are independent of  $P_x$ . Next, we note that, in the recurrences, the coefficients  $X_{PA}$  and  $X_{PB}$  are both equal to  $X_{AB}$  scaled by some constant factor – see (9.2.30) and (9.2.31). The recurrence relations (9.5.6) and (9.5.7) are therefore independent of  $P_x$  and we conclude that the coefficients themselves must be independent of  $P_x$  (9.5.10).

The expressions (9.5.6) and (9.5.7) are three-term recurrence relations. A simpler set of relations may be obtained from the invariance (9.5.10). Differentiating (9.5.1) with respect to  $P_x$ , we obtain [4]

$$\frac{\partial \Omega_{ij}}{\partial P_x} = \sum_{t=0}^{i+j} E_t^{ij} \frac{\partial \Lambda_t}{\partial P_x} \quad (9.5.11)$$

since the coefficients are independent of  $P_x$ . Applying (9.2.36) to the left-hand side of this expression and (9.4.5) to the right-hand side, we find

$$2a\Omega_{i+1,j}^x + 2b\Omega_{i,j+1}^x - i\Omega_{i-1,j}^x - j\Omega_{i,j-1}^x = \sum_{t=0}^{i+j} E_t^{ij} \Lambda_{t+1} \quad (9.5.12)$$

Next, inserting the expansion (9.5.1) on the left-hand side and collecting terms to the same order in  $t$ , we obtain the following relationship between the coefficients:

$$2aE_t^{i+1,j} + 2bE_t^{i,j+1} - iE_t^{i-1,j} - jE_t^{i,j-1} = E_{t-1}^{ij} \quad (9.5.13)$$

On the left-hand side, we now substitute (9.5.6) and (9.5.7) for  $E_t^{i+1,j}$  and  $E_t^{i,j+1}$ . Using (9.2.11) and (9.2.13) and making the global substitution  $t \rightarrow t - 1$ , we arrive at the following simple two-term recurrence relation for the expansion coefficients:

$$2ptE_t^{ij} = iE_{t-1}^{i-1,j} + jE_{t-1}^{i,j-1} \quad (9.5.14)$$

Note that this relation, which is the same for the three Cartesian directions, determines all coefficients with  $t > 0$ . Restricting the recurrence relations (9.5.6) and (9.5.7) to  $t = 0$ , we have the following three *two-term recurrences*:

$$E_0^{i+1,j} = X_{PA}E_0^{ij} + E_1^{ij} \quad (9.5.15)$$

$$E_0^{i,j+1} = X_{PB}E_0^{ij} + E_1^{ij} \quad (9.5.16)$$

$$E_t^{ij} = \frac{1}{2pt}(iE_{t-1}^{i-1,j} + jE_{t-1}^{i,j-1}), \quad t > 0 \quad (9.5.17)$$

from which the full set of coefficients may be generated, starting with (9.5.8). We note the following special cases

$$E_t^{i0} = (2p)^{-t} \binom{i}{t} E_0^{i-t,0} \quad (9.5.18)$$

$$E_t^{0j} = (2p)^{-t} \binom{j}{t} E_0^{0,j-t} \quad (9.5.19)$$

which are easily obtained from (9.5.17) by iteration.

One more set of recurrence relations for the expansion coefficients should be pointed out. Combining (9.5.6) and (9.5.17), we obtain

$$E_t^{i+1,j} = X_{\text{PA}} E_t^{ij} + \frac{1}{2p} (iE_t^{i-1,j} + jE_t^{i,j-1} + E_{t-1}^{ij}) \quad (9.5.20)$$

$$E_t^{i,j+1} = X_{\text{PB}} E_t^{ij} + \frac{1}{2p} (iE_t^{i-1,j} + jE_t^{i,j-1} + E_{t-1}^{ij}) \quad (9.5.21)$$

where the last equation follows from (9.5.20) and (9.5.9). These recurrence relations, which are reminiscent of the Obara–Saika relations (9.3.8) and (9.3.9), will later prove useful when setting up the Obara–Saika scheme for the Coulomb integrals.

### 9.5.2 OVERLAP DISTRIBUTIONS FROM HERMITE GAUSSIANS BY RECURSION

In Section 9.5.1, the Cartesian overlap distributions were generated from the one-centre Hermite Gaussians by explicit expansion, using the expansion coefficients  $E_t^{ij}$ . These distributions may be generated recursively as well. For this purpose, we introduce the auxiliary distributions

$$\Omega_{ij}^t = K_{ab}^x x_A^i x_B^j \Lambda_t(x_P) \quad (9.5.22)$$

which contain as special cases the Cartesian overlap distributions ( $t = 0$ ) and the Hermite Gaussians ( $i = j = 0$ ). To relate these hybrid, auxiliary functions by recursion, we first multiply the recurrence relation for Hermite Gaussians (9.4.10) by  $K_{ab}^x x_A^i x_B^j$  to give

$$x_P \Omega_{ij}^t = \frac{1}{2p} \Omega_{ij}^{t+1} + t \Omega_{ij}^{t-1} \quad (9.5.23)$$

noting from (9.4.9) that

$$\Omega_{ij}^t = 0, \quad t < 0 \quad (9.5.24)$$

Next, substituting (9.2.22) and (9.2.23) and noting from (9.2.9) that

$$x_A \Omega_{ij}^t = \Omega_{i+1,j}^t \quad (9.5.25)$$

$$x_B \Omega_{ij}^t = \Omega_{i,j+1}^t \quad (9.5.26)$$

we arrive at the McMurchie–Davidson recurrence relations for the auxiliary functions:

$$\Omega_{i+1,j}^t = t \Omega_{ij}^{t-1} + X_{\text{PA}} \Omega_{ij}^t + \frac{1}{2p} \Omega_{ij}^{t+1} \quad (9.5.27)$$

$$\Omega_{i,j+1}^t = t \Omega_{ij}^{t-1} + X_{\text{PB}} \Omega_{ij}^t + \frac{1}{2p} \Omega_{ij}^{t+1} \quad (9.5.28)$$

Using these relations, we may generate the Cartesian overlap distributions recursively from the Hermite Gaussians.

### 9.5.3 THE McMURCHIE-DAVIDSON SCHEME FOR MULTIPOLE-MOMENT INTEGRALS

Having investigated the properties of the Hermite Gaussians and having considered the expansion of the Cartesian overlap distributions in such Gaussians, we are now ready to consider the evaluation of one-electron integrals in the McMurchie-Davidson scheme. However, since a rather complete treatment of the more important simple one-electron integrals was given in Section 9.3 in connection with the Obara-Saika scheme, our treatment will be restricted to multipole-moment integrals, bearing in mind that the techniques presented here can be applied also to the other integrals.

Let us consider again the  $x$  component of the Cartesian multipole-moment integrals (9.3.11):

$$S_{ij}^e = \langle G_i | x_C^e | G_j \rangle \quad (9.5.29)$$

Inserting the Hermite expansion of the overlap distribution (9.5.1), we obtain

$$S_{ij}^e = \sum_{t=0}^{i+j} E_t^{ij} \int_{-\infty}^{+\infty} x_C^e \Lambda_t \, dx = \sum_{t=0}^{i+j} E_t^{ij} M_t^e \quad (9.5.30)$$

where the Hermite multipole-moment integrals are given by

$$M_t^e = \int_{-\infty}^{+\infty} x_C^e \Lambda_t \, dx \quad (9.5.31)$$

The expansion coefficients  $E_t^{ij}$  may be calculated according to the recurrence relations (9.5.6)–(9.5.8) and we here discuss only the evaluation of the Hermite integrals (9.5.31).

First, consider the Hermite integrals with  $e = 0$ . From (9.4.12), we know that these Hermite integrals reduce to

$$M_t^0 = \delta_{t0} \sqrt{\frac{\pi}{p}} \quad (9.5.32)$$

which vanishes for  $t > 0$ . The remaining Hermite integrals (with  $e > 0$ ) may be generated by recursion. Incrementing  $e$ , we obtain

$$M_t^{e+1} = \int_{-\infty}^{+\infty} x_C^e x_C \Lambda_t \, dx \quad (9.5.33)$$

Making the substitution

$$x_C = x_P + X_{PC} \quad (9.5.34)$$

and applying the basic Hermite recurrence relation (9.4.10) in the usual way, we find

$$x_C \Lambda_t = x_P \Lambda_t + X_{PC} \Lambda_t = \frac{1}{2p} \Lambda_{t+1} + t \Lambda_{t-1} + X_{PC} \Lambda_t \quad (9.5.35)$$

which may be inserted into the Hermite integral (9.5.33) to yield

$$M_t^{e+1} = t M_{t-1}^e + X_{PC} M_t^e + \frac{1}{2p} M_{t+1}^e \quad (9.5.36)$$

Together with (9.5.32), this expression allows us to generate recursively the higher-order multipole moments from those of lower orders, noting that all Hermite integrals with  $t > e$  are zero:

$$M_t^e = 0, \quad t > e \quad (9.5.37)$$

To demonstrate (9.5.37), we apply partial integration to (9.5.31)

$$\begin{aligned} M_t^e &= \int_{-\infty}^{+\infty} x_C^e \left[ \frac{\partial^t \exp(-px_P^2)}{\partial P_x^t} \right] dx = (-1)^t \int_{-\infty}^{+\infty} x_C^e \left[ \frac{\partial^t \exp(-px_P^2)}{\partial x^t} \right] dx \\ &= \int_{-\infty}^{+\infty} \left( \frac{\partial^t x_C^e}{\partial x^t} \right) \exp(-px_P^2) dx \end{aligned} \quad (9.5.38)$$

and note that the derivative in the integrand vanishes for  $t > e$ . The final expression for the Cartesian multipole-moment integrals therefore becomes [4]

$$S_{ij}^e = \sum_{t=0}^{\min(i+j,e)} E_t^{ij} M_t^e \quad (9.5.39)$$

where the Hermite-to-Cartesian coefficients are calculated recursively from (9.5.6) and (9.5.7), and the Hermite multipole-moment integrals are calculated recursively from (9.5.36).

Let us consider two examples. According to the above discussion, the  $x$  component of the overlap integral is simply

$$S_{ij}^0 = E_0^{ij} \sqrt{\frac{\pi}{p}} \quad (9.5.40)$$

and the total integral is therefore

$$S_{ab}^{000} = E_0^{ij} E_0^{kl} E_0^{mn} \left( \frac{\pi}{p} \right)^{3/2} \quad (9.5.41)$$

If we assume  $s$  orbitals, this expression becomes (see (9.5.8))

$$S_{ab}^{000} = \exp(-\mu R_{AB}^2) \left( \frac{\pi}{p} \right)^{3/2} \quad (9.5.42)$$

in accordance with (9.2.41). The  $x$  component of the dipole integral contains two terms (the first vanishes when both orbitals are of  $s$  type):

$$S_{ij}^1 = (E_1^{ij} + X_{PC} E_0^{ij}) \sqrt{\frac{\pi}{p}} \quad (9.5.43)$$

as is easily established from the recurrence relation of the Hermite multipole-moment integrals (9.5.36).

## 9.6 Gaussian quadrature for simple integrals

In the previous sections, we have studied two different approaches to the calculation of the simple one-electron integrals over Cartesian Gaussians – the Obara–Saika and McMurchie–Davidson

schemes. Before discussing the evaluation of the more complicated Coulomb integrals by means of these techniques, we shall consider a third method for the evaluation of simple one-electron integrals over Cartesian Gaussians – *Gaussian quadrature* [8,9]. The purpose of this section is not only to present a useful method for the evaluation of the simple one-electron integrals, but also to serve as an introduction to the use of Gaussian quadrature in molecular calculations. As such, the present section provides the necessary mathematical background for understanding the Rys method [10] for the evaluation of Coulomb integrals in Section 9.11.

### 9.6.1 ORTHOGONAL POLYNOMIALS

Consider a set of polynomials  $p_n(x)$  that are *orthogonal* in the sense that

$$\int_a^b p_m(x) p_n(x) W(x) dx = h_n \delta_{mn} \quad (9.6.1)$$

where  $W(x)$  is a *weight function* that is positive in the interval  $[a, b]$  [8,9]. Standard examples of such *orthogonal polynomials* are the *Legendre polynomials*  $P_n(x)$  of Section 6.4.1, the *Laguerre polynomials*  $L_n^\alpha(x)$  of Section 6.5.1, the *Hermite polynomials*  $H_n(x)$  of Section 6.6.6 and the *Chebyshev polynomials*  $T_n(x)$ , which fulfil the following *orthogonality relations*:

$$\int_{-1}^1 P_m(x) P_n(x) dx = \frac{2}{2n+1} \delta_{mn} \quad (9.6.2)$$

$$\int_0^\infty L_m^\alpha(x) L_n^\alpha(x) x^\alpha \exp(-x) dx = \frac{\Gamma(n+\alpha+1)}{n!} \delta_{mn} \quad (9.6.3)$$

$$\int_{-\infty}^\infty H_m(x) H_n(x) \exp(-x^2) dx = \sqrt{\pi} 2^n n! \delta_{mn} \quad (9.6.4)$$

$$\int_{-1}^1 \frac{T_m(x) T_n(x)}{\sqrt{1-x^2}} dx = \frac{\pi}{2} (1 + \delta_{n0}) \delta_{mn} \quad (9.6.5)$$

Except for an overall scaling factor, these relations determine the orthogonal polynomials uniquely in the sense that the full set of polynomials to a given degree  $N$  may be generated by a Gram–Schmidt orthogonalization of the monomials  $x^k$  for  $0 \leq k \leq N$ . Alternatively, we may generate the same polynomials using a Rodrigues formula such as those given in Chapter 6 or by means of a *two-term recurrence relation*

$$(n+1)P_{n+1} = (2n+1)xP_n - nP_{n-1} \quad (9.6.6)$$

$$(n+1)L_{n+1}^\alpha = (2n+1+\alpha-x)L_n^\alpha - (n+\alpha)L_{n-1}^\alpha \quad (9.6.7)$$

$$H_{n+1} = 2xH_n - 2nH_{n-1} \quad (9.6.8)$$

$$T_{n+1} = 2xT_n - T_{n-1} \quad (9.6.9)$$

starting in all cases with

$$p_{-1}(x) = 0 \quad (9.6.10)$$

$$p_0(x) = 1 \quad (9.6.11)$$

The reader may wish to derive the recurrence relations for the Legendre, Laguerre and Hermite polynomials from the Rodrigues expressions (6.4.4), (6.5.1) and (6.6.29).

These and other orthogonal polynomials have many properties in common. We shall not attempt to explore in detail their common properties here, but we note (without proof) the nontrivial fact that an orthogonal polynomial  $p_n(x)$  of degree  $n$  has  $n$  distinct *roots* or *zeros*

$$p_n(x_i) = 0, \quad 1 \leq i \leq n \quad (9.6.12)$$

in the interval  $[a, b]$  interleaving the  $n - 1$  roots of the polynomial  $p_{n-1}(x)$ . As we shall see in the remainder of this section, the roots of orthogonal polynomials play an important role in the theory of Gaussian quadrature.

### 9.6.2 GAUSSIAN QUADRATURE

Consider a general polynomial  $f_k(x)$  of degree  $k$

$$f_k(x) = \sum_{j=0}^k c_j x^j \quad (9.6.13)$$

and let  $x_i$  be the  $n$  distinct roots (9.6.12) of the polynomial  $p_n(x)$  orthogonal in the interval  $[a, b]$  with weight function  $W(x)$ ; see (9.6.1). If  $k < 2n$ , then [8,9]

$$\int_a^b f_k(x) W(x) dx = \sum_{i=1}^n w_i f_k(x_i) \quad (9.6.14)$$

where

$$w_i = \int_a^b W(x) \prod_{\substack{j=1 \\ j \neq i}}^n \frac{x - x_j}{x_i - x_j} dx \quad (9.6.15)$$

as shown in Section 9.6.3. In the  $n$ -point quadrature formula (9.6.14), the  $x_i$  are known as the *abscissae* and the  $w_i$  as the *weights*. The abscissae and weights are independent of the polynomial  $f_k(x)$  but depend on the number of quadrature points  $n$ . Depending on what particular weight function and polynomials are used, the resulting quadrature schemes are known as Gauss–Legendre quadrature, Gauss–Laguerre quadrature, Gauss–Hermite quadrature, and so on.

The great advantage of *Gaussian quadrature* over other quadrature schemes is that an  $n$ -point integration is exact for all polynomials of degree  $k < 2n$ . Thus, if the abscissae had been chosen in a different manner – for example, distributed evenly in the interval  $[a, b]$  rather than at the nodes of the orthogonal polynomials – then we would have to carry out a  $2n$ -point quadrature to make integration exact for all polynomials of degree  $k < 2n$ . In our applications, where the polynomial form in (9.6.13) is of known degree but rather complicated, the use of Gaussian quadrature greatly improves the efficiency of the evaluation, reducing the cost of evaluating the exact integral roughly by a factor of 2.

The application of Gaussian quadrature is not restricted to polynomial functions  $f(x)$ . Indeed, in most applications of Gaussian quadrature, the functions  $f(x)$  are not polynomials but some more complicated function, the analytical integration over which presents difficulties [8]. In such cases, we employ Gaussian quadrature to provide an accurate numerical estimate of the true integral. By carrying out quadrature over a sufficiently large number of points (which is equivalent to approximating the integrand by a polynomial of sufficiently high degree) and by a clever choice of weight function  $W(x)$  (which need not be present in the original integrand), we may hope to obtain an accurate numerical estimate of the true integral.

### 9.6.3 PROOF OF THE GAUSSIAN-QUADRATURE FORMULA

We shall demonstrate that (9.6.14) and (9.6.15) hold for all polynomials  $f_k(x)$  of degree  $k < 2n$ . Such polynomials may be written in the form

$$f_k(x) = Q_q(x)p_n(x) + R_r(x) \quad (9.6.16)$$

where  $p_n(x)$  is the orthogonal polynomial of degree  $n$  and  $Q_q(x)$  and  $R_r(x)$  are polynomials of degrees  $q < n$  and  $r < n$ . In this expression, we may consider  $Q_q(x)$  the quotient of  $f_k(x)$  and  $p_n(x)$ , with  $R_r(x)$  being the remainder.

With this decomposition of the polynomial (9.6.16), the integral over  $f_k(x)$  may be written as

$$\int_a^b f_k(x)W(x) dx = \int_a^b R_r(x)W(x) dx \quad (9.6.17)$$

since, according to (9.6.1), the polynomial  $p_n(x)$  is orthogonal to all polynomials of degree  $q < n$ :

$$\int_a^b Q_q(x)p_n(x)W(x) dx = 0 \quad (9.6.18)$$

To evaluate the integral over the remainder in (9.6.17), we note that  $R_r(x)$  may be written as a *Lagrange interpolating polynomial*

$$R_r(x) = \sum_{i=1}^n R_r(x_i) \prod_{\substack{j=1 \\ j \neq i}}^n \frac{x - x_j}{x_i - x_j} \quad (9.6.19)$$

as may be verified by direct substitution of the  $n$  distinct abscissae  $x_i$ , using the fact that two polynomials of degree less than  $n$  are identical if they have the same values at  $n$  points. Inserting this expression in (9.6.17), we obtain

$$\int_a^b f_k(x)W(x) dx = \sum_{i=1}^n R_r(x_i) \int_a^b W(x) \prod_{\substack{j=1 \\ j \neq i}}^n \frac{x - x_j}{x_i - x_j} dx \quad (9.6.20)$$

which, combined with (9.6.15), yields the  $n$ -point quadrature expression, given as

$$\int_a^b f_k(x)W(x) dx = \sum_{i=1}^n w_i R_r(x_i) \quad (9.6.21)$$

The final quadrature formula (9.6.14) now follows immediately from the fact that

$$f_k(x_i) = Q_q(x_i)p_n(x_i) + R_r(x_i) = R_r(x_i) \quad (9.6.22)$$

since  $p_n(x)$  evaluates to zero at the roots  $x_i$ . Whereas the identity (9.6.17) follows from the use of the orthogonal polynomials  $p_n(x)$  when rewriting  $f_k(x)$  according to (9.6.16), the identity (9.6.22) follows from the use of the roots (9.6.12) as the grid points.

#### 9.6.4 GAUSS–HERMITE QUADRATURE FOR SIMPLE INTEGRALS

Consider the evaluation of the multipole-moment integrals of the type

$$S_{ij}^e = \langle G_i | x_{\text{C}}^e | G_j \rangle \quad (9.6.23)$$

Using the Gaussian product rule (9.2.21), this integral becomes

$$S_{ij}^e = K_{ab}^x \int_{-\infty}^{\infty} x_{\text{A}}^i x_{\text{B}}^j x_{\text{C}}^e \exp(-px_{\text{P}}^2) dx \quad (9.6.24)$$

where  $K_{ab}^x$  is given by (9.2.15). Making a simple substitution of variables, this integral may be written in the form

$$S_{ij}^e = \frac{K_{ab}^x}{\sqrt{p}} \int_{-\infty}^{\infty} \left( \frac{x}{\sqrt{p}} + X_{\text{PA}} \right)^i \left( \frac{x}{\sqrt{p}} + X_{\text{PB}} \right)^j \left( \frac{x}{\sqrt{p}} + X_{\text{PC}} \right)^e \exp(-x^2) dx \quad (9.6.25)$$

which, according to the theory of Gaussian quadrature, may be evaluated exactly as

$$S_{ij}^e = \frac{K_{ab}^x}{\sqrt{p}} \sum_{\kappa=1}^{\gamma} w_{\kappa} \left( \frac{x_{\kappa}}{\sqrt{p}} + X_{\text{PA}} \right)^i \left( \frac{x_{\kappa}}{\sqrt{p}} + X_{\text{PB}} \right)^j \left( \frac{x_{\kappa}}{\sqrt{p}} + X_{\text{PC}} \right)^e \quad (9.6.26)$$

where  $x_{\kappa}$  and  $w_{\kappa}$  are the  $\gamma$  roots and weights of the Hermite polynomial  $H_{\gamma}(x)$  of degree

$$\gamma = \left[ \frac{i+j+e}{2} \right] + 1 \quad (9.6.27)$$

Note that, in (9.6.26), the abscissae and weights are the same for all integrals of the same quantum number  $i + j + e$ . The Gauss–Hermite scheme for multipole-moment integrals may easily be extended to the evaluation of kinetic-energy integrals.

## 9.7 Coulomb integrals over spherical Gaussians

Coulomb-interaction integrals cannot be expressed in a closed analytical form. They may, however, be reduced to one-dimensional integrals, the numerical evaluation of which is relatively straightforward. In the present section, we begin our discussion of Coulomb integrals by considering the electrostatics of simple spherical Gaussian charge distributions. In particular, we shall demonstrate that the potential arising from a spherical Gaussian distribution as well as the Coulomb repulsion between two such distributions may be described by means of a special mathematical function – the Boys function – related to the incomplete gamma function, whose mathematical properties and evaluation are considered in Section 9.8.

#### 9.7.1 SPHERICAL GAUSSIAN CHARGE DISTRIBUTIONS

We consider the electrostatics of two *spherical Gaussian charge distributions* of exponents  $p$  and  $q$ , centred at  $\mathbf{P}$  and  $\mathbf{Q}$ :

$$\rho_p(\mathbf{r}_{\text{P}}) = \left( \frac{p}{\pi} \right)^{3/2} \exp(-pr_{\text{P}}^2) \quad (9.7.1)$$

$$\rho_q(\mathbf{r}_{\text{Q}}) = \left( \frac{q}{\pi} \right)^{3/2} \exp(-qr_{\text{Q}}^2) \quad (9.7.2)$$

Each of these distributions corresponds to a positive unit charge since from (9.2.39)

$$\int \rho_p(\mathbf{r}_P) d\mathbf{r} = \int \rho_q(\mathbf{r}_Q) d\mathbf{r} = 1 \quad (9.7.3)$$

In this section, we shall consider the electrostatic potential at  $\mathbf{C}$  due to  $\rho_p(\mathbf{r}_P)$

$$V_p(\mathbf{C}) = \int \frac{\rho_p(\mathbf{r}_P)}{r_C} d\mathbf{r} \quad (9.7.4)$$

and the energy of repulsion between  $\rho_p(\mathbf{r}_{1P})$  and  $\rho_q(\mathbf{r}_{2Q})$ :

$$V_{pq} = \iint \frac{\rho_p(\mathbf{r}_{1P})\rho_q(\mathbf{r}_{2Q})}{r_{12}} d\mathbf{r}_1 d\mathbf{r}_2 \quad (9.7.5)$$

We expect the electrostatic potential and the repulsion energy to depend on the exponents and on the separations  $R_{PC}$  and  $R_{PQ}$ . For large separations, they should reduce to the expressions for point charges (i.e. charge distributions with infinite exponents).

### 9.7.2 THE POTENTIAL FROM A SPHERICAL GAUSSIAN CHARGE DISTRIBUTION

Unlike the simple one-electron integrals discussed in Sections 9.3–9.6, the potential integral (9.7.4) cannot be factorized in the Cartesian directions, the complications arising from the presence of the inverse operator  $r_C^{-1}$ . However, using (9.2.39), we may re-express the inverse operator in terms of a one-dimensional integral over a Gaussian function, which is separable in the Cartesian directions [1]:

$$\frac{1}{r_C} = \frac{1}{\sqrt{\pi}} \int_{-\infty}^{+\infty} \exp(-r_C^2 t^2) dt \quad (9.7.6)$$

This is the key step in treating integrals involving Coulomb interactions and Gaussian orbitals. We obtain the following expression for the potential  $V_p(\mathbf{C})$ :

$$V_p(\mathbf{C}) = \frac{p^{3/2}}{\pi^2} \int \exp(-pr_P^2) \left[ \int_{-\infty}^{+\infty} \exp(-t^2 r_C^2) dt \right] d\mathbf{r} \quad (9.7.7)$$

We now invoke the Gaussian product rule (9.2.10)

$$V_p(\mathbf{C}) = \frac{p^{3/2}}{\pi^2} \int_{-\infty}^{+\infty} \left\{ \int \exp[-(p+t^2)r_S^2] d\mathbf{r} \right\} \exp\left(-\frac{pt^2}{p+t^2} R_{PC}^2\right) dt \quad (9.7.8)$$

where  $\mathbf{S}$  is a point on the line connecting  $\mathbf{C}$  and  $\mathbf{P}$ :

$$\mathbf{S} = \frac{p\mathbf{P} + t^2\mathbf{C}}{p + t^2} \quad (9.7.9)$$

Integration over the spatial coordinates now gives

$$V_p(\mathbf{C}) = \frac{2p^{3/2}}{\sqrt{\pi}} \int_0^{\infty} (p+t^2)^{-3/2} \exp\left(-pR_{PC}^2 \frac{t^2}{p+t^2}\right) dt \quad (9.7.10)$$

where, to reduce the integration interval, we have used the fact that the integrand is a quadratic function in  $t$ . The variable substitution

$$u^2 = \frac{t^2}{p+t^2} \quad (9.7.11)$$

gives

$$dt = \sqrt{p}(1 - u^2)^{-3/2} du \quad (9.7.12)$$

with integration limits 0 and 1 for  $u$ . The integral (9.7.10) now becomes

$$V_p(\mathbf{C}) = \sqrt{\frac{4p}{\pi}} \int_0^1 \exp(-pR_{\text{PC}}^2 u^2) du \quad (9.7.13)$$

We have thus replaced integration over all space in (9.7.4) by a one-dimensional integration over a finite interval.

The integral appearing on the right-hand side of (9.7.13) is of central importance in the calculation of Coulomb-interaction integrals over Gaussian distributions. It belongs to a class of functions that we shall refer to as the *Boys function*

$$F_n(x) = \int_0^1 \exp(-xt^2) t^{2n} dt \quad (9.7.14)$$

The potential from the Gaussian charge distribution of a positive unit charge may therefore be written as

$$V_p(\mathbf{C}) = \sqrt{\frac{4p}{\pi}} F_0(pR_{\text{PC}}^2) \quad (9.7.15)$$

in terms of the Boys function. As we shall see, this special function also arises when we calculate the energy of interaction for two Gaussian charge distributions.

### 9.7.3 THE REPULSION BETWEEN SPHERICAL GAUSSIAN CHARGE DISTRIBUTIONS

The interaction between two charge distributions (9.7.5) may be calculated as the electrostatic energy of the second distribution in the potential due to the first distribution:

$$V_{pq} = \int V_p(\mathbf{r}_2) \rho_q(\mathbf{r}_{2Q}) d\mathbf{r}_2 \quad (9.7.16)$$

Since we have expressed the potential from the first charge distribution in terms of the Boys function (9.7.15), this interaction becomes

$$V_{pq} = \sqrt{\frac{4p}{\pi}} \left(\frac{q}{\pi}\right)^{3/2} \int F_0(pr_{2P}^2) \exp(-qr_{2Q}^2) d\mathbf{r}_2 \quad (9.7.17)$$

We now insert the definition of the Boys function (9.7.14), use the Gaussian product rule (9.2.10) and integrate over all space. We obtain

$$V_{pq} = \sqrt{\frac{4pq}{\pi}} \int_0^1 \frac{q}{(pt^2 + q)^{3/2}} \exp\left(-\frac{pqt^2 R_{\text{PQ}}^2}{pt^2 + q}\right) dt \quad (9.7.18)$$

Making the substitution

$$u^2 = \frac{p+q}{pt^2 + q} t^2 \quad (9.7.19)$$

with

$$dt = \frac{p+q}{(p+q-u^2 p)^{3/2}} \sqrt{q} du \quad (9.7.20)$$

we obtain the final result for the repulsion energy [1]

$$V_{pq} = \sqrt{\frac{4\alpha}{\pi}} F_0(\alpha R_{PQ}^2) \quad (9.7.21)$$

where  $\alpha$  is the *reduced exponent*

$$\alpha = \frac{pq}{p+q} \quad (9.7.22)$$

The interaction between two spherical Gaussian distributions may therefore also be expressed in terms of the Boys function.

#### 9.7.4 THE ELECTROSTATICS OF SPHERICAL GAUSSIAN DISTRIBUTIONS

To summarize the results from Sections 9.7.2 and 9.7.3, we have found that the following relationships hold for spherical Gaussian distributions of unit charge (9.7.1) and (9.7.2):

$$V_p(\mathbf{C}) = \int \frac{\rho_p(\mathbf{r}_P)}{r_C} d\mathbf{r} = \sqrt{\frac{4p}{\pi}} F_0(p R_{PC}^2) \quad (9.7.23)$$

$$V_{pq} = \iint \frac{\rho_p(\mathbf{r}_{1P})\rho_q(\mathbf{r}_{2Q})}{r_{12}} d\mathbf{r}_1 d\mathbf{r}_2 = \sqrt{\frac{4\alpha}{\pi}} F_0(\alpha R_{PQ}^2) \quad (9.7.24)$$

These equations replace the usual classical electrostatic expressions  $R_{PC}^{-1}$  and  $R_{PQ}^{-1}$  for the interactions of unit point charges.

Figure 9.4 illustrates the potentials arising from positive unit Gaussian distributions of different exponents compared with that from a point charge. At large separations, the potential from a

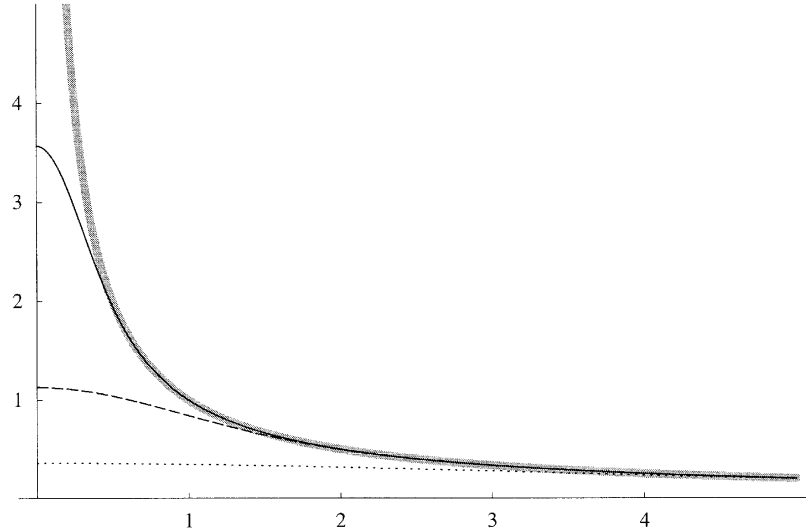


**Fig. 9.4.** The potentials from spherical Gaussian distributions of unit charge with exponents 10 (full line), 1 (dashed line) and  $\frac{1}{10}$  (dotted line) plotted as functions of the distance from the centre of the charge distribution and compared with the corresponding potential from a point charge (thick grey line).

Gaussian distribution approaches closely that of a point-charge potential; at short distances, it is reduced. At the centre of the charge distribution, the potential is finite.

## 9.8 The Boys function

In Section 9.7, we found that the electrostatics of spherical Gaussian charge distributions are determined by the Boys function  $F_n(x)$ . Since this function plays such an important role in the evaluation of molecular integrals over Gaussian functions, we shall in this section discuss its properties and evaluation in more detail.

### 9.8.1 THE BOYS FUNCTION

The *Boys function* of order  $n$  is defined by

$$F_n(x) = \int_0^1 \exp(-xt^2)t^{2n} dt \quad (9.8.1)$$

for  $x \geq 0$  [1,11]. It is a strictly positive function since the integrand is positive:

$$F_n(x) > 0 \quad (9.8.2)$$

Its derivatives are negative

$$\frac{dF_n(x)}{dx} = -F_{n+1}(x) < 0 \quad (9.8.3)$$

and the Boys function is therefore a strictly decreasing function. We also note that

$$F_n(x) - F_{n+1}(x) = \int_0^1 \exp(-xt^2)t^{2n}(1-t^2) dt > 0 \quad (9.8.4)$$

since the integrand is positive within the integration range. We therefore obtain

$$F_n(x) > F_{n+1}(x) \quad (9.8.5)$$

for all  $n$ . The values at  $x = 0$  may be expressed in closed form

$$F_n(0) = \int_0^1 t^{2n} dt = \frac{1}{2n+1} \quad (9.8.6)$$

which, since the function is strictly decreasing, implies that

$$F_n(x) \leq \frac{1}{2n+1} \quad (9.8.7)$$

For large values of  $x$ , we may determine the Boys function approximately from

$$F_n(x) = \int_0^1 \exp(-xt^2)t^{2n} dt \approx \int_0^\infty \exp(-xt^2)t^{2n} dt \quad (x \text{ large}) \quad (9.8.8)$$

The latter integral can be integrated (see (6E.9.2)) to give

$$F_n(x) \approx \frac{(2n-1)!!}{2^{n+1}} \sqrt{\frac{\pi}{x^{2n+1}}} \quad (x \text{ large}) \quad (9.8.9)$$

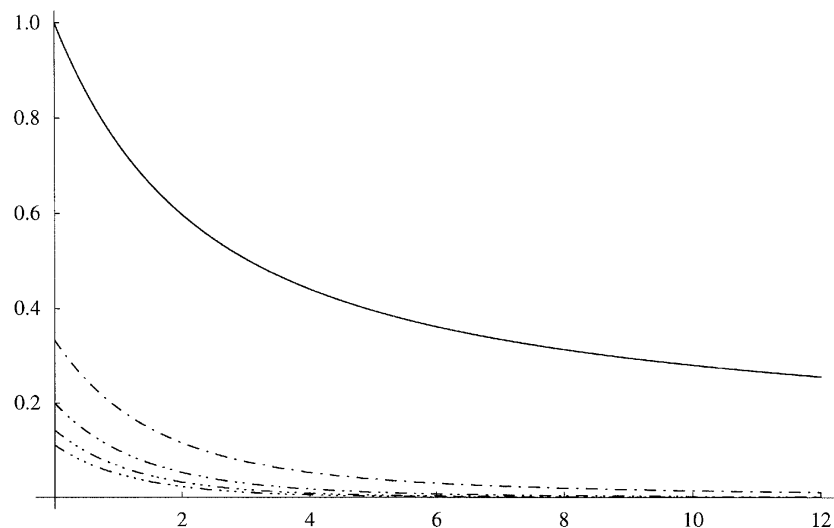


**Fig. 9.5.** The Boys function  $F_n(x)$  for  $0 \leq n \leq 4$ . The number of consecutive dots in the lines corresponds to the order  $n$  of the function.

from which we conclude that the Boys function tends to zero as  $x$  tends to infinity. From (9.8.8), we also note that, for all  $x$ , the Boys function is bounded as

$$F_n(x) \leq \frac{(2n-1)!!}{2^{n+1}} \sqrt{\frac{\pi}{x^{2n+1}}} \quad (9.8.10)$$

The properties discussed above are illustrated for  $n \leq 4$  in Figure 9.5.

### 9.8.2 EVALUATION OF THE BOYS FUNCTION

We now consider the evaluation of the Boys function. Since this function is at the centre of integral evaluation, it is important that it is calculated efficiently. Different methods of evaluating the Boys function have been suggested in the literature [11]. Some of these approaches are discussed in the present subsection.

We first note that, for large  $x$ , (9.8.9) provides a good estimate. For small  $x$ , this approximation breaks down. However, since we know both the function and its derivatives at  $x = 0$  in closed form (see (9.8.3) and (9.8.6)), we may easily construct a Taylor expansion for small values:

$$F_n(x) = \sum_{k=0}^{\infty} \frac{(-x)^k}{k!(2n+2k+1)} \quad (9.8.11)$$

These two approximations – (9.8.9) for large values of  $x$  and (9.8.11) truncated at  $k = 6$  for small values – are illustrated for  $F_0(x)$  in Figure 9.6. Although we have a reasonable approximation to the Boys function by these two methods, they are inadequate for use in integral calculations, in which we would like errors of order  $10^{-10}$  or smaller. Using the above two approximations, this accuracy is attained only in the regions  $x < 0.18$  and  $x > 19.35$ . More accurate methods are therefore needed in practice.

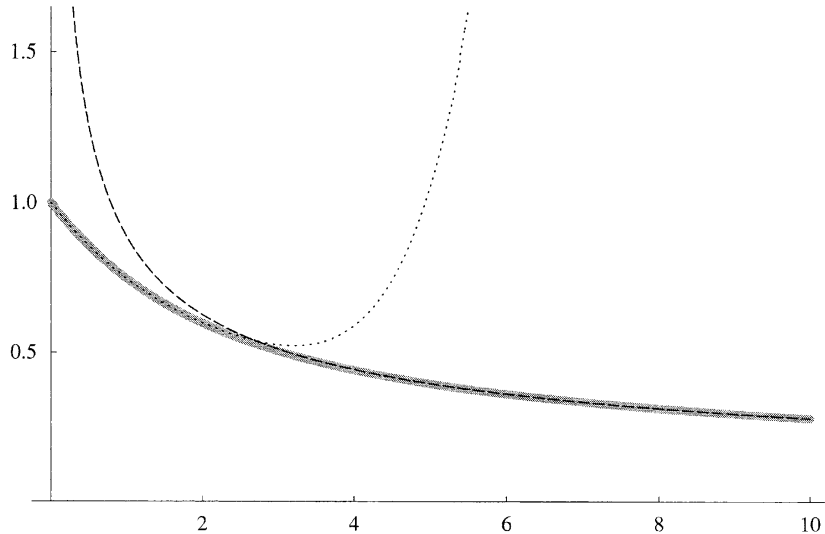


**Fig. 9.6.** The Boys function  $F_0(x)$  (thick grey line) as approximated by the long-range formula (9.8.9) for large  $x$  (dashed line) and by a sixth-order Taylor expansion (9.8.11) around  $x = 0$  for small  $x$  (dotted line).

A practicable alternative is to pretabulate the function at regular intervals  $x_t$  for small arguments. During the calculation of the integrals, the Boys function at  $x$  is then expanded around the nearest tabulated point  $x_t = x - \Delta x$ :

$$F_n(x_t + \Delta x) = \sum_{k=0}^{\infty} \frac{F_{n+k}(x_t)(-\Delta x)^k}{k!} \quad (9.8.12)$$

Using intervals of 0.1, convergence to errors smaller than  $10^{-14}$  is obtained after six terms. For large arguments, the asymptotic formula (9.8.9) may be used. Other methods are also used in practice – for large arguments, the asymptotic formula (9.8.9) may be supplemented with more accurate asymptotic expansions, which are valid in a larger region; for small arguments, various polynomial fitting schemes may be applied, based for example on the use of Chebyshev polynomials.

The Boys functions of different orders are related by recursion. Integrating the Boys function by parts, we obtain for upward recursion (see Exercise 9.3)

$$F_{n+1}(x) = \frac{(2n+1)F_n(x) - \exp(-x)}{2x} \quad (9.8.13)$$

and for downward recursion

$$F_n(x) = \frac{2xF_{n+1}(x) + \exp(-x)}{2n+1} \quad (9.8.14)$$

We therefore only need to calculate the Boys function for the highest or the lowest order needed, obtaining the others by downward or upward recursion. For small  $x$ , upward recursion is unstable since it involves the difference between two almost equal numbers, making downward recursion the preferred strategy.

### 9.8.3 THE INCOMPLETE GAMMA FUNCTION

The Boys function is related to the incomplete gamma function, one of the special functions of mathematical physics. From Section 6.5.1, we recall that the *Euler gamma function* is defined as

$$\Gamma(n) = \int_0^\infty \exp(-t)t^{n-1} dt \quad (9.8.15)$$

where  $n > 0$  is not necessarily an integer. As generalizations of the gamma function, the *incomplete gamma function*  $P(n, x)$  and its complement  $Q(n, x)$  are given by ( $x > 0$ ) [8,9]

$$P(n, x) = \frac{\gamma(n, x)}{\Gamma(n)} = \frac{1}{\Gamma(n)} \int_0^x \exp(-t)t^{n-1} dt \quad (9.8.16)$$

$$Q(n, x) = \frac{\Gamma(n, x)}{\Gamma(n)} = \frac{1}{\Gamma(n)} \int_x^\infty \exp(-t)t^{n-1} dt \quad (9.8.17)$$

and satisfy the relation

$$P(n, x) + Q(n, x) = 1 \quad (9.8.18)$$

For fixed  $n$ , the incomplete gamma function  $P(n, x)$  increases strictly from 0 to 1 as  $x$  tends to infinity (see Figure 9.7).

To establish the relation of the Boys function to the incomplete gamma function, we substitute  $u = xt^2$  in  $F_{n-1/2}(x)$  and obtain

$$F_{n-1/2}(x) = \frac{1}{2x^n} \int_0^x \exp(-u)u^{n-1} du \quad (9.8.19)$$

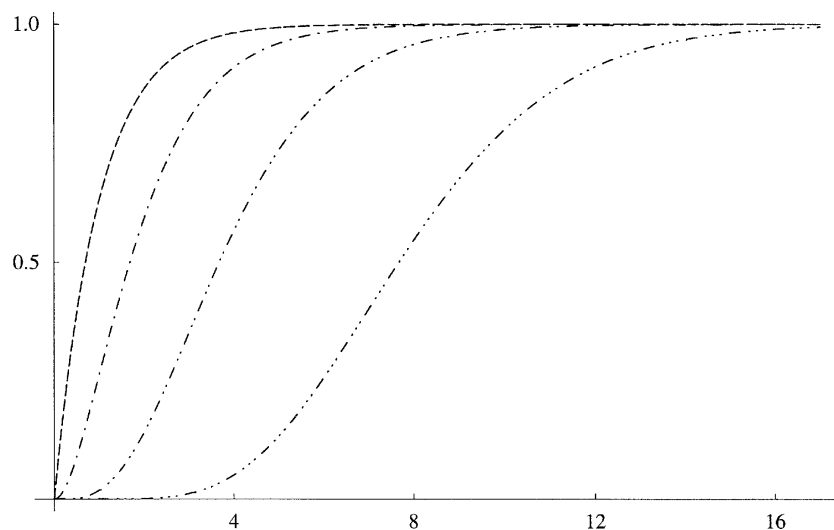


**Fig. 9.7.** The incomplete gamma function  $P(n, x)$  plotted as a function of  $x$  for  $n = 1$  (no dots),  $n = 2$  (one dot),  $n = 4$  (two dots) and  $n = 8$  (three dots).

From this expression, we note the following close relationship between the Boys function and the incomplete gamma function:

$$F_n(x) = \frac{\gamma(n + \frac{1}{2}, x)}{2x^{n+1/2}} = \frac{\Gamma(n + \frac{1}{2}) P(n + \frac{1}{2}, x)}{2x^{n+1/2}} \quad (9.8.20)$$

Indeed, in electronic-structure theory,  $F_n(x)$  is often loosely referred to as the *incomplete gamma function*. In order to avoid any confusion with the special functions  $P(n, x)$  and  $\gamma(n, x)$ , we have here adopted the term the *Boys function* for  $F_n(x)$ . From (9.8.20), we may interpret the Boys function as the function  $\frac{1}{2}\Gamma(n + \frac{1}{2})x^{-1/2-n}$  weighted by the incomplete gamma function  $P(n + \frac{1}{2}, x)$ . For large  $x$ ,

$$F_n(x) = P(n + \frac{1}{2}, x) \frac{\Gamma(n + \frac{1}{2})}{2x^{n+1/2}} \approx \frac{\Gamma(n + \frac{1}{2})}{2x^{n+1/2}} \quad (\text{large } x) \quad (9.8.21)$$

since  $P(n + \frac{1}{2}, x)$  tends to 1 at infinity. Using (6.5.8), this expression can be reduced to (9.8.9).

#### 9.8.4 THE ERROR FUNCTION

Another important special function of mathematical physics is the *error function* [8,9]

$$\text{erf}(x) = \frac{2}{\sqrt{\pi}} \int_0^x \exp(-t^2) dt \quad (9.8.22)$$

Using (9.8.16) and (6.5.8) and carrying out a substitution of variables, we find that the error function is closely related to the incomplete gamma function

$$\text{erf}(x) = P(\frac{1}{2}, x^2) \quad (9.8.23)$$

and therefore also to the Boys function:

$$F_0(x) = \sqrt{\frac{\pi}{4x}} \text{erf}(\sqrt{x}) \quad (9.8.24)$$

Returning to the expressions (9.7.23) and (9.7.24) of electrostatics in Section 9.7, we note that these may now be cast in the simple form

$$\int \frac{\rho_p(\mathbf{r}_P)}{r_C} d\mathbf{r} = \frac{\text{erf}(\sqrt{p}R_{PC})}{R_{PC}} \quad (9.8.25)$$

$$\iint \frac{\rho_p(\mathbf{r}_{1P})\rho_q(\mathbf{r}_{2Q})}{r_{12}} d\mathbf{r}_1 d\mathbf{r}_2 = \frac{\text{erf}(\sqrt{\alpha}R_{PQ})}{R_{PQ}} \quad (9.8.26)$$

which makes their relationship to Coulomb's law and electrostatics particularly clear. For example, for a charge distribution of unit exponent, the error function  $\text{erf}(R_{PC})$  represents the part of the charge which is inside a sphere centred at  $P$  and which extends to the point  $C$  where the potential is measured. Only this part of the total Gaussian charge distribution contributes to the potential at  $C$ . As the exponent  $p$  tends to infinity, the error function tends to 1 and we recover the usual expression for a point charge. For an illustration of the error function and its relationship to the Coulomb potential, see Figure 9.8.

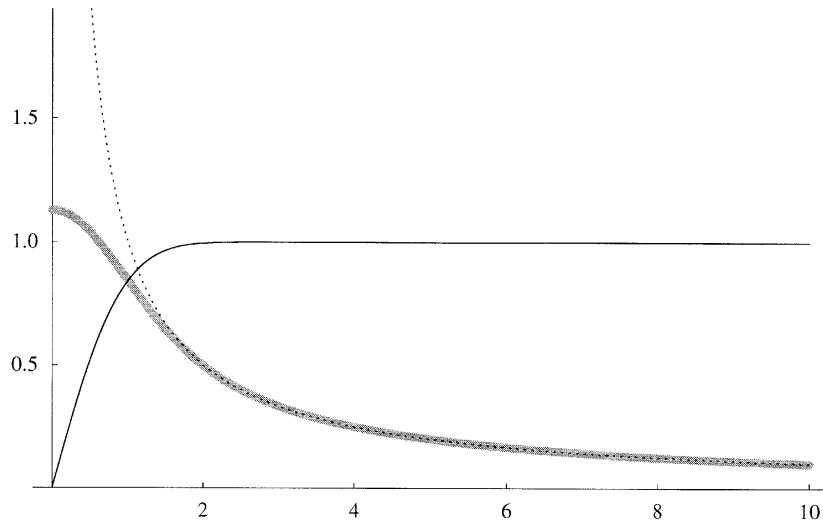


**Fig. 9.8.** The error function  $\text{erf}(x)$  (thin black line). Also plotted are the Coulomb potential from a unit point charge  $1/x$  (dotted line) and from a Gaussian charge distribution of exponent 1 (thick grey line). The latter potential is equal to the point-charge Coulomb potential multiplied by the error function.

#### 9.8.5 THE COMPLEMENTARY ERROR FUNCTION

The *complementary error function* [8,9] is defined as

$$\text{erfc}(x) = 1 - \text{erf}(x) \quad (9.8.27)$$

and may be used to characterize the deviation of the interaction of unit Gaussian charges from that of point charges:

$$\frac{1}{R_{\text{PC}}} - \int \frac{\rho_p(\mathbf{r}_P)}{r_C} d\mathbf{r} = \frac{\text{erfc}(\sqrt{p}R_{\text{PC}})}{R_{\text{PC}}} \quad (9.8.28)$$

$$\frac{1}{R_{\text{PQ}}} - \iint \frac{\rho_p(\mathbf{r}_{1P})\rho_q(\mathbf{r}_{2Q})}{r_{12}} d\mathbf{r}_1 d\mathbf{r}_2 = \frac{\text{erfc}(\sqrt{\alpha}R_{\text{PQ}})}{R_{\text{PQ}}} \quad (9.8.29)$$

An upper bound to the complementary error function is easily established. From (9.8.22), we note that the complementary error function may be written in the form

$$\text{erfc}(x) = \frac{2}{\sqrt{\pi}} \int_x^\infty \exp(-t^2) dt \quad (9.8.30)$$

Rewriting the integrand and integrating by parts, we obtain

$$\text{erfc}(x) = -\frac{1}{\sqrt{\pi}} \int_x^\infty \frac{1}{t} \left[ \frac{d}{dt} \exp(-t^2) \right] dt = \frac{\exp(-x^2)}{\sqrt{\pi}x} - \int_x^\infty \frac{\exp(-t^2)}{\sqrt{\pi}t^2} dt \quad (9.8.31)$$

Since the final integrand is positive, we find that the complementary error function is bounded as

$$\text{erfc}(x) \leq \frac{\exp(-x^2)}{\sqrt{\pi}x} \quad (9.8.32)$$

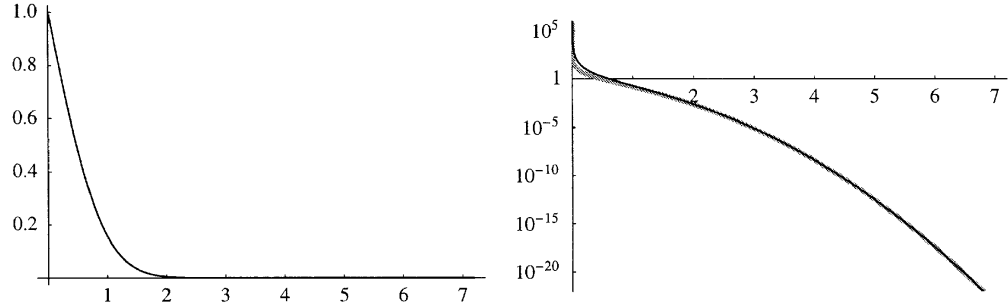


**Fig. 9.9.** The complementary error function  $\text{erfc}(x)$ . On the left, we have plotted  $\text{erfc}(x)$  on a linear scale. On the right, we have plotted the function  $\text{erfc}(x)/x$  of (9.8.28) and (9.8.29) (grey line) and its upper bound  $\exp(-x^2)/(\sqrt{\pi}x^2)$  (black line) on a logarithmic scale. The function  $\text{erfc}(x)/x$  represents the error incurred by calculating interactions between Gaussian charge distributions using point-charge models.

Consequently, we have the following upper bounds to the errors incurred by treating the interactions of unit Gaussians like those of point charges:

$$\frac{1}{R_{\text{PC}}} - \int \frac{\rho_p(\mathbf{r}_P)}{r_C} d\mathbf{r} \leq \frac{\exp(-pR_{\text{PC}}^2)}{\sqrt{\pi p} R_{\text{PC}}} \quad (9.8.33)$$

$$\frac{1}{R_{\text{PQ}}} - \iint \frac{\rho_p(\mathbf{r}_{1P})\rho_q(\mathbf{r}_{2Q})}{r_{12}} d\mathbf{r}_1 d\mathbf{r}_2 \leq \frac{\exp(-\alpha R_{\text{PQ}}^2)}{\sqrt{\pi \alpha} R_{\text{PQ}}^2} \quad (9.8.34)$$

In Figure 9.9, we have illustrated the validity of this approximation, which may be used to decide what integrals may be treated by multipole expansions.

#### 9.8.6 THE CONFLUENT HYPERGEOMETRIC FUNCTION

Many functions of mathematical physics are related to the *Kummer confluent hypergeometric function*, defined as [9]:

$$M(a, b, x) = \sum_{k=0}^{\infty} \frac{(a)_k}{k!(b)_k} x^k \quad (9.8.35)$$

Here  $(a)_k$  is the *Pochhammer symbol*

$$(a)_k = \frac{\Gamma(a+k)}{\Gamma(a)} \quad (9.8.36)$$

which for integral  $k$  takes on the values

$$(a)_k = \begin{cases} 1 & k = 0 \\ a(a+1)(a+2)\cdots(a+k-1) & k > 0 \\ \frac{1}{(a-1)(a-2)\cdots(a-k)} & k < 0 \end{cases} \quad (9.8.37)$$

For negative integers  $a$ ,  $M(a, b, x)$  yields a polynomial provided  $b < a < 0$  or  $a < 0 < b$ ; when neither  $a$  nor  $b$  is a negative integer,  $M(a, b, x)$  constitutes an infinite convergent series. Among its many special cases are the Hermite and Laguerre polynomials and the exponential function  $\exp(x)$ .

We are here interested in the relationship of the Kummer function to the Boys function. From (9.8.35) we obtain, using (9.8.37),

$$M\left(n + \frac{1}{2}, n + \frac{3}{2}, -x\right) = (2n + 1) \sum_{k=0}^{\infty} \frac{(-x)^k}{k!(2n + 2k + 1)} \quad (9.8.38)$$

Comparing with (9.8.11), we find that the Boys function is a (renormalized) special case of the Kummer function:

$$F_n(x) = \frac{M\left(n + \frac{1}{2}, n + \frac{3}{2}, -x\right)}{2n + 1} \quad (9.8.39)$$

Therefore, the standard relations that have been established for the Kummer function hold for the Boys function as well. For example, for the Boys function, the general relations [9]

$$M'(a, b, x) = \frac{a}{b} M(a + 1, b + 1, x) \quad (9.8.40)$$

$$M(a + 1, b + 1, x) = \frac{b(x - b + 1)M(a, b, x) + b(b - 1)M(a - 1, b - 1, x)}{ax} \quad (9.8.41)$$

reduce to

$$F'_n(x) = -F_{n+1}(x) \quad (9.8.42)$$

$$F_{n+1}(x) = \frac{(2x + 2n + 1)F_n(x) - (2n - 1)F_{n-1}(x)}{2x} \quad (9.8.43)$$

The first relation is the usual differentiation formula (9.8.3) and the second is equivalent to the recurrence relation (9.8.13), from which it may be obtained by elimination of  $\exp(-x)$ .

## 9.9 The McMurchie–Davidson scheme for Coulomb integrals

Having discussed the electrostatics of spherical Gaussian distributions and the Boys function, we are now in a position to consider the evaluation of one- and two-electron Coulomb integrals over nonspherical Gaussians. For this task, several schemes have been developed. In the present chapter, we shall consider three such schemes: the McMurchie–Davidson scheme [6], in which the Cartesian integrals are expanded in an intermediate set of integrals over Hermite Gaussians; the Obara–Saika scheme [5], in which the Cartesian Coulomb integrals are obtained directly from the Boys function by recursion; and the Rys-polynomial scheme [10], in which the evaluation of the Boys function is avoided by the application of a special Gaussian-quadrature scheme. Different modifications and further developments of these schemes exist – in the PRISM scheme, for example, the formation of contracted integrals (for segmented sets) is carried out in a particularly efficient manner [12,13].

In the present section, we consider the evaluation of Cartesian Coulomb integrals by the McMurchie–Davidson scheme. First, we show how Coulomb integrals over Hermite Gaussians

may be obtained by differentiating the Boys function, and we derive a set of recurrence relations for obtaining these derivatives. Next, we discuss how Coulomb integrals over Cartesian Gaussians may be obtained from integrals over Hermite Gaussians by expansion or recursion.

### 9.9.1 HERMITE COULOMB INTEGRALS

In Section 9.7, we discussed the evaluation of Coulomb integrals over spherical Gaussians. We now go one step further and consider nonspherical electron distributions as described by Hermite Gaussians. The one-electron Coulomb integral can then be expressed as

$$V_{tuv}^{efg} = \int \Lambda_{tuv}(\mathbf{r}) \left( \frac{\partial}{\partial C_x} \right)^e \left( \frac{\partial}{\partial C_y} \right)^f \left( \frac{\partial}{\partial C_z} \right)^g r_C^{-1} d\mathbf{r} \quad (9.9.1)$$

where, for example,  $V_{tuv}^{000}$  is the potential and  $V_{tuv}^{100}$ ,  $V_{tuv}^{010}$  and  $V_{tuv}^{001}$  are the three components of the electric field. The two-electron Coulomb-interaction integral is

$$V_{tuv;tv\phi} = \iint \frac{\Lambda_{tuv}(\mathbf{r}_1) \Lambda_{tv\phi}(\mathbf{r}_2)}{r_{12}} d\mathbf{r}_1 d\mathbf{r}_2 \quad (9.9.2)$$

where  $\Lambda_{tuv}$  is a Hermite Gaussian of exponent  $p$  centred on  $\mathbf{P}$  and  $\Lambda_{tv\phi}$  a Hermite Gaussian of exponent  $q$  centred on  $\mathbf{Q}$ . Inserting the definition of Hermite Gaussians (9.4.1) and taking the differential operators outside the integration sign, we obtain

$$V_{tuv}^{efg} = \left( \frac{\partial}{\partial P_x} \right)^t \left( \frac{\partial}{\partial P_y} \right)^u \left( \frac{\partial}{\partial P_z} \right)^v \left( \frac{\partial}{\partial C_x} \right)^e \left( \frac{\partial}{\partial C_y} \right)^f \left( \frac{\partial}{\partial C_z} \right)^g \int \frac{\exp(-pr_P^2)}{r_C} d\mathbf{r} \quad (9.9.3)$$

and

$$\begin{aligned} V_{tuv;tv\phi} = & \left( \frac{\partial}{\partial P_x} \right)^t \left( \frac{\partial}{\partial P_y} \right)^u \left( \frac{\partial}{\partial P_z} \right)^v \left( \frac{\partial}{\partial Q_x} \right)^{\tau} \left( \frac{\partial}{\partial Q_y} \right)^{\nu} \left( \frac{\partial}{\partial Q_z} \right)^{\phi} \\ & \times \iint \frac{\exp(-pr_P^2) \exp(-qr_Q^2)}{r_{12}} d\mathbf{r}_1 d\mathbf{r}_2 \end{aligned} \quad (9.9.4)$$

The integrals appearing in these expressions are the Coulomb potential and interaction integrals for spherical charge distributions, introduced in Section 9.7.1. Equations (9.7.23) and (9.7.24) may now be used to replace these integrals by the Boys function. Taking the normalization of the charge distributions (9.7.1) and (9.7.2) into account, we obtain

$$V_{tuv}^{efg} = \frac{2\pi}{p} \left( \frac{\partial}{\partial P_x} \right)^t \left( \frac{\partial}{\partial P_y} \right)^u \left( \frac{\partial}{\partial P_z} \right)^v \left( \frac{\partial}{\partial C_x} \right)^e \left( \frac{\partial}{\partial C_y} \right)^f \left( \frac{\partial}{\partial C_z} \right)^g F_0(pr_{PC}^2) \quad (9.9.5)$$

and

$$V_{tuv;tv\phi} = \frac{2\pi^{5/2}}{pq\sqrt{p+q}} \left( \frac{\partial}{\partial P_x} \right)^t \left( \frac{\partial}{\partial P_y} \right)^u \left( \frac{\partial}{\partial P_z} \right)^v \left( \frac{\partial}{\partial Q_x} \right)^{\tau} \left( \frac{\partial}{\partial Q_y} \right)^{\nu} \left( \frac{\partial}{\partial Q_z} \right)^{\phi} F_0(\alpha r_{PQ}^2) \quad (9.9.6)$$

The definition of Hermite Gaussians in terms of differentiation has thus enabled us to express integrals over nonspherical distributions as derivatives of integrals over spherical distributions.

These derivatives may be further simplified since the Boys function depends only on the relative separation of the two centres, giving the following major simplifications:

$$V_{tuv}^{efg} = (-1)^{e+f+g} \frac{2\pi}{p} \left( \frac{\partial}{\partial \mathbf{P}_x} \right)^{t+e} \left( \frac{\partial}{\partial \mathbf{P}_y} \right)^{u+f} \left( \frac{\partial}{\partial \mathbf{P}_z} \right)^{v+g} F_0(pR_{\text{PC}}^2) \quad (9.9.7)$$

and

$$V_{tuv;\tau\nu\phi} = (-1)^{\tau+\nu+\phi} \frac{2\pi^{5/2}}{pq\sqrt{p+q}} \left( \frac{\partial}{\partial \mathbf{P}_x} \right)^{t+\tau} \left( \frac{\partial}{\partial \mathbf{P}_y} \right)^{u+\nu} \left( \frac{\partial}{\partial \mathbf{P}_z} \right)^{v+\phi} F_0(\alpha R_{\text{PQ}}^2) \quad (9.9.8)$$

These simplifications occur since we use Hermite (rather than Cartesian) Gaussians to describe the nonspherical distributions. Since the derivatives of the Boys function play such an important role, we introduce the Hermite Coulomb integrals

$$R_{tuv}(p, \mathbf{R}_{\text{PC}}) = \left( \frac{\partial}{\partial \mathbf{P}_x} \right)^t \left( \frac{\partial}{\partial \mathbf{P}_y} \right)^u \left( \frac{\partial}{\partial \mathbf{P}_z} \right)^v F_0(pR_{\text{PC}}^2) \quad (9.9.9)$$

The one- and two-electron Hermite Coulomb integrals (9.9.1) and (9.9.2) may now be expressed as [6]

$$\begin{aligned} V_{tuv}^{efg} &= \int \Lambda_{tuv}(\mathbf{r}) \left( \frac{\partial}{\partial \mathbf{C}_x} \right)^e \left( \frac{\partial}{\partial \mathbf{C}_y} \right)^f \left( \frac{\partial}{\partial \mathbf{C}_z} \right)^g r_{\text{C}}^{-1} d\mathbf{r} \\ &= (-1)^{e+f+g} \frac{2\pi}{p} R_{t+e, u+f, v+g}(p, \mathbf{R}_{\text{PC}}) \end{aligned} \quad (9.9.10)$$

and

$$\begin{aligned} V_{tuv;\tau\nu\phi} &= \iint \frac{\Lambda_{tuv}(\mathbf{r}_1) \Lambda_{\tau\nu\phi}(\mathbf{r}_2)}{r_{12}} d\mathbf{r}_1 d\mathbf{r}_2 \\ &= (-1)^{\tau+\nu+\phi} \frac{2\pi^{5/2}}{pq\sqrt{p+q}} R_{t+\tau, u+\nu, v+\phi}(\alpha, \mathbf{R}_{\text{PQ}}) \end{aligned} \quad (9.9.11)$$

Hence, to calculate Coulomb integrals over Hermite Gaussians, we simply take the derivatives of the Boys function. We also see that field and field-gradient integrals may be calculated in the same way as Coulomb-potential integrals. It remains, however, to develop a method for calculating the derivatives of the Boys function.

### 9.9.2 THE EVALUATION OF HERMITE COULOMB INTEGRALS

To develop a scheme for evaluating the Hermite Coulomb integrals (9.9.9), we note that the first derivative involves the first-order Boys function

$$R_{100}(p, \mathbf{R}_{\text{PC}}) = -2pX_{\text{PC}} \int_0^1 \exp(-pR_{\text{PC}}^2 t^2) t^2 dt = -2pX_{\text{PC}} F_1(pR_{\text{PC}}^2) \quad (9.9.12)$$

In general, therefore, higher derivatives are linear combinations of Boys functions of different orders and our task is now to develop a recursive scheme by which the Hermite integrals  $R_{tuv}$  for

$t + u + v \leq N$  may be calculated from the Boys functions  $F_n$  of order  $n \leq N$ . To this end, we introduce the auxiliary integrals

$$R_{tuv}^n(p, \mathbf{R}_{\text{PC}}) = \left( \frac{\partial}{\partial P_x} \right)^t \left( \frac{\partial}{\partial P_y} \right)^u \left( \frac{\partial}{\partial P_z} \right)^v R_{000}^n(p, \mathbf{R}_{\text{PC}}) \quad (9.9.13)$$

where

$$R_{000}^n(p, \mathbf{R}_{\text{PC}}) = (-2p)^n F_n(p R_{\text{PC}}^2) \quad (9.9.14)$$

Note that the definition (9.9.13) includes the integrals  $R_{tuv}$  and  $F_n$  as special cases. We must now relate the integrals  $R_{tuv}^n$  by recursion. Incrementing  $t$ , we obtain

$$R_{t+1,u,v}^n(p, \mathbf{R}_{\text{PC}}) = \left( \frac{\partial}{\partial P_x} \right)^t \left( \frac{\partial}{\partial P_y} \right)^u \left( \frac{\partial}{\partial P_z} \right)^v \frac{\partial R_{000}^n(p, \mathbf{R}_{\text{PC}})}{\partial P_x} \quad (9.9.15)$$

Using (9.9.14) and differentiating the  $n$ th order Boys function, we find

$$R_{t+1,u,v}^n(p, \mathbf{R}_{\text{PC}}) = \left( \frac{\partial}{\partial P_x} \right)^t X_{\text{PC}} R_{0uv}^{n+1}(p, \mathbf{R}_{\text{PC}}) \quad (9.9.16)$$

The operator on the right-hand side may be written as

$$\left( \frac{\partial}{\partial P_x} \right)^t X_{\text{PC}} = \left[ \left( \frac{\partial}{\partial P_x} \right)^t, X_{\text{PC}} \right] + X_{\text{PC}} \left( \frac{\partial}{\partial P_x} \right)^t = t \left( \frac{\partial}{\partial P_x} \right)^{t-1} + X_{\text{PC}} \left( \frac{\partial}{\partial P_x} \right)^t \quad (9.9.17)$$

where we have used (9.4.7). Inserting (9.9.17) in (9.9.16), we obtain the recurrence relation for the Hermite integrals. The formulae for increments in the three indices are [6]

$$R_{t+1,u,v}^n(p, \mathbf{R}_{\text{PC}}) = t R_{t-1,u,v}^{n+1}(p, \mathbf{R}_{\text{PC}}) + X_{\text{PC}} R_{0uv}^{n+1}(p, \mathbf{R}_{\text{PC}}) \quad (9.9.18)$$

$$R_{t,u+1,v}^n(p, \mathbf{R}_{\text{PC}}) = u R_{t,u-1,v}^{n+1}(p, \mathbf{R}_{\text{PC}}) + Y_{\text{PC}} R_{0uv}^{n+1}(p, \mathbf{R}_{\text{PC}}) \quad (9.9.19)$$

$$R_{t,u,v+1}^n(p, \mathbf{R}_{\text{PC}}) = v R_{t,u,v-1}^{n+1}(p, \mathbf{R}_{\text{PC}}) + Z_{\text{PC}} R_{0uv}^{n+1}(p, \mathbf{R}_{\text{PC}}) \quad (9.9.20)$$

In this way, all Hermite Gaussians of order  $t + u + v \leq N$  may be calculated from the Boys functions of order  $n \leq N$  by recursion. The same recurrences may be used to evaluate the integrals (9.9.11) except that  $X_{\text{PQ}}$  replaces  $X_{\text{PC}}$  and so on.

To summarize, we have shown that the Coulomb integrals over Hermite Gaussians (9.9.10) and (9.9.11) may be obtained from the Boys function by three simple recurrence relations (9.9.18)–(9.9.20). The one- and two-electron Coulomb integrals follow essentially the same scheme; field and field-gradient integrals may be calculated in the same way as the one-electron Coulomb integrals. The remaining task is to generate the integrals over Cartesian Gaussians from the Hermite integrals.

### 9.9.3 CARTESIAN COULOMB INTEGRALS BY HERMITE EXPANSION

Having obtained the Hermite Coulomb integrals, we are now in a position to calculate the Cartesian Coulomb integrals

$$V_{ab}^{efg} = \langle G_a | \left( \frac{\partial}{\partial C_x} \right)^e \left( \frac{\partial}{\partial C_y} \right)^f \left( \frac{\partial}{\partial C_z} \right)^g r_{\text{C}}^{-1} | G_b \rangle \quad (9.9.21)$$

$$g_{abcd} = \langle G_a(\mathbf{r}_1) G_b(\mathbf{r}_1) | \frac{1}{r_{12}} | G_c(\mathbf{r}_2) G_d(\mathbf{r}_2) \rangle \quad (9.9.22)$$

In terms of overlap distributions, these integrals are given by

$$V_{ab}^{efg} = \int \Omega_{ab}(\mathbf{r}) \left( \frac{\partial}{\partial C_x} \right)^e \left( \frac{\partial}{\partial C_y} \right)^f \left( \frac{\partial}{\partial C_z} \right)^g r_C^{-1} d\mathbf{r} \quad (9.9.23)$$

$$g_{abcd} = \iint \frac{\Omega_{ab}(\mathbf{r}_1) \Omega_{cd}(\mathbf{r}_2)}{r_{12}} d\mathbf{r}_1 d\mathbf{r}_2 \quad (9.9.24)$$

Inserting the Hermite expansions of the overlap distributions (9.5.1), we obtain

$$V_{ab}^{efg} = \sum_{tuv} E_{tuv}^{ab} \int \Lambda_{tuv}(\mathbf{r}) \left( \frac{\partial}{\partial C_x} \right)^e \left( \frac{\partial}{\partial C_y} \right)^f \left( \frac{\partial}{\partial C_z} \right)^g r_C^{-1} d\mathbf{r} \quad (9.9.25)$$

$$g_{abcd} = \sum_{tuv} E_{tuv}^{ab} \sum_{\tau\phi} E_{\tau\phi}^{cd} \iint \frac{\Lambda_{tuv}(\mathbf{r}_1) \Lambda_{\tau\phi}(\mathbf{r}_2)}{r_{12}} d\mathbf{r}_1 d\mathbf{r}_2 \quad (9.9.26)$$

with the notation

$$E_{tuv}^{ab} = E_t^{ij} E_u^{kl} E_v^{mn} \quad (9.9.27)$$

We recall that  $\Lambda_{tuv}$  is a Hermite Gaussian of exponent  $p$  centred on  $\mathbf{P}$

$$p = a + b \quad (9.9.28)$$

$$\mathbf{P} = \frac{a\mathbf{A} + b\mathbf{B}}{p} \quad (9.9.29)$$

and that  $\Lambda_{\tau\phi}$  is a Hermite Gaussian of exponent  $q$  centred on  $\mathbf{Q}$

$$q = c + d \quad (9.9.30)$$

$$\mathbf{Q} = \frac{c\mathbf{C} + d\mathbf{D}}{q} \quad (9.9.31)$$

Inserting the Hermite integrals (9.9.10) and (9.9.11) in the expressions for the Cartesian integrals (9.9.25) and (9.9.26), we obtain the final expressions for Cartesian Coulomb integrals [6]:

$$V_{ab}^{efg} = (-1)^{e+f+g} \frac{2\pi}{p} \sum_{tuv} E_{tuv}^{ab} R_{t+e,u+f,v+g}(p, \mathbf{R}_{PC}) \quad (9.9.32)$$

$$g_{abcd} = \frac{2\pi^{5/2}}{pq\sqrt{p+q}} \sum_{tuv} E_{tuv}^{ab} \sum_{\tau\phi} (-1)^{\tau+\nu+\phi} E_{\tau\phi}^{cd} R_{t+\tau,u+\nu,v+\phi}(\alpha, \mathbf{R}_{PQ}) \quad (9.9.33)$$

We see that the Cartesian integrals may be calculated straightforwardly from the Hermite integrals of Section 9.9.2, the basic manipulation being a transformation of an array from one basis (Hermite Gaussian overlap distributions) to another basis (Cartesian Gaussian overlap distributions). In practice, this transformation (9.9.33) is the time-consuming step in the evaluation of two-electron integrals. Note that, once the Hermite Coulomb integrals have been generated, the calculation of field and field-gradient integrals is no more expensive than the calculation of the one-electron Coulomb integrals since the summations are the same.

The nuclear-attraction part of the one-electron Hamiltonian contains one contribution from each nucleus, obtained by multiplying the charge of the nucleus by the potential at its position. Introducing the charges of  $-1$  for the electron and  $Z_K$  for the nuclei, we obtain

$$h_{ab}^{\text{NA}} = - \sum_K Z_K V_{ab}^{000}(\mathbf{C}_K) = - \frac{2\pi}{p} \sum_{tuv} E_{tuv}^{ab} \sum_K Z_K R_{tuv}(p, \mathbf{R}_{\text{PC}_K}) \quad (9.9.34)$$

where the summation is over the full set of nuclei. Note that the contributions from all the nuclei may be added together before we transform from Hermite to Cartesian integrals.

#### 9.9.4 CARTESIAN COULOMB INTEGRALS BY HERMITE RECURSION

Having derived formulae for calculating the Coulomb integrals by expansion, we now discuss their calculation by recursion. To avoid complicated notation, we consider only the one-electron potential integrals. One-electron field and field-gradient integrals, as well as two-electron integrals, are obtained by a straightforward modification of the scheme. We introduce the integrals

$$\Phi_{ijklmn}^{tuv} = \int \frac{\Omega_{ij}^t \Omega_{kl}^u \Omega_{mn}^v}{r_C} d\mathbf{r} \quad (9.9.35)$$

where we use the mixed Cartesian and Hermite overlap distributions defined in (9.5.22). These integrals contain as special cases the Cartesian and Hermite integrals

$$\Phi_{ijklmn}^{000} = V_{ab}^{000} \quad (9.9.36)$$

$$\Phi_{000000}^{tuv} = K_{ab}^{xyz} \int \frac{\Lambda_{tuv}(\mathbf{r})}{r_C} d\mathbf{r} \quad (9.9.37)$$

where  $K_{ab}^{xyz}$  is the product of three preexponential factors, one for each Cartesian direction (9.2.15). Using the recurrence relations for the mixed overlap distributions (9.5.27) and (9.5.28), we obtain from (9.9.35) the following recurrences

$$\Phi_{i+1,j,k,l,m,n}^{tuv} = \frac{1}{2p} \Phi_{ijklmn}^{t+1,u,v} + X_{\text{PA}} \Phi_{ijklmn}^{tuv} + t \Phi_{ijklmn}^{t-1,u,v} \quad (9.9.38)$$

$$\Phi_{i,j+1,k,l,m,n}^{tuv} = \frac{1}{2p} \Phi_{ijklmn}^{t+1,u,v} + X_{\text{PB}} \Phi_{ijklmn}^{tuv} + t \Phi_{ijklmn}^{t-1,u,v} \quad (9.9.39)$$

and similarly for increments in the other indices. Starting from the Hermite integrals (9.9.37) with  $t \leq N$ ,  $u \leq N$  and  $v \leq N$ , we may use these relations to generate all Cartesian integrals with  $i + j \leq N$ ,  $k + l \leq N$  and  $m + n \leq N$ .

#### 9.9.5 COMPUTATIONAL CONSIDERATIONS FOR THE ONE-ELECTRON INTEGRALS

The calculation of integrals is a complicated business, where compromises must be made between considerations such as efficiency, memory usage, and programming effort. Moreover, different implementations may be superior in different ways – some for basis sets consisting of highly contracted functions of low angular momentum, others for basis sets with a large number of functions of high angular momentum, and so on. In the following, we shall give some consideration to the different algorithms that may be used in order to calculate integrals efficiently. Although

the time-critical task is the calculation of two-electron integrals, we begin by considering in this subsection the one-electron Coulomb integrals within the McMurchie–Davidson scheme, noting that many of the considerations apply also to the two-electron integrals discussed in Section 9.9.6 as well as to the Obara–Saika and Rys schemes discussed in Sections 9.10 and 9.11.

In the McMurchie–Davidson scheme, the one-electron Coulomb integrals may be written in the following manner

$$V_{ijklmn}^{000} = \frac{2\pi}{p} \sum_{tuv} E_t^{ij} E_u^{kl} E_v^{mn} R_{tuv} \quad (9.9.40)$$

In our analysis, we shall assume that both orbitals have angular momentum  $L$  and contain  $p$  primitive functions. Each shell then contains  $(L+1)(L+2)/2$  orbitals in the Cartesian basis and  $2L+1$  orbitals in the spherical-harmonic basis.

The obvious way to generate the integrals (9.9.40) is first to calculate the expansion coefficients and Hermite integrals and then to carry out the summation. As the number of Cartesian orbitals in each shell scales as  $L^2$ , the number of Cartesian integrals scales as  $L^4 p^2$ . For each Cartesian integral, we carry out a simultaneous summation over three indices, each of which scales as  $L$ , so the total operation count scales as  $L^7 p^2$ .

We must also consider the cost of generating the expansion coefficients and the Hermite integrals in (9.9.40). The number of Hermite integrals scales as  $L^3 p^2$  and their evaluation scales as  $L^4 p^2$ . The  $L^4 p^2$  dependence for the construction arises from the use of the auxiliary four-index integrals  $R_{tuv}^n$ , where each index scales as  $L$ . The evaluation of the Boys function scales only as  $Lp^2$ . Finally, the number of expansion coefficients  $E_t^{ij}$  scales as  $L^3 p^2$  and their evaluation also as  $L^3 p^2$  since no auxiliary elements are used in the calculation. The evaluation of the primitive Cartesian integrals is therefore dominated by the transformation (9.9.40), with a total cost of  $L^7 p^2$ .

To produce the final integrals over contracted functions in a spherical-harmonic basis, we must carry out a set of transformations of the primitive Cartesian integrals. Assuming a segmented basis set, the transformation to the contracted basis is a simple data reduction step, with a cost that scales as the number of primitive Cartesian functions – that is, as  $L^4 p^2$ . The generation of integrals over spherical-harmonic Gaussians requires one transformation for each orbital index. The transformation of the first orbital scales as  $L^5$  and that of the second orbital as  $L^4$ . The overall cost of the Cartesian-to-spherical transformation then scales as  $L^5$ , assuming that it is carried out after the transformation of primitive to contracted functions. We conclude that the overall cost for the calculation of the one-electron Coulomb integrals (as described here) is  $L^7 p^2$ .

There is one obvious way to bring this cost down. Rewriting the Cartesian integrals in terms of three partial summations, we obtain

$$V_{ijklmn}^{000} = \frac{2\pi}{p} \sum_t E_t^{ij} \sum_u E_u^{kl} \sum_v E_v^{mn} R_{tuv} \quad (9.9.41)$$

Noting that the upper indices of the expansion coefficients  $mn$  scale as  $L^2 p^2$ , we find that the first partial summation scales as  $L^5 p^2$  and produces  $L^4 p^2$  intermediates. In the second transformation, we combine these  $L^4 p^2$  intermediates with  $L^3 p^2$  expansion coefficients, in a process that scales as  $L^6 p^2$  and produces  $L^5 p^2$  new intermediates. Finally, in the last summation, the upper indices  $ij$  are fixed by the requirement that the total angular momentum of each orbital is equal to  $L$ . In this step, therefore, we combine  $Lp^2$  coefficients with  $L^5 p^2$  intermediates in a step that scales as  $L^5 p^2$  and produces  $L^4 p^2$  integrals. The overall scaling of the integration has thus been reduced to  $L^6 p^2$ .

**Table 9.1** Cost and memory requirements of the McMurchie–Davidson scheme for one-electron Coulomb integrals

	Cost	Memory
Boys functions	$Lp^2$	$Lp^2$
Hermite integrals	$L^4p^2$	$L^3p^2$
Expansion coefficients	$L^3p^2$	$L^3p^2$
Cartesian integrals	$L^7p^2/L^6p^2$	$L^4p^2$
Primitive contraction	$L^4p^2$	$L^4$
Solid harmonics	$L^5$	$L^2$

The cost of the two schemes (9.9.40) and (9.9.41) for the evaluation of the one-electron Coulomb integrals is summarized in Table 9.1. At this point, it is worth noting that factors such as  $L^6p^2$  and  $L^7p^2$  are not always good indicators of the overall cost of a given process. For low angular momentum, in particular, lower-order terms may dominate the evaluation, making the cost analysis rather difficult. In practice, except for orbitals of high angular momentum, the three-step transformation (9.9.41) will not be faster than the original one-step transformation (9.9.40).

Let us now consider a somewhat different approach where, in the first *vertical step*, we evaluate integrals of the form

$$V_{i0k0m0}^{000} = \frac{2\pi}{p} \sum_{tuv} E_t^{i0} E_u^{k0} E_v^{m0} R_{tuv} \quad (9.9.42)$$

Next, we transform the integrals to the contracted basis and then, in the *horizontal step*, we apply recurrence relations such as

$$V_{i,j+1,k,l,m,n}^{000} = V_{i+1,j,k,l,m,n}^{000} + X_{AB} V_{ijklmn}^{000} \quad (9.9.43)$$

to transfer angular momentum from the first to the second orbital; see (9.5.9). This step may be carried out after the transformation to the contracted basis since it does not depend on the exponents of the primitive functions. In the final step, the orbitals are transformed to the spherical-harmonic basis.

For this procedure to work, we must in the vertical step (9.9.42) generate integrals not only of angular momentum  $L$ , but of all angular momenta from  $L$  to  $2L$  since these are all needed in the horizontal step (9.9.43). Still, since the functions of nonzero angular momentum are restricted to the first orbital, the number of Cartesian integrals in (9.9.42) scales as  $L^3p^2$  rather than as  $L^4p^2$  for (9.9.40), reducing the cost of this step to  $L^6p^2$  or  $L^4p^2$  (if carried out in a three-step manner). The cost of the various steps of this *vertical–horizontal algorithm* is given in Table 9.2. This algorithm should be contrasted with the original scheme in Table 9.1, with an overall cost of  $L^7p^2$  for the first step (9.9.40) and  $L^4p^2$  for the contraction.

### 9.9.6 COMPUTATIONAL CONSIDERATIONS FOR THE TWO-ELECTRON INTEGRALS

Having considered the evaluation of the one-electron Coulomb integrals, let us turn our attention to the two-electron repulsion integrals within the McMurchie–Davidson scheme. Clearly, many of the considerations for the one-electron integrals apply also to the two-electron integrals. In addition, some new considerations arise because of the higher complexity of the two-electron integrals.

**Table 9.2** Cost and memory requirements of the vertical–horizontal McMurchie–Davidson scheme for one-electron Coulomb integrals

	Cost	Memory
Boys functions	$Lp^2$	$Lp^2$
Hermite integrals	$L^4p^2$	$L^3p^2$
Expansion coefficients	$L^2p^2$	$L^2p^2$
Vertical transformation	$L^6p^2/L^4p^2$	$L^3p^2$
Primitive contraction	$L^3p^2$	$L^3$
Horizontal transformation	$L^6$	$L^4$
Solid harmonics	$L^5$	$L^2$

We begin our discussion by noting that the two-electron integrals (9.9.33) may be written in the manner

$$g_{abcd} = \sum_{\substack{tuv \\ \tau\phi}} E_{tuv}^{ab} F_{\tau\phi}^{cd} \mathfrak{R}_{t+\tau, u+v, v+\phi}(\alpha, \mathbf{R}_{\text{PQ}}) \quad (9.9.44)$$

where we have introduced

$$F_{\tau\phi}^{cd} = (-1)^{\tau+v+\phi} E_{\tau\phi}^{cd} \quad (9.9.45)$$

$$\mathfrak{R}_{t+\tau, u+v, v+\phi}(\alpha, \mathbf{R}_{\text{PQ}}) = \frac{2\pi^{5/2}}{pq\sqrt{p+q}} R_{t+\tau, u+v, v+\phi}(\alpha, \mathbf{R}_{\text{PQ}}) \quad (9.9.46)$$

We now observe that the evaluation of the two-electron integrals is best carried out in two steps:

$$g_{tuv}^{cd} = \sum_{\tau\phi} F_{\tau\phi}^{cd} \mathfrak{R}_{t+\tau, u+v, v+\phi}(\alpha, \mathbf{R}_{\text{PQ}}) \quad (9.9.47)$$

$$g_{abcd} = \sum_{tuv} E_{tuv}^{ab} g_{tuv}^{cd} \quad (9.9.48)$$

The advantage of carrying out this partial summation is that the operation count is brought down from  $L^{14}p^4$  for (9.9.44) to  $L^{10}p^4$  for (9.9.47) and  $L^{11}p^4$  for (9.9.48), clearly a major improvement. Next, we note that, once the first Hermite-to-Cartesian step has been completed, we may carry out the transformation to the contracted spherical-harmonic basis for the first electron before we go on to the second Hermite-to-Cartesian transformation (9.9.48), bringing the number of integrals for the second step (9.9.48) down from  $L^7p^4$  to  $L^5p^2$ . The cost is  $L^7p^4$  for the contraction and  $L^8p^2$  for the spherical-harmonic transformation. As a result, the cost of the second step (9.9.48) is reduced from  $L^{11}p^4$  to  $L^9p^2$ . To conclude our calculation, a contraction and transformation to the spherical-harmonic basis must be carried out for the second electron, at the costs  $L^6p^2$  and  $L^7$ , respectively. The cost of the evaluation of the different steps is given in Table 9.3, where, for the Hermite-to-Cartesian steps, we have given also the costs  $L^8p^4$  and  $L^8p^2$  for the alternative partial summations analogous to (9.9.41). For reasons that will become clear shortly, we shall refer to this algorithm as MD4.

As for the one-electron integrals, we may reduce the cost of the integration (at the expense of a somewhat more complicated algorithm) by employing vertical and horizontal transformations for the Hermite-to-Cartesian step. The same arguments apply as for the one-electron integrals in Section 9.9.5, and the costs of the various steps are given in Table 9.4. The overall cost of the evaluation of the two-electron integrals now scales as  $L^7p^4$  (for the  $p^4$  steps) and  $L^9p^2$  (for the  $p^2$  steps). Since we now use the McMurchie–Davidson expansion to generate integrals with nonzero

**Table 9.3** Cost and memory requirements of the two-electron MD4 scheme

	First electron		Second electron	
	Cost	Memory	Cost	Memory
Boys functions	$Lp^4$	$Lp^4$		
Hermite integrals	$L^4p^4$	$L^3p^4$		
Expansion coefficients	$L^3p^2$	$L^3p^2$		
Cartesian integrals	$L^{10}p^4/L^8p^4$	$L^7p^4$	$L^3p^2$	$L^3p^2$
Primitive contraction	$L^7p^4$	$L^7p^2$	$L^6p^2$	$L^6$
Solid harmonics	$L^8p^2$	$L^5p^2$	$L^7$	$L^4$

**Table 9.4** Cost and memory requirements of the two-electron MD2 scheme

	First electron		Second electron	
	Cost	Memory	Cost	Memory
Boys functions	$Lp^4$	$Lp^4$		
Hermite integrals	$L^4p^4$	$L^3p^4$		
Expansion coefficients	$L^2p^2$	$L^2p^2$		
Vertical transformation	$L^9p^4/L^7p^4$	$L^6p^4$	$L^8p^2/L^6p^2$	$L^5p^2$
Primitive contraction	$L^6p^4$	$L^6p^2$	$L^5p^2$	$L^5$
Horizontal transformation	$L^9p^2$	$L^7p^2$	$L^8$	$L^6$
Solid harmonics	$L^8p^2$	$L^5p^2$	$L^7$	$L^4$

angular momentum only for the first and third indices, we shall refer to this scheme as MD2. In the limit of high angular momentum, the MD2 scheme appears to be a substantial improvement on the MD4 scheme. For integrals of low angular momentum, the simpler MD4 scheme is usually more efficient.

The separate treatment of the two electrons in the McMurchie–Davidson scheme may be very useful in some circumstances. Consider, for example, the calculation of the Coulomb contribution to the Fock matrix, which, in the primitive Cartesian basis, may be written in the manner

$$f_{ab}^{\text{cou}} = \sum_{cd} g_{abcd} D_{cd}^{\text{AO}} \quad (9.9.49)$$

as discussed in Section 10.6.3. Combining these expressions with (9.9.44)–(9.9.48), we find that the contribution to the Fock matrix may be obtained in the following two steps:

$$g_{tuv} = \sum_{cd} g_{tuv}^{cd} D_{cd}^{\text{AO}} \quad (9.9.50)$$

$$f_{ab}^{\text{cou}} = \sum_{tuv} E_{tuv}^{ab} g_{tuv} \quad (9.9.51)$$

reducing the cost for the second electron in direct Hartree–Fock calculations significantly.

## 9.10 The Obara–Saika scheme for Coulomb integrals

In the McMurchie–Davidson scheme, we begin by calculating the Boys function; next, we generate the Hermite integrals; and, finally, we arrive at the Cartesian integrals by combination of the Hermite integrals. We shall now investigate a different route to the Coulomb integrals – the

Obara–Saika scheme [5] – in which we avoid the intermediate Hermite integrals altogether, obtaining the final Cartesian integrals by recursion directly from the Boys function.

### 9.10.1 THE OBARA–SAIKA SCHEME FOR ONE-ELECTRON COULOMB INTEGRALS

According to our discussion in Section 9.9, the Coulomb-potential integrals may be written in the form (9.9.32)

$$V_{ijklmn}^{000} = \frac{2\pi}{p} \sum_{tuv} E_t^{ij} E_u^{kl} E_v^{mn} R_{tuv} \quad (9.10.1)$$

To derive the Obara–Saika recurrence relations, we introduce the auxiliary integrals

$$\Theta_{ijklmn}^N = \frac{2\pi}{p} (-2p)^{-N} \sum_{tuv} E_t^{ij} E_u^{kl} E_v^{mn} R_{tuv}^N \quad (9.10.2)$$

For lower indices equal to 0, these integrals represent the (scaled) Boys function; for 0 upper index, they represent the final Cartesian integrals:

$$\Theta_{000000}^N = \frac{2\pi}{p} (-2p)^{-N} K_{ab}^{xyz} R_{000}^N = \frac{2\pi}{p} K_{ab}^{xyz} F_N(pR_{\text{PC}}^2) \quad (9.10.3)$$

$$\Theta_{ijklmn}^0 = V_{ijklmn}^{000} \quad (9.10.4)$$

To obtain (9.10.3), we have used (9.5.8) and (9.9.14). Our task is now to develop a set of recurrence relations by means of which we may arrive at the target integrals (9.10.4) starting from the source integrals (9.10.3).

We shall derive the recurrence relations for the Coulomb-potential integrals from the recurrence relations for the expansion coefficients in Section 9.5.1 and for the Hermite integrals in Section 9.9.2. Consider the integral (9.10.2) with  $i$  incremented by 1:

$$\Theta_{i+1,j}^N = \frac{2\pi}{p} (-2p)^{-N} \sum_{tuv} E_t^{i+1,j} E_u^{kl} E_v^{mn} R_{tuv}^N \quad (9.10.5)$$

where, for ease of notation, we have omitted the Cartesian quantum numbers  $kl$  and  $mn$  for the  $y$  and  $z$  directions and written  $\Theta_{i+1,j}^N$  rather than  $\Theta_{i+1,j,k,l,m,n}^N$ . First, we insert the recurrence relation for the expansion coefficients (9.5.20) and replace  $t$  by  $t+1$  in the summation:

$$\Theta_{i+1,j}^N = X_{\text{PA}} \Theta_{ij}^N + \frac{1}{2p} (i \Theta_{i-1,j}^N + j \Theta_{i,j-1}^N) - \frac{2\pi}{p} (-2p)^{-N-1} \sum_{tuv} E_t^{ij} E_u^{kl} E_v^{mn} R_{t+1,u,v}^N \quad (9.10.6)$$

Next, we invoke the recurrence relation for the Hermite integrals (9.9.18):

$$\begin{aligned} \Theta_{i+1,j}^N &= X_{\text{PA}} \Theta_{ij}^N + \frac{1}{2p} (i \Theta_{i-1,j}^N + j \Theta_{i,j-1}^N) - \frac{2\pi}{p} (-2p)^{-N-1} X_{\text{PC}} \sum_{tuv} E_t^{ij} E_u^{kl} E_v^{mn} R_{tuv}^{N+1} \\ &\quad + \frac{2\pi}{p} (-2p)^{-N-2} \sum_{tuv} (2pt E_t^{ij}) E_u^{kl} E_v^{mn} R_{t-1,u,v}^{N+1} \end{aligned} \quad (9.10.7)$$

Finally, using the relation (9.5.14) for the expansion coefficients and reintroducing the full set of indices, we arrive at the *Obara–Saika recurrence relations* for the Coulomb-potential integral [5]:

$$\begin{aligned} \Theta_{i+1,j,k,l,m,n}^N &= X_{\text{PA}} \Theta_{ijklmn}^N + \frac{1}{2p} (i \Theta_{i-1,j,k,l,m,n}^N + j \Theta_{i,j-1,k,l,m,n}^N) \\ &\quad - X_{\text{PC}} \Theta_{ijklmn}^{N+1} - \frac{1}{2p} (i \Theta_{i-1,j,k,l,m,n}^{N+1} + j \Theta_{i,j-1,k,l,m,n}^{N+1}) \end{aligned} \quad (9.10.8)$$

$$\begin{aligned}\Theta_{i,j+1,k,l,m,n}^N &= X_{\text{PB}} \Theta_{ijklmn}^N + \frac{1}{2p} (i \Theta_{i-1,j,k,l,m,n}^N + j \Theta_{i,j-1,k,l,m,n}^N) \\ &\quad - X_{\text{PC}} \Theta_{ijklmn}^{N+1} - \frac{1}{2p} (i \Theta_{i-1,j,k,l,m,n}^{N+1} + j \Theta_{i,j-1,k,l,m,n}^{N+1})\end{aligned}\quad (9.10.9)$$

The recurrence relation (9.10.9) is identical to (9.10.8) except that  $X_{\text{PA}}$  is replaced by  $X_{\text{PB}}$  and is most easily obtain from the horizontal recurrence

$$\Theta_{i+1,j,k,l,m,n}^N = \Theta_{i,j+1,k,l,m,n}^N - X_{\text{AB}} \Theta_{ijklmn}^N \quad (9.10.10)$$

Using these recurrences and their analogues for the remaining four Cartesian indices, we may generate the full set of Cartesian integrals starting from the Boys function.

Comparing the recurrence relations (9.10.8) and (9.10.9) with those for the simple one-electron integrals in Section 9.3, we note that the recurrences for the Coulomb-potential integrals are considerably more complicated, containing as many as six terms – three terms with an unmodified upper index  $N$  and three terms with an incremented upper index  $N + 1$ .

### 9.10.2 THE OBARA–SAIKA SCHEME FOR TWO-ELECTRON COULOMB INTEGRALS

To derive the Obara–Saika recurrence relations for the two-electron Coulomb integral, we begin by setting up the following auxiliary integral

$$\begin{aligned}\Theta_{i_x j_x k_x l_x; i_y j_y k_y l_y; i_z j_z k_z l_z}^N &= \frac{2\pi^{5/2}}{pq\sqrt{p+q}} (-2\alpha)^{-N} \\ &\quad \times \sum_{\substack{tuv \\ \tau\phi}} (-1)^{\tau+v+\phi} E_t^{i_x j_x} E_{\tau}^{k_x l_x} E_u^{i_y j_y} E_v^{k_y l_y} E_v^{i_z j_z} E_{\phi}^{k_z l_z} R_{t+\tau, u+v, v+\phi}^N\end{aligned}\quad (9.10.11)$$

From (9.5.8), (9.9.14) and (9.9.33), this integral is seen to contain as special cases the source and target integrals:

$$\Theta_{0000;0000;0000}^N = \frac{2\pi^{5/2}}{pq\sqrt{p+q}} K_{ab}^{xyz} K_{cd}^{xyz} F_N(\alpha R_{\text{PQ}}^2) \quad (9.10.12)$$

$$\Theta_{i_x j_x k_x l_x; i_y j_y k_y l_y; i_z j_z k_z l_z}^0 = g_{i_x j_x k_x l_x; i_y j_y k_y l_y; i_z j_z k_z l_z} \quad (9.10.13)$$

To simplify notation, we shall write the auxiliary integral in the form

$$\Theta_{ijkl}^N = A_N \sum_{\substack{tuv \\ \tau\phi}} (-1)^{\tau+v+\phi} E_t^{ij} E_{\tau}^{kl} E_{uv\phi} R_{t+\tau, u+v, v+\phi}^N \quad (9.10.14)$$

where  $i, j, k, l$  are the Cartesian quantum numbers for orbitals  $a, b, c, d$  in the  $x$  direction, and where we have introduced the quantities

$$A_N = \frac{2\pi^{5/2}}{pq\sqrt{p+q}} (-2\alpha)^{-N} \quad (9.10.15)$$

$$E_{uv\phi} = E_u^{i_y j_y} E_v^{k_y l_y} E_v^{i_z j_z} E_{\phi}^{k_z l_z} \quad (9.10.16)$$

Note that the Cartesian quantum numbers for the  $y$  and  $z$  directions are not affected by the recurrence relations to be developed here. Also, the recurrences for the  $y$  and  $z$  directions may be easily set up by analogy with the recurrences for the  $x$  direction.

Our development follows closely that for the one-electron Coulomb integrals in Section 9.10.1. In the incremented integral

$$\Theta_{i+1,j,k,l}^N = A_N \sum_{\substack{uvw \\ \tau v \phi}} (-1)^{\tau+v+\phi} E_t^{i+1,j} E_\tau^{kl} E_{uvv\phi} R_{t+\tau, u+v, v+\phi}^N \quad (9.10.17)$$

we insert (9.5.20) and replace  $t$  by  $t+1$  to obtain

$$\Theta_{i+1,j,k,l}^N = X_{\text{PA}} \Theta_{ijkl}^N + \frac{1}{2p} (i \Theta_{i-1,j,k,l}^N + j \Theta_{i,j-1,k,l}^N) - \frac{1}{2p} Q_{ijkl}^N \quad (9.10.18)$$

where we have introduced

$$Q_{ijkl}^N = -A_N \sum_{\substack{uvw \\ \tau v \phi}} (-1)^{\tau+v+\phi} E_t^{ij} E_\tau^{kl} E_{uvv\phi} R_{t+\tau+1, u+v, v+\phi}^N \quad (9.10.19)$$

which represents the original integral  $\Theta_{ijkl}^N$  differentiated with respect to  $Q_x$ . To evaluate  $Q_{ijkl}^N$ , we invoke the Hermite recurrence (9.9.18) in the form

$$R_{t+\tau+1, u+v, v+\phi}^N = (t+\tau) R_{t+\tau-1, u+v, v+\phi}^{N+1} + X_{\text{PQ}} R_{t+\tau, u+v, v+\phi}^{N+1} \quad (9.10.20)$$

Inserting this expression in (9.10.19) and rearranging terms, we obtain

$$\begin{aligned} Q_{ijkl}^N &= 2\alpha X_{\text{PQ}} A_{N+1} \sum_{\substack{uvw \\ \tau v \phi}} (-1)^{\tau+v+\phi} E_t^{ij} E_\tau^{kl} E_{uvv\phi} R_{t+\tau, u+v, v+\phi}^{N+1} \\ &\quad + \frac{\alpha}{p} A_{N+1} \sum_{\substack{uvw \\ \tau v \phi}} (-1)^{\tau+v+\phi} (2pt E_t^{ij}) E_\tau^{kl} E_{uvv\phi} R_{t+\tau-1, u+v, v+\phi}^{N+1} \\ &\quad + \frac{\alpha}{q} A_{N+1} \sum_{\substack{uvw \\ \tau v \phi}} (-1)^{\tau+v+\phi} E_t^{ij} (2q\tau E_\tau^{kl}) E_{uvv\phi} R_{t+\tau-1, u+v, v+\phi}^{N+1} \end{aligned} \quad (9.10.21)$$

We now invoke (9.5.14) for the expressions  $2pt E_t^{ij}$  and  $2q\tau E_\tau^{kl}$

$$\begin{aligned} Q_{ijkl}^N &= 2\alpha X_{\text{PQ}} \Theta_{ijkl}^{N+1} + i \frac{\alpha}{p} A_{N+1} \sum_{\substack{uvw \\ \tau v \phi}} (-1)^{\tau+v+\phi} E_{t-1}^{i-1,j} E_\tau^{kl} E_{uvv\phi} R_{t+\tau-1, u+v, v+\phi}^{N+1} \\ &\quad + j \frac{\alpha}{p} A_{N+1} \sum_{\substack{uvw \\ \tau v \phi}} (-1)^{\tau+v+\phi} E_{t-1}^{i,j-1} E_\tau^{kl} E_{uvv\phi} R_{t+\tau-1, u+v, v+\phi}^{N+1} \\ &\quad - k \frac{\alpha}{q} A_{N+1} \sum_{\substack{uvw \\ \tau v \phi}} (-1)^{\tau-1+v+\phi} E_t^{ij} E_{\tau-1}^{k-1,l} E_{uvv\phi} R_{t+\tau-1, u+v, v+\phi}^{N+1} \\ &\quad - l \frac{\alpha}{q} A_{N+1} \sum_{\substack{uvw \\ \tau v \phi}} (-1)^{\tau-1+v+\phi} E_t^{ij} E_{\tau-1}^{k,l-1} E_{uvv\phi} R_{t+\tau-1, u+v, v+\phi}^{N+1} \end{aligned} \quad (9.10.22)$$

which yields the expression

$$Q_{ijkl}^N = 2\alpha X_{PQ} \Theta_{ijkl}^{N+1} + \frac{\alpha}{p} (i\Theta_{i-1,j,k,l}^{N+1} + j\Theta_{i,j-1,k,l}^{N+1}) - \frac{\alpha}{q} (k\Theta_{i,j,k-1,l}^{N+1} + l\Theta_{i,j,k,l-1}^{N+1}) \quad (9.10.23)$$

for the integral  $\Theta_{ijkl}^N$  differentiated with respect to  $Q_x$ .

Inserting (9.10.23) in (9.10.18), we obtain the Obara–Saika two-electron recurrence relation [5]

$$\begin{aligned} \Theta_{i+1,j,k,l}^N = & X_{PA} \Theta_{ijkl}^N - \frac{\alpha}{p} X_{PQ} \Theta_{ijkl}^{N+1} + \frac{i}{2p} \left( \Theta_{i-1,j,k,l}^N - \frac{\alpha}{p} \Theta_{i-1,j,k,l}^{N+1} \right) \\ & + \frac{j}{2p} \left( \Theta_{i,j-1,k,l}^N - \frac{\alpha}{p} \Theta_{i,j-1,k,l}^{N+1} \right) + \frac{k}{2(p+q)} \Theta_{i,j,k-1,l}^{N+1} + \frac{l}{2(p+q)} \Theta_{i,j,k,l-1}^{N+1} \end{aligned} \quad (9.10.24)$$

Using the horizontal recurrence relation (9.10.10), a similar relation may be written down for increments in  $j$ , replacing  $X_{PA}$  with  $X_{PB}$ . For completeness, we give also the recurrence relation for increments in  $k$  for the second electron:

$$\begin{aligned} \Theta_{i,j,k+1,l}^N = & X_{QC} \Theta_{ijkl}^N + \frac{\alpha}{q} X_{PQ} \Theta_{ijkl}^{N+1} + \frac{k}{2q} \left( \Theta_{i,j,k-1,l}^N - \frac{\alpha}{q} \Theta_{i,j,k-1,l}^{N+1} \right) \\ & + \frac{l}{2q} \left( \Theta_{i,j,k,l-1}^N - \frac{\alpha}{q} \Theta_{i,j,k,l-1}^{N+1} \right) + \frac{i}{2(p+q)} \Theta_{i-1,j,k,l}^{N+1} + \frac{j}{2(p+q)} \Theta_{i,j-1,k,l}^{N+1} \end{aligned} \quad (9.10.25)$$

Note that (9.10.25) can be obtained from (9.10.24) by index substitution and renaming of variables. Similar recurrence relations are easily set up for the remaining two Cartesian directions. Note that the recurrence (9.10.24) reduces to that for the one-electron Coulomb integrals of Section 9.10.1 – see (9.10.8) – when  $k = l = 0$  and when  $q$  (i.e. the sum of the exponents for the second electron) tends to infinity.

We have now succeeded in setting up a set of recurrence relations by means of which the two-electron Cartesian integrals may be obtained from the Boys function. The resulting expressions are rather complicated, however, involving as many as eight distinct contributions. Unlike the McMurchie–Davidson scheme, the Obara–Saika scheme does not treat the two electrons separately since the recurrences (9.10.24) and (9.10.25), for example, affect the indices of all four orbitals. In Section 9.10.3, we shall see how the Obara–Saika recurrences may be simplified considerably when used in conjunction with two other types of recurrence relations: the electron-transfer recurrences and the horizontal recurrences.

### 9.10.3 THE ELECTRON-TRANSFER AND HORIZONTAL RECURRENCE RELATIONS

In the original Obara–Saika scheme, the two-electron integrals are generated from the Boys function by means of rather unwieldy recurrence relations such as (9.10.24). It is possible, however, to break the generation of the two-electron integrals up into several smaller steps, each of which involves a simpler set of recurrences. Consider the following three-step path to the Cartesian integrals.

First, a set of two-electron integrals with  $j = k = l = 0$  is generated by means of the following special four-term version of the *Obara–Saika recurrence relation*:

$$\Theta_{i+1,0,0,0}^N = X_{PA} \Theta_{i000}^N - \frac{\alpha}{p} X_{PQ} \Theta_{i000}^{N+1} + \frac{i}{2p} \left( \Theta_{i-1,0,0,0}^N - \frac{\alpha}{p} \Theta_{i-1,0,0,0}^{N+1} \right) \quad (9.10.26)$$

In the next step, we transfer Cartesian powers from the first to the second electron by the *electron-transfer recurrence relation* [14,15]

$$\Theta_{i,0,k+1,0}^N = -\frac{bX_{AB} + dX_{CD}}{q} \Theta_{i0k0}^N + \frac{i}{2q} \Theta_{i-1,0,k,0}^N + \frac{k}{2q} \Theta_{i,0,k-1,0}^N - \frac{p}{q} \Theta_{i+1,0,k,0}^N \quad (9.10.27)$$

to be proved shortly. In the final step, we transfer Cartesian powers between the orbitals of the same electron, using the simple two-term *horizontal recurrence relations* [16]:

$$\Theta_{i,j+1,k,l}^N = \Theta_{i+1,j,k,l}^N + X_{AB} \Theta_{ijkl}^N \quad (9.10.28)$$

$$\Theta_{i,j,k,l+1}^N = \Theta_{i,j,k+1,l}^N + X_{CD} \Theta_{ijkl}^N \quad (9.10.29)$$

In this way, we may build up the full set of Cartesian integrals by the use of three sets of recurrence relations, each of which is considerably simpler than the full Obara–Saika scheme. The horizontal recurrences (9.10.28) and (9.10.29) do not involve the orbital exponents and may therefore be applied *after* the transformation of the integrals to the contracted basis, as will be discussed later. In passing, we note that this procedure may also be used for the one-electron integrals, replacing the first step by the similar recurrence relation

$$\Theta_{i+1,0}^N = X_{PA} \Theta_{i0}^N - X_{PC} \Theta_{i0}^{N+1} + \frac{i}{2p} (\Theta_{i-1,0}^N - \Theta_{i-1,0}^{N+1}) \quad (9.10.30)$$

omitting the electron-transfer step, and carrying out the horizontal recursion in the final step

$$\Theta_{i,j+1}^N = \Theta_{i+1,j}^N + X_{AB} \Theta_{ij}^N \quad (9.10.31)$$

using the same notation as for the two-electron integrals. Clearly, in this method, the same set of routines may be used for the one- and two-electron integrals.

We conclude this subsection by deriving the electron-transfer recurrence relation (9.10.27). As in the derivation of the Obara–Saika recurrence relations, we begin by setting up the translational condition on the integrals:

$$\frac{\partial \Theta_{i0k0}^N}{\partial A_x} + \frac{\partial \Theta_{i0k0}^N}{\partial B_x} + \frac{\partial \Theta_{i0k0}^N}{\partial C_x} + \frac{\partial \Theta_{i0k0}^N}{\partial D_x} = 0 \quad (9.10.32)$$

Differentiating each orbital separately, we obtain

$$2a\Theta_{i+1,0,k,0}^N + 2b\Theta_{i1k0}^N + 2c\Theta_{i,0,k+1,0}^N + 2d\Theta_{i0k1}^N - i\Theta_{i-1,0,k,0}^N - k\Theta_{i,0,k-1,0}^N = 0 \quad (9.10.33)$$

Applying the horizontal recurrences (9.2.27), we arrive at the expression

$$2p\Theta_{i+1,0,k,0}^N + 2bX_{AB}\Theta_{i0k0}^N + 2q\Theta_{i,0,k+1,0}^N + 2dX_{CD}\Theta_{i0k0}^N - i\Theta_{i-1,0,k,0}^N - k\Theta_{i,0,k-1,0}^N = 0 \quad (9.10.34)$$

which may be rearranged to yield the transfer relation (9.10.27).

#### 9.10.4 COMPUTATIONAL CONSIDERATIONS FOR THE TWO-ELECTRON INTEGRALS

From our discussion of the Obara–Saika scheme three techniques emerge, differing in the use of the electron-transfer and the horizontal recurrence relations; see Table 9.5. In the OS4 scheme, no use is made of the transfer and horizontal recurrences – the primitive Cartesian integrals  $\Theta_{ijkl}^0$

**Table 9.5** Cost and memory requirements of the two-electron Obara–Saika scheme

	OS4		OS2		OS1	
	Cost	Memory	Cost	Memory	Cost	Memory
Boys functions	$Lp^4$	$Lp^4$	$Lp^4$	$Lp^4$	$Lp^4$	$Lp^4$
Vertical recursion	$L^{13}p^4$	$L^8p^4$	$L^7p^4$	$L^6p^4$	$L^4p^4$	$L^3p^4$
Transfer recursion					$L^6p^4$	$L^6p^4$
Primitive contraction	$L^8p^4$	$L^8$	$L^6p^4$	$L^6$	$L^6p^4$	$L^6$
Horizontal recursion 1			$L^9$	$L^7$	$L^9$	$L^7$
Solid harmonics 1	$L^9$	$L^6$	$L^8$	$L^5$	$L^8$	$L^5$
Horizontal recursion 2				$L^8$	$L^8$	$L^6$
Solid harmonics 2	$L^7$	$L^4$	$L^7$	$L^4$	$L^7$	$L^4$

are generated directly by the Obara–Saika recurrence relations (9.10.24) and (9.10.25) [5]. The cost of the OS4 scheme is high, scaling as  $L^{13}p^4$ , where  $L$  is the angular momentum and  $p$  the number of primitive functions for each contracted orbital. Substantial reductions may be obtained, however, by avoiding unnecessary intermediates in the construction of the integrals.

In the OS2 scheme, we generate the Cartesian integrals of the type  $\Theta_{i0k0}^0$  from the Obara–Saika recurrence relations (9.10.24) and (9.10.25) and the remaining ones by means of the horizontal relations (9.10.28) and (9.10.29) [16]. The OS2 scheme is a substantial improvement on the OS4 scheme, scaling as  $L^7p^4$  in the vertical part and  $L^9$  in the horizontal part. Finally, in the OS1 scheme, we use the electron-transfer as well as the horizontal recurrence relations (as described in Section 9.10.3), generating in the first step integrals of the type  $\Theta_{i000}^0$ . The OS1 scheme appears to be the superior one, at least for orbitals of high angular momentum – the cost of the Obara–Saika step has been reduced to  $L^4p^4$ , whereas the transfer step scales as  $L^6p^4$  and the horizontal step as  $L^9$ .

Comparing the Obara–Saika and McMurchie–Davidson schemes, we find that MD4 scales more favourably than OS4, with a highest cost of  $L^{10}p^4$  (or  $L^8p^4$ ) rather than  $L^{13}p^4$ . However, a simple order analysis (like that carried out here) is not sufficiently detailed to allow us to distinguish between the two schemes except in the limit of high  $L$ . The MD4 scheme involves a rather large number of steps, most of which must be repeated for both electrons. In the OS4 scheme, on the other hand, the key recurrence relations are complicated, involving as many as 15 floating-point operations (9.10.24) compared with 3 in the time-consuming MD4 step (9.9.47). A more satisfactory comparison would require a careful count of all operations.

The MD2 and OS2 schemes are similar, with highest costs of  $L^9p^4$  (or  $L^7p^4$ ) and  $L^9p^2$  for MD2 and  $L^7p^4$  and  $L^9$  for OS2, but both schemes appear to be slower than OS1 for integrals of high angular momentum. At this point, we note that it is perfectly possible to set up an MD1 scheme, where we first generate – by means of the McMurchie–Davidson algorithm – integrals of the type  $\Theta_{i000}^0$  and then proceed exactly as for OS1. Thus, for high angular-momentum functions, the efficiency of the calculation appears to be more dependent on the use of electron-transfer and horizontal recurrence relations than on the type of algorithm used for the generation of Cartesian integrals from the Boys function.

## 9.11 Rys quadrature for Coulomb integrals

In the previous sections, we considered two approaches to the calculation of Coulomb integrals over Gaussian orbitals – the McMurchie–Davidson scheme and the Obara–Saika scheme – both of which employ Boys functions as intermediates. In the present section, a different approach is

explored, in which the construction of the Boys function is bypassed altogether and replaced by a Gaussian-quadrature scheme [10], providing an interesting alternative to the McMurchie–Davidson and Obara–Saika schemes.

### 9.11.1 MOTIVATION FOR THE GAUSSIAN-QUADRATURE SCHEME

In the McMurchie–Davidson and Obara–Saika schemes, the Coulomb integrals are generated as linear combinations of Boys functions  $F_n(x)$  of different orders  $n$ . Referring back to the discussion of these schemes, we find that the two-electron integrals may be written in the form

$$g_{abcd} = \sum_{n=0}^L c_n F_n(\alpha R_{\text{PQ}}^2) \quad (9.11.1)$$

where  $L$  is the sum of the total angular momentum of the four orbitals and where the coefficients  $c_n$  depend on the coordinates and exponents of these orbitals – see, for example, Section 9.10.2. Since the Boys function (9.8.1) is given by

$$F_n(x) = \int_0^1 t^{2n} \exp(-xt^2) dt \quad (9.11.2)$$

we conclude that the two-electron integrals may be written in the form

$$g_{abcd} = \int_0^1 f_L(t^2) \exp(-\alpha R_{\text{PQ}}^2 t^2) dt \quad (9.11.3)$$

where the integrand is an exponential in  $t^2$  times a polynomial of degree  $L$  in  $t^2$

$$f_L(t^2) = \sum_{n=0}^L c_n t^{2n} \quad (9.11.4)$$

According to the discussion in Section 9.6, such integrals can be evaluated exactly by *Gaussian quadrature* over  $L + 1$  points

$$g_{abcd} = \sum_{\kappa=1}^{L+1} w_{\kappa} f_L(t_{\kappa}^2) \quad (9.11.5)$$

where the abscissae  $t_{\kappa}$  and weights  $w_{\kappa}$  are determined by the general rules of Gaussian-quadrature theory. This observation forms the basis for the Rys-polynomial scheme for the evaluation of Coulomb integrals over Gaussian functions [10].

In the following, we shall first show how Gaussian quadrature can be simplified for the special case of even polynomials and weight functions such as those in (9.11.3). The orthogonal polynomials needed for the calculation of Coulomb integrals (9.11.3) are then introduced, and finally we show how a Gaussian-quadrature scheme for the evaluation of Coulomb integrals can be developed based on the McMurchie–Davidson and Obara–Saika schemes.

### 9.11.2 GAUSSIAN QUADRATURE FOR EVEN POLYNOMIALS AND WEIGHT FUNCTIONS

Consider the Gaussian quadrature for integrals such as

$$I_k = \int_{-a}^a f_k(x^2) W(x^2) dx \quad (9.11.6)$$

where  $f_k(x^2)$  is a polynomial of degree  $k$  in  $x^2$  and where the weight function  $W(x^2)$  is symmetric about the origin. According to the general theory of Gaussian quadrature, such integrals can be

evaluated exactly in terms of the roots and weights of a polynomial  $p_n(x)$  of degree  $n > k$ , provided the polynomials satisfy the orthonormality relations

$$\int_{-a}^a p_n(x) p_m(x) W(x^2) dx = \delta_{mn} \quad (9.11.7)$$

In the present subsection, we shall see that the symmetry of the integrand about the origin (9.11.6) reduces the number of quadrature points needed for exact integration by a factor of 2 relative to the requirement  $n > k$ .

In setting up the quadrature scheme for (9.11.6), the orthogonal polynomials  $p_n(x)$  may be generated by a Gram–Schmidt orthogonalization of the monomials  $x^i$  using the inner product (9.11.7). In this process, the inner product between an even function and an odd function vanishes trivially and it follows that  $p_{2n}(x)$  contains only monomials of even degree in  $x$  and that  $p_{2n+1}(x)$  contains only monomials of odd degree in  $x$ . Moreover, the roots of the orthogonal polynomials are distributed symmetrically about the origin – the even polynomial  $p_{2n}(x)$  has  $n$  positive and  $n$  negative roots, whereas the odd polynomial  $p_{2n+1}(x)$  has an additional root at the origin.

The symmetrical distribution of the roots about the origin for  $p_n(x)$  leads to identical weights (9.6.15) at the roots  $x_i$  and  $-x_i$ :

$$\begin{aligned} w_{n;-x_i} &= \int_{-a}^a W(x^2) \prod_{\substack{j=1 \\ x_j \neq -x_i}}^n \frac{x - x_j}{(-x_i) - x_j} dx \\ &= \int_{-a}^a W(x^2) \prod_{\substack{j=1 \\ x_j \neq x_i}}^n \frac{x - (-x_j)}{(-x_i) - (-x_j)} dx = w_{n;x_i} \end{aligned} \quad (9.11.8)$$

The quadrature for (9.11.6) can therefore be reduced to a sum over just the positive roots of a polynomial  $p_n(x)$  of even degree  $n$ . To obtain an exact quadrature for a polynomial  $f_k(x^2)$ , we must – according to the general theory – use a polynomial  $p_n(x)$  with  $n > k$ . The smallest even integer that satisfies this requirement is  $n = 2[k/2] + 2$ . The associated polynomial has  $[k/2] + 1$  positive roots, and we may consequently obtain the integral exactly as

$$\int_{-a}^a f_k(x^2) W(x^2) dx = 2 \sum_{i=1}^{[k/2]+1} w_{2[k/2]+2;i} f_k(x_{2[k/2]+2;i}) \quad (9.11.9)$$

in terms of the positive roots and weights of the polynomial  $p_{2[k/2]+2}(x)$ . We also note that the calculation of the weights can be simplified in the following manner:

$$\begin{aligned} w_{2[k/2]+2;i} &= \int_{-a}^a W(x^2) \prod_{\substack{j=1 \\ j \neq i}}^{2[k/2]+2} \frac{x - x_j}{x_i - x_j} dx \\ &= \int_{-a}^a W(x^2) \frac{x + x_i}{2x_i} \prod_{\substack{j=1 \\ j \neq i}}^{[k/2]+1} \frac{x^2 - x_j^2}{x_i^2 - x_j^2} dx \\ &= \int_0^a W(x^2) \prod_{\substack{j=1 \\ j \neq i}}^{[k/2]+1} \frac{x^2 - x_j^2}{x_i^2 - x_j^2} dx \end{aligned} \quad (9.11.10)$$

where the product is over only the positive roots and the integration over positive  $x$ .

Since only the even polynomials  $p_{2n}(x)$  are needed for the quadrature and since the integration may be restricted to positive  $x$ , we introduce the new polynomials

$$q_n(x) = \sqrt{2} p_{2n}(x) \quad (9.11.11)$$

that satisfy the orthonormality relations

$$\int_0^a q_m(x) q_n(x) W(x^2) dx = \delta_{mn} \quad (9.11.12)$$

Using the  $n$  roots of  $q_n(x)$  in the interval  $[0, a]$  to define the weights as in (9.11.10), we now obtain the following simple expression for the Gaussian quadrature of a polynomial of degree  $k$  in  $x^2$

$$\int_0^a f_k(x^2) W(x^2) dx = \sum_{i=1}^n w_{n;i} f_k(x_{n;i}^2) \quad (9.11.13)$$

where the number of quadrature points is given by

$$n = \left[ \frac{k}{2} \right] + 1 \quad (9.11.14)$$

This result should be contrasted with the general Gaussian-quadrature scheme, which requires  $k + 1$  quadrature points for a general polynomial of degree  $2k$ .

### 9.11.3 RYS POLYNOMIALS AND GAUSS–RYS QUADRATURE

We now return to the Gaussian quadrature of the Coulomb integrals such as that given in (9.11.3):

$$g_{abcd} = \int_0^1 f_L(t^2) \exp(-\alpha R_{PQ}^2 t^2) dt \quad (9.11.15)$$

In accordance with the discussion of Section 9.11.2, we introduce for this purpose the *J-type Rys polynomials*  $J_n^\alpha(x)$  of degree  $n$ , orthonormal on the interval  $[-1, 1]$  with weight function  $\exp(-\alpha x^2)$  [17]:

$$\int_{-1}^1 J_m^\alpha(x) J_n^\alpha(x) \exp(-\alpha x^2) dx = \delta_{mn} \quad (9.11.16)$$

Since only the even members of the J-type Rys polynomials are needed, we also introduce the *R-type Rys polynomials* of degree  $2n$  [17]

$$R_n^\alpha(x) = \sqrt{2} J_{2n}^\alpha(x) \quad (9.11.17)$$

which are orthogonal on the interval  $[0, 1]$  with weight function  $\exp(-\alpha x^2)$ :

$$\int_0^1 R_m^\alpha(x) R_n^\alpha(x) \exp(-\alpha x^2) dx = \delta_{mn} \quad (9.11.18)$$

In terms of the roots and weights of these polynomials, we may write the Coulomb integrals as

$$\int_0^1 f_L(x^2) \exp(-\alpha x^2) dx = \sum_{i=1}^n w_{n;i} f_L(x_{n;i}^2) \quad (9.11.19)$$

where the number of quadrature points is given by

$$n = \left[ \frac{L}{2} \right] + 1 \quad (9.11.20)$$

as discussed in Section 9.11.2.

The weight function of the Rys polynomials  $J_n^\alpha(x)$  and  $R_n^\alpha(x)$  depends on the real parameter  $\alpha \geq 0$ . These polynomials consequently constitute a manifold of polynomials, one for each  $\alpha$ . In Figure 9.10, we have plotted the first four Rys polynomials for several values of the weight parameter  $\alpha$ . As  $\alpha$  increases, the Rys roots shift towards the origin. At  $\alpha = 0$ , the weight function becomes equal to unity and the Rys polynomials turn into the scaled Legendre polynomials (9.6.2)

$$J_n^0(x) = \sqrt{\frac{2n+1}{2}} P_n(x) \quad (9.11.21)$$

On the other hand, in the limit as  $\alpha$  tends to infinity, we may in (9.11.16) integrate over the full set of real numbers and the Rys polynomials may then be related to the Hermite functions as

$$J_n^\alpha(x) \approx \frac{1}{\sqrt{2^n n!}} \left( \frac{\alpha}{\pi} \right)^{1/4} H_n(\sqrt{\alpha}x) \quad (\text{large } \alpha) \quad (9.11.22)$$

From these expressions, we conclude that the roots of the Rys polynomials coincide with the roots of the Legendre polynomials for  $\alpha = 0$  and with the scaled roots of the Hermite polynomials for large  $\alpha$ :

$$x_{n;i}^J = x_{n;i}^L \quad (\alpha = 0) \quad (9.11.23)$$

$$x_{n;i}^J \approx \alpha^{-1/2} x_{n;i}^H \quad (\text{large } \alpha) \quad (9.11.24)$$

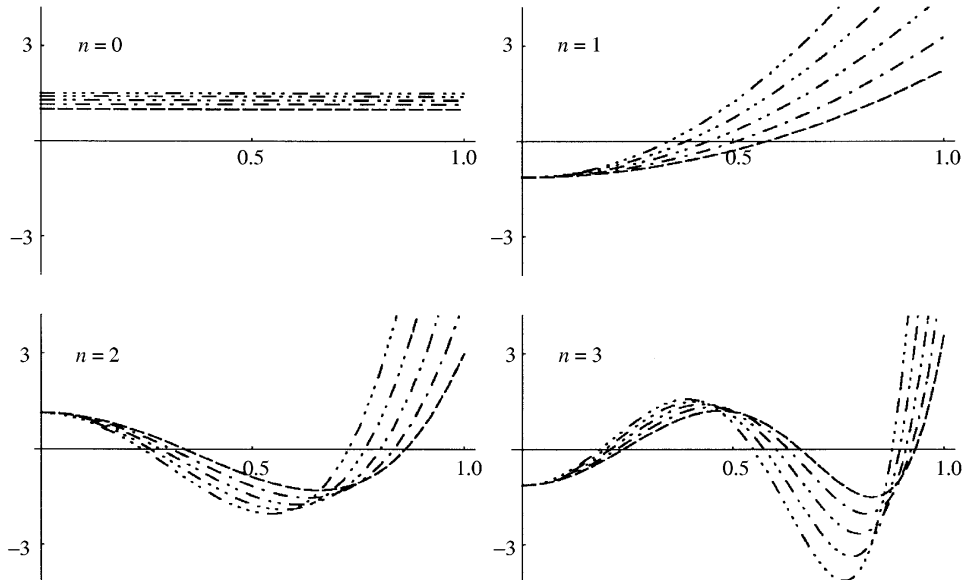


**Fig. 9.10.** The Rys polynomials  $R_n^\alpha(x)$  of degree  $2n \leq 6$  for  $\alpha = 0, 1, 2, 3, 4$ , with the number of consecutive dots in the lines increasing with  $\alpha$ .

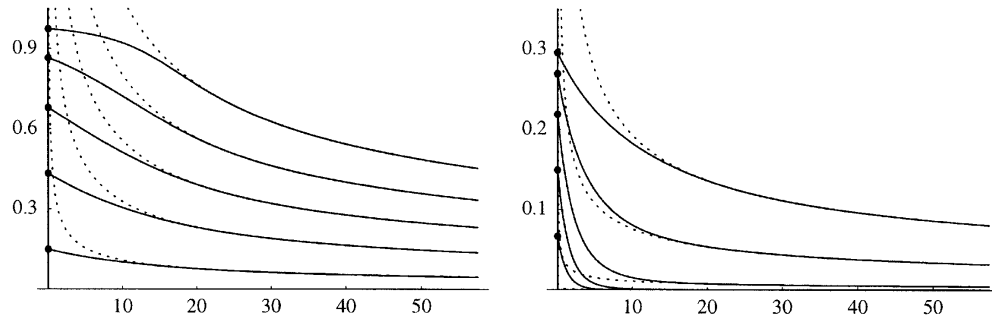


**Fig. 9.11.** The roots and weights of the Rys polynomials  $R_5^\alpha(x)$ . On the left, the roots of  $R_5^\alpha(x)$  have been plotted as functions  $\alpha$ ; the dotted lines represent the five positive roots of  $H_{10}(\sqrt{\alpha}x)$  and the dots at  $\alpha = 0$  the five positive roots of  $L_{10}(x)$ . On the right, the weights of  $R_5^\alpha(x)$  have been plotted as functions  $\alpha$ ; the dotted lines represent the corresponding five weights of  $H_{10}(\sqrt{\alpha}x)$  and the dots at  $\alpha = 0$  the five weights of  $L_{10}(x)$ .

These relationships are illustrated in Figure 9.11, where, in the left-hand plot, we have plotted the five roots of the Rys polynomials  $R_5^\alpha(x)$  as a function of  $\alpha$ , superimposed on the positive roots of the Hermite polynomial  $H_{10}(\sqrt{\alpha}x)$  multiplied by  $\alpha^{-1/2}$  (dotted lines) and with the positive roots of the Legendre polynomial  $L_{10}(x)$  indicated with black dots at  $\alpha = 0$ .

The weights of the Rys polynomials are related to the weights of the Legendre and Hermite polynomials in the same manner as for the roots (9.11.23) and (9.11.24)

$$w_{n,i}^J = w_{n,i}^L \quad (\alpha = 0) \quad (9.11.25)$$

$$w_{n,i}^J \approx \alpha^{-1/2} w_{n,i}^H \quad (\text{large } \alpha) \quad (9.11.26)$$

as may be ascertained by considering (9.6.15). On the right in Figure 9.11, we have drawn a plot of the Rys weights of  $R_5^\alpha(x)$  analogous to the left-hand plot of the roots. Clearly, for  $\alpha = 0$ , we may obtain the roots and weights from the Legendre polynomials and, for large  $\alpha$ , the roots and the weights are obtained by a simple scaling of the Hermite roots and weights. In the intermediate region, a more elaborate technique must be employed, based, for example, on the use of Taylor expansions or Chebyshev polynomials. Thus, the evaluation of the roots and weights of the Rys polynomials proceeds in a similar manner as for the Boys function in Section 9.8.2, where the short- and long-range forms are obtained in a simple manner and more elaborate techniques must be used in the intermediate region.

#### 9.11.4 THE RYS SCHEME FOR HERMITE COULOMB INTEGRALS

Having introduced and discussed the Rys polynomials, we are now in a position to consider the evaluation of Hermite Coulomb integrals by Gaussian quadrature. In this subsection, we consider the one-electron Hermite Coulomb integrals (9.9.9)

$$R_{tuv}(p, \mathbf{R}_{\text{PC}}) = \left( \frac{\partial}{\partial P_x} \right)^t \left( \frac{\partial}{\partial P_y} \right)^u \left( \frac{\partial}{\partial P_z} \right)^v F_0(pR_{\text{PC}}^2) \quad (9.11.27)$$

which may be calculated recursively as discussed in Section 9.9.2. The calculation of the corresponding two-electron integrals of the form  $R_{tuv}(\alpha, \mathbf{R}_{\text{PQ}})$  may be carried out in exactly the same manner, replacing  $p$  by  $\alpha$  and  $\mathbf{C}$  by  $\mathbf{Q}$ .

Inserting the definition of the Boys function (9.8.1) in (9.11.27), we may write the Hermite integral in the following manner:

$$R_{tuv}(p, \mathbf{R}_{\text{PC}}) = \int_0^1 \left( \frac{\partial}{\partial P_x} \right)^t \left( \frac{\partial}{\partial P_y} \right)^u \left( \frac{\partial}{\partial P_z} \right)^v \exp(-pR_{\text{PC}}^2 s^2) ds \quad (9.11.28)$$

We now introduce the auxiliary polynomials

$$\bar{H}_t(s^2) = \exp(pX_{\text{PC}}^2 s^2) \left( \frac{\partial}{\partial P_x} \right)^t \exp(-pX_{\text{PC}}^2 s^2) \quad (9.11.29)$$

These polynomials, which are of degree  $t$  in  $s^2$ , are related to the Hermite polynomials by

$$\bar{H}_t(s^2) = (-\sqrt{p}s)^t H_t(\sqrt{p}X_{\text{PC}} s) \quad (9.11.30)$$

as may be verified using the Rodrigues expression (6.6.29). In terms of the modified Hermite polynomials (9.11.29) and their counterparts for the  $y$  and  $z$  directions, we may write the Hermite integrals as

$$R_{tuv}(p, \mathbf{R}_{\text{PC}}) = \int_0^1 \bar{H}_t(s^2) \bar{H}_u(s^2) \bar{H}_v(s^2) \exp(-pR_{\text{PC}}^2 s^2) ds \quad (9.11.31)$$

This expression is in the appropriate form for Gauss–Rys quadrature (9.11.19) and may thus be evaluated exactly as

$$R_{tuv}(p, \mathbf{R}_{\text{PC}}) = \sum_{\kappa=1}^{\gamma} w_{\kappa} \bar{H}_t(s_{\kappa}^2) \bar{H}_u(s_{\kappa}^2) \bar{H}_v(s_{\kappa}^2) \quad (9.11.32)$$

where the number of quadrature points is given by

$$\gamma = \left[ \frac{t+u+v}{2} \right] + 1 \quad (9.11.33)$$

and where  $s_{\kappa}$  and  $w_{\kappa}$  are the abscissae and weights of the Rys polynomial  $R_{\gamma}^{\alpha}(s)$  with

$$\alpha = pR_{\text{PC}}^2 \quad (9.11.34)$$

To complete the evaluation of the Hermite integrals by Rys quadrature, we must derive a scheme for the evaluation of the modified Hermite polynomials.

To evaluate the modified Hermite polynomials (9.11.29) for a given argument  $s$ , we shall employ a recursive scheme. Incrementing  $t$  by 1, we obtain

$$\begin{aligned} \bar{H}_{t+1}(s^2) &= \exp(pX_{\text{PC}}^2 s^2) \left( \frac{\partial}{\partial P_x} \right)^{t+1} \exp(-pX_{\text{PC}}^2 s^2) \\ &= -2ps^2 \exp(pX_{\text{PC}}^2 s^2) \left( \frac{\partial}{\partial P_x} \right)^t X_{\text{PC}} \exp(-pX_{\text{PC}}^2 s^2) \end{aligned} \quad (9.11.35)$$

Using (9.9.17), we arrive at the recurrence relation [18]

$$\bar{H}_{t+1}(s^2) = -2ps^2 [X_{\text{PC}} \bar{H}_t(s^2) + t \bar{H}_{t-1}(s^2)] \quad (9.11.36)$$

Starting from the polynomial

$$\bar{H}_0(s^2) = 1 \quad (9.11.37)$$

we may use (9.11.36) to generate  $\bar{H}_t(s^2)$  for a given argument  $s$  and a given degree  $t$ . The recurrences for the  $y$  and  $z$  directions are similar, replacing  $X_{\text{PC}}$  by  $Y_{\text{PC}}$  and  $Z_{\text{PC}}$ , respectively. Note the similarity with (9.9.18).

In the two-electron case, we may calculate the Hermite integrals in the same manner

$$R_{tuv}(\alpha, \mathbf{R}_{\text{PQ}}) = \sum_{\kappa=1}^{\gamma} w_{\kappa} \bar{H}_t(s_{\kappa}^2) \bar{H}_u(s_{\kappa}^2) \bar{H}_v(s_{\kappa}^2) \quad (9.11.38)$$

using the recurrence relation [18]

$$\bar{H}_{t+1}(s^2) = -2\alpha s^2 [X_{\text{PQ}} \bar{H}_t(s^2) + i \bar{H}_{t-1}(s^2)] \quad (9.11.39)$$

and similarly for the other directions.

### 9.11.5 THE RYS SCHEME FOR CARTESIAN COULOMB INTEGRALS

To calculate the one-electron Coulomb integrals by Rys quadrature, we write the integrals in the standard McMurchie–Davidson form (9.9.32)

$$V_{ijklmn}^{000} = \frac{2\pi}{p} \sum_{tuv} E_t^{ij} E_u^{kl} E_v^{mn} R_{tuv}(p, \mathbf{R}_{\text{PC}}) \quad (9.11.40)$$

Inserting the quadrature expression (9.11.32) in (9.11.40), we obtain

$$V_{ijklmn}^{000} = \frac{2\pi}{p} \sum_{\kappa=1}^{\gamma} w_{\kappa} \sum_{tuv} E_t^{ij} E_u^{kl} E_v^{mn} \bar{H}_t(s_{\kappa}^2) \bar{H}_u(s_{\kappa}^2) \bar{H}_v(s_{\kappa}^2) \quad (9.11.41)$$

This expression may be rearranged to give

$$V_{ijklmn}^{000} = \frac{2\pi}{p} \sum_{\kappa=1}^{\gamma} w_{\kappa} I_{ij}(s_{\kappa}^2) I_{kl}(s_{\kappa}^2) I_{mn}(s_{\kappa}^2) \quad (9.11.42)$$

where we have introduced the one-dimensional Cartesian integrals

$$I_{ij}(s^2) = \sum_t E_t^{ij} \bar{H}_t(s^2) \quad (9.11.43)$$

$$I_{kl}(s^2) = \sum_u E_u^{kl} \bar{H}_u(s^2) \quad (9.11.44)$$

$$I_{mn}(s^2) = \sum_v E_v^{mn} \bar{H}_v(s^2) \quad (9.11.45)$$

Equation (9.11.42) constitutes the final expression for the one-electron Coulomb integrals in the Rys scheme [10].

We have now developed a complete scheme for the evaluation of one-electron Coulomb integrals by Gaussian quadrature. First, we calculate (by some numerical scheme) the abscissae and weights

of the Rys polynomial of degree

$$\gamma = \left[ \frac{L}{2} \right] + 1 \quad (9.11.46)$$

where  $L$  is the sum of the quantum numbers of the two orbitals (which is the same for all orbitals in the same shell)

$$L = i + j + k + l + m + n \quad (9.11.47)$$

Next, at each abscissa, we calculate the modified Hermite polynomials (9.11.30) using the recurrence relations (9.11.36). The resulting polynomial values are then contracted with the Hermite-to-Cartesian expansion coefficients, yielding the one-dimensional Cartesian integrals (9.11.43)–(9.11.45). The expansion coefficients, which may be obtained from the two-term recurrence relations (9.5.15)–(9.5.17), are the same for all the abscissae. The final Cartesian one-electron Coulomb integral is obtained by carrying out the summation (9.11.42).

The two-electron integrals are obtained in the same manner. Starting from (9.9.33), we obtain the expression [10]

$$g_{abcd} = \frac{2\pi^{5/2}}{pq\sqrt{p+q}} \sum_{\kappa=1}^{\gamma} w_{\kappa} I_x(s_{\kappa}^2) I_y(s_{\kappa}^2) I_z(s_{\kappa}^2) \quad (9.11.48)$$

The two-dimensional Cartesian integrals are given by

$$I_x(s^2) = \sum_{tt} (-1)^t E_t^{i_x j_x} E_t^{k_x l_x} \bar{H}_{t+\tau}(s^2) \quad (9.11.49)$$

$$I_y(s^2) = \sum_{uv} (-1)^u E_u^{i_y j_y} E_v^{k_y l_y} \bar{H}_{u+v}(s^2) \quad (9.11.50)$$

$$I_z(s^2) = \sum_{v\phi} (-1)^{\phi} E_v^{i_z j_z} E_{\phi}^{k_z l_z} \bar{H}_{v+\phi}(s^2) \quad (9.11.51)$$

and are evaluated in terms of the modified Hermite polynomials, obtained by using recurrence relations such as (9.11.39). The number of quadrature points is again obtained from (9.11.46), where  $L$  is now the sum of the quantum numbers for all four orbitals. Thus, there is one quadrature point for (ssss) and (psss) integrals, two quadrature points for (ppss) and (ppps) integrals, three for a (pppp) integral, and so on. In general, for an integral with all orbitals of angular momentum  $l$ , the number of quadrature points is equal to  $2l + 1$ ; therefore, we must calculate  $2l + 1$  abscissae and  $2l + 1$  weights. These numbers should be compared with the number of Boys-function evaluations needed for the same integral ( $4l + 1$ ).

### 9.11.6 OBARA–SAIKA RECURSION FOR THE TWO-DIMENSIONAL RYS INTEGRALS

In the Rys-quadrature scheme presented above, the one- and two-dimensional integrals were calculated using the McMurchie–Davidson scheme. These integrals may also be obtained from the Obara–Saika scheme, as we shall now discuss.

Let us first consider the one-dimensional integrals needed for the one-electron Coulomb integral. For the  $x$  direction, these are given by (9.11.43)

$$I_{ij}(s^2) = \sum_t E_t^{ij} \bar{H}_t(s^2) \quad (9.11.52)$$

We proceed in the same manner as in Section 9.10.1. Incrementing the first index and using the recurrence relation (9.5.20), we obtain

$$I_{i+1,j} = X_{\text{PA}} I_{ij} + \frac{1}{2p} (iI_{i-1,j} + jI_{i,j-1}) + \frac{1}{2p} \sum_t E_t^{ij} \bar{H}_{t+1} \quad (9.11.53)$$

where we have omitted the argument  $s^2$  and have substituted  $t$  for  $t - 1$  in the summation. Next, we invoke the recurrence relation (9.11.36)

$$I_{i+1,j} = X_{\text{PA}} I_{ij} + \frac{1}{2p} (iI_{i-1,j} + jI_{i,j-1}) - s^2 X_{\text{PC}} I_{ij} - \frac{s^2}{2p} \sum_t 2pt E_t^{ij} \bar{H}_{t-1} \quad (9.11.54)$$

and finally the identity (9.5.14). We then arrive at the following recurrence relations for the one-dimensional integrals [19]

$$I_{i+1,j} = (X_{\text{PA}} - s^2 X_{\text{PC}}) I_{ij} + \frac{1}{2p} (1 - s^2) (iI_{i-1,j} + jI_{i,j-1}) \quad (9.11.55)$$

$$I_{i,j+1} = (X_{\text{PB}} - s^2 X_{\text{PC}}) I_{ij} + \frac{1}{2p} (1 - s^2) (iI_{i-1,j} + jI_{i,j-1}) \quad (9.11.56)$$

where the latter relation is obtained from (9.11.55) by using (9.5.9). Starting from the integral

$$I_{00} = K_{ab}^x \quad (9.11.57)$$

we may then generate the full set of one-dimensional integrals needed for Rys quadrature. The one-dimensional recurrence relations (9.11.55) and (9.11.56) should be compared with their three-dimensional counterparts (9.10.8) and (9.10.9). We note that increments in the upper index for the three-dimensional integrals have been replaced by multiplication by a factor of  $s^2$  for the one-dimensional ones.

The recurrence relations for the two-dimensional two-electron integrals are worked out in the same manner. Consider the integral (9.11.49) for the  $x$  direction

$$I_{ijkl} = \sum_{t\tau} (-1)^\tau E_t^{ij} E_\tau^{kl} \bar{H}_{t+\tau} \quad (9.11.58)$$

Incrementing the first index and invoking the recurrence relation (9.5.20), we obtain

$$I_{i+1,j,k,l} = X_{\text{PA}} I_{ijkl} + \frac{1}{2p} (iI_{i-1,j,k,l} + jI_{i,j-1,k,l}) + \frac{1}{2p} \sum_{t\tau} (-1)^\tau E_t^{ij} E_\tau^{kl} \bar{H}_{t+\tau+1} \quad (9.11.59)$$

The recurrence relation for the modified Hermite polynomials (9.11.39) in the form

$$\bar{H}_{t+\tau+1} = -2\alpha s^2 [X_{\text{PQ}} \bar{H}_{t+\tau} + (t + \tau) \bar{H}_{t+\tau-1}] \quad (9.11.60)$$

gives us

$$\begin{aligned} I_{i+1,j,k,l} &= (X_{\text{PA}} - \frac{\alpha}{p} s^2 X_{\text{PQ}}) I_{ijkl} + \frac{1}{2p} (iI_{i-1,j,k,l} + jI_{i,j-1,k,l}) \\ &\quad - \frac{\alpha}{p} s^2 \sum_{t\tau} (-1)^\tau t E_t^{ij} E_\tau^{kl} \bar{H}_{t+\tau-1} - \frac{\alpha}{p} s^2 \sum_{t\tau} (-1)^\tau E_t^{ij} \tau E_\tau^{kl} \bar{H}_{t+\tau-1} \end{aligned} \quad (9.11.61)$$

Finally, for the last two terms, we employ (9.5.17) and obtain the following recurrence relation for increments in the first index [19]:

$$\begin{aligned} I_{i+1,j,k,l} = & \left( X_{PA} - \frac{\alpha}{p} X_{PQ} s^2 \right) I_{ijkl} + \frac{1}{2p} \left( 1 - \frac{\alpha}{p} s^2 \right) (iI_{i-1,j,k,l} + jI_{i,j-1,k,l}) \\ & + \frac{s^2}{2(p+q)} (kI_{i,j,k-1,l} + lI_{i,j,k,l-1}) \end{aligned} \quad (9.11.62)$$

The corresponding recurrence relation for increments in the second index is identical except that  $X_{PA}$  is replaced by  $X_{PB}$ . The recurrence relation for increments in the third index is obtained from (9.11.62) by interchange of the quantities that refer to particles 1 and 2:

$$\begin{aligned} I_{i,j,k+1,l} = & \left( X_{QC} + \frac{\alpha}{q} X_{PQ} s^2 \right) I_{ijkl} + \frac{1}{2q} \left( 1 - \frac{\alpha}{q} s^2 \right) (kI_{i,j,k-1,l} + lI_{i,j,k,l-1}) \\ & + \frac{s^2}{2(p+q)} (iI_{i-1,j,k,l} + jI_{i,j-1,k,l}) \end{aligned} \quad (9.11.63)$$

and, for the fourth index, we simply replace  $X_{QC}$  by  $X_{QD}$ . Comparing the recurrence relations (9.11.62) and (9.11.63) with the Obara–Saika recurrences for the six-dimensional integrals (9.10.24) and (9.10.25), we find (as in the one-electron case) that increments in the upper index of the six-dimensional integrals have been replaced by multiplication by the factor  $s^2$  in the two-dimensional integrals.

It is of course possible to simplify the recurrence relations for the two-dimensional two-electron integrals considerably by considering only the integrals  $I_{i0k0}$ . We then obtain the following two recurrence relations [19]

$$I_{i+1,0,k,0} = \left( X_{PA} - \frac{\alpha}{p} s^2 X_{PQ} \right) I_{i0k0} + \frac{1}{2p} \left( 1 - \frac{\alpha}{p} s^2 \right) iI_{i-1,0,k,0} + \frac{s^2}{2(p+q)} kI_{i,0,k-1,0} \quad (9.11.64)$$

$$I_{i,0,k+1,0} = \left( X_{QC} + \frac{\alpha}{q} s^2 X_{PQ} \right) I_{i0k0} + \frac{1}{2q} \left( 1 - \frac{\alpha}{q} s^2 \right) kI_{i,0,k-1,0} + \frac{s^2}{2(p+q)} iI_{i-1,0,k,0} \quad (9.11.65)$$

The remaining integrals may then be generated by the standard horizontal recurrence relations. Also, we may specialize (9.11.64) to integrals of the form  $I_{i000}$ , resulting in a simple two-term recurrence relation; the final integrals are then obtained using an electron-transfer relation. Finally, we note that there is no need to carry out either the horizontal or the electron-transfer relations until after the six-dimensional integrals have been calculated.

### 9.11.7 COMPUTATIONAL CONSIDERATIONS FOR THE TWO-ELECTRON INTEGRALS

Just as in the Obara–Saika scheme, we may set up three different algorithms for the evaluation of two-electron integrals by the Rys scheme. In the R4 scheme, we use the four-index recurrence relations such as (9.11.62) and (9.11.63) to generate the two-dimensional integrals (9.11.49)–(9.11.51) at each of the  $\gamma$  abscissae; the final six-dimensional Cartesian integrals are then obtained from the quadrature formula (9.11.48) [10]. In the R2 scheme, we first use the simpler two-index recurrence relations (9.11.64) and (9.11.65) for the two-dimensional integrals; next, we generate by quadrature six-dimensional Cartesian integrals with the angular momentum distributed between two orbitals only; in the final step, we invoke the horizontal recurrence relations to distribute the

**Table 9.6** Cost and memory requirements of the two-electron Rys scheme

	R4		R2		R1	
	Cost	Memory	Cost	Memory	Cost	Memory
Rys weights and roots	$Lp^4$	$Lp^4$	$Lp^4$	$Lp^4$	$Lp^4$	$Lp^4$
2-D integrals	$L^5 p^4$	$L^5 p^4$	$L^3 p^4$	$L^3 p^4$	$L^2 p^4$	$L^2 p^4$
6-D integrals	$L^9 p^4$	$L^8 p^4$	$L^7 p^4$	$L^6 p^4$	$L^4 p^4$	$L^3 p^4$
Transfer recursion					$L^6 p^4$	$L^6 p^4$
Primitive contraction	$L^8 p^4$	$L^8$	$L^6 p^4$	$L^6$	$L^6 p^4$	$L^6$
Horizontal recursion 1			$L^9$	$L^7$	$L^9$	$L^7$
Solid harmonics 1	$L^9$	$L^6$	$L^8$	$L^5$	$L^8$	$L^5$
Horizontal recursion 2			$L^8$	$L^6$	$L^8$	$L^6$
Solid harmonics 2	$L^7$	$L^4$	$L^7$	$L^4$	$L^7$	$L^4$

angular momentum among all four orbitals [19]. In the R1 scheme, we first generate one-index two-dimensional integrals; next, we generate from these integrals six-dimensional Cartesian integrals with the angular momentum on only one orbital; the final integrals are then obtained by distributing the angular momentum using the electron-transfer recurrence relations and finally the horizontal recurrence relations [15]. The cost of these different schemes is given in Table 9.6.

Comparing with the McMurchie–Davidson scheme in Section 9.9.6 and the Obara–Saika scheme in Section 9.10.4, we note that the cost scales in the same manner for the schemes that employ the electron-transfer relation – the MD1, OS1 and R1 schemes, all of which are dominated by the electron-transfer step ( $L^6 p^4$ ) and by the horizontal step ( $L^9$ ). For high angular momentum, these appear to be the preferred schemes – in particular the Obara–Saika scheme, which involves a smaller number of steps.

Comparing the vertical–horizontal schemes MD2, OS2 and R2, we note that these perform similarly ( $L^9 p^4 + L^9 p^2$  or  $L^7 p^4 + L^9 p^2$  for MD2, and  $L^7 p^4 + L^9$  for OS2 and R2) and a more careful analysis is needed to distinguish between them. Finally, for the schemes that do not employ either the transfer or the horizontal recurrences, the cost is similar for MD4 ( $L^{10} p^4$  or  $L^8 p^4$ ) and R4 ( $L^9 p^4$ ) and less favourable for OS4 ( $L^{13} p^4$ ).

## 9.12 Scaling properties of the molecular integrals

Using the techniques developed in the preceding sections, the molecular integrals may be calculated to any desired accuracy. In practice, however, we are interested in calculating the integrals to some fixed absolute accuracy, discarding all integrals whose magnitude is smaller than the allowed error. In large systems, in particular, most integrals are small and it becomes imperative to detect these integrals in advance so that their evaluation can be avoided. In the present section, we shall examine molecular integrals in large systems – in particular, their scaling properties (i.e. the dependence of the number of significant integrals on the size of the system) and techniques for their pre-screening.

### 9.12.1 LINEAR SCALING OF THE OVERLAP AND KINETIC-ENERGY INTEGRALS

To study the scaling properties of the integrals, we consider a linear model system consisting of  $n$  hydrogen atoms, separated from one another by  $1a_0$ . To each atom, we attach a single primitive Gaussian 1s function of unit exponent. In Figure 9.12, we have plotted, for this model system, the number of overlap, kinetic-energy, nuclear-attraction, and electron-repulsion integrals as a function of  $n$ . Full lines are used for the total number of integrals and dotted lines for the number

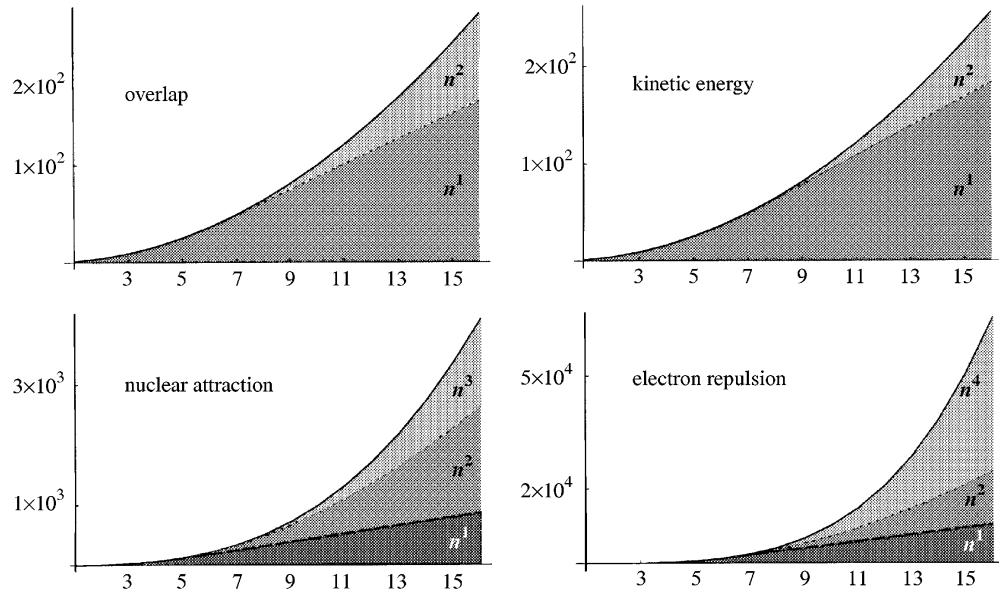


**Fig. 9.12.** The scaling properties of the molecular integrals. The full line represents the total number of integrals as a function of  $n$ , where  $n$  is the number of 1s AOs of unit exponent in a linear system of  $n$  hydrogen atoms, separated from one another by  $1a_0$ . The dotted line represents the number of significant integrals (i.e. integrals larger than  $10^{-10}$  in magnitude). Finally, for the Coulomb integrals, the dashed line represents the number of integrals that cannot be calculated classically (by multipole expansions) since their charge distributions overlap. Note the differences in the vertical scales (approximately  $10^2$ ,  $10^2$ ,  $10^3$  and  $10^4$ ), which reflect the different scaling properties of the integrals.

of significant integrals, which we here take to be integrals larger than  $10^{-10}$  in magnitude. For small  $n$ , all integrals are significant and must be calculated. However, as the number of atoms increases, many of the integrals become insignificant and may be neglected when the calculations are carried out to a given finite precision.

Let us consider the overlap integrals. For our model system consisting of  $n$  atoms, the total number of overlap integrals is equal to  $n^2$ . Thus, formally at least, the number of overlap integrals scales quadratically with the size of the system, as indicated by the full line in Figure 9.12. However, as seen from the dotted line in the same figure, the number of *significant* integrals scales only *linearly* with the size of the system. To understand how this linear dependence on the size of the system arises, consider the expression for the overlap between two Gaussian  $s$  functions (9.2.41):

$$S_{ab} = \left( \frac{\pi}{a+b} \right)^{3/2} \exp \left( -\frac{ab}{a+b} R_{AB}^2 \right) \quad (9.12.1)$$

This integral decreases exponentially with the square of the distance between the functions. To determine the distance  $d_s$  where this integral becomes smaller than  $10^{-k}$ , we consider the Gaussian with the smallest exponent  $a_{\min}$ . Some simple algebra then shows that all  $s$  functions separated by more than

$$d_s = \sqrt{a_{\min}^{-1} \log \left[ \left( \frac{\pi}{2a_{\min}} \right)^3 10^{2k} \right]} \quad (9.12.2)$$

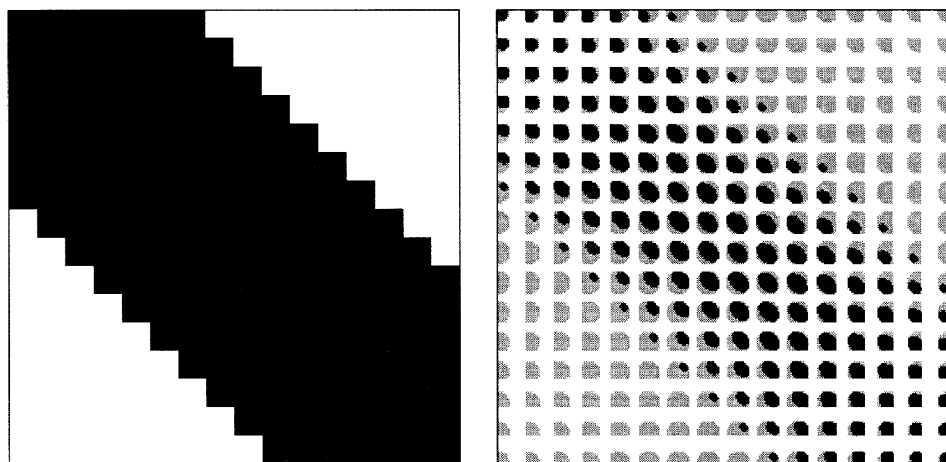


**Fig. 9.13.** The sparsity of the  $16 \times 16$  overlap matrix (left) and the  $256 \times 256$  electron-repulsion matrix (right) for a linear model system of 16 Gaussian  $1s$  functions of unit exponent, separated from one another by  $1a_0$ . In the overlap matrix, the significant integrals (i.e. integrals larger than  $10^{-10}$ ) appear in black and the remaining, insignificant integrals in white. In the electron-repulsion matrix, the nonclassical significant integrals appear in black, the classical significant integrals in grey and the insignificant integrals in white.

are smaller than  $10^{-k}$  in magnitude. In particular, in our model system (where the exponents are all equal to 1), all overlaps for functions separated by more than  $6.9a_0$  will be smaller than  $10^{-10}$ , giving rise to the banded matrix in Figure 9.13. Clearly, as the length of the chain increases, there is a crossover point, beyond which the number of significant overlap integrals increases only linearly with the size of the system. In our model, this crossover occurs for systems containing about seven atoms – see Figure 9.12.

In a more realistic system, the AOs will be less uniformly distributed in space and there will be a range of orbital exponents. The crossover to linear scaling will then be less sharply defined. Nevertheless, for any molecular system, there will be a characteristic distance  $d_s$  beyond which all overlap integrals are negligible. When the size of the system increases beyond  $d_s$ , the amount of work required for the evaluation of the overlap integrals will begin to increase linearly with the size of the system – provided, of course, that the evaluation of the insignificant integrals is avoided by the application of some screening mechanism such as testing against  $d_s$ .

Since the kinetic-energy integrals are fixed linear combinations of overlap integrals (of higher angular momentum), there will also be a characteristic distance beyond which all kinetic-energy integrals are negligible, leading to linear scaling for these integrals as well – see Figure 9.12. For the kinetic-energy integrals, the crossover to linear scaling appears to occur somewhat later than for the overlap integrals.

### 9.12.2 QUADRATIC SCALING OF THE COULOMB INTEGRALS

Having considered the scaling properties of the overlap and kinetic-energy integrals, we now turn our attention to the Coulomb integrals and, in particular, to the two-electron integrals. For  $s$  orbitals (the only orbitals present in our model system), we may write the two-electron Coulomb integrals in the form

$$g_{abcd} = \sqrt{\frac{4\alpha}{\pi}} S_{ab} S_{cd} F_0(\alpha R_{PQ}^2) \quad (9.12.3)$$

which is the generalization of (9.7.24) to unnormalized charge distributions, obtained by using the Gaussian product rule (9.2.10) for the overlap distributions and then (9.12.1) and (9.7.24). We recall here that  $R_{PQ}$  is the separation between the overlap distributions of the two electrons and that  $\alpha$  is the reduced exponent  $pq/(p+q)$ . To study the scaling properties of the two-electron integrals, we note that the integral (9.12.3) is bounded by

$$g_{abcd} \leq \min \left( \sqrt{\frac{4\alpha}{\pi}} S_{ab} S_{cd}, \frac{S_{ab} S_{cd}}{R_{PQ}} \right) \quad (9.12.4)$$

where the first upper bound represents the short-range limit and the second bound the long-range limit. These bounds for the integrals follow from the corresponding upper bounds to the Boys function (9.8.7) and (9.8.10).

For small systems, all integrals are significant (in the absence of symmetries) and the number of two-electron integrals increases as  $n^4$ . However, when the system increases beyond  $d_s$  and the number of significant overlap integrals begins to increase as  $n$ , the number of significant two-electron integrals will begin to increase as  $n^2$  [20]. This crossover from quartic to *quadratic scaling* is clearly seen in Figure 9.12. In Figure 9.13, we have depicted the sparse structure of the two-electron integral matrix for  $n = 16$ , with the significant integrals shaded in grey or black, depending on whether they represent classical or nonclassical interactions as explained in Section 9.12.3.

From the long-range upper bound in (9.12.4), we conclude that the number of significant two-electron integrals should eventually increase *linearly* with the size of the system. However, for this to happen, the system must become truly macroscopic in size, with typical separations  $R_{PQ}$  greater than  $1 \text{ m} \approx 10^{10} a_0$ . For all practical purposes, therefore, the number of significant two-electron integrals will depend at least quadratically on the size of the system.

### 9.12.3 LINEAR SCALING OF THE NONCLASSICAL COULOMB INTEGRALS

Although, in large molecular systems, the number of significant two-electron integrals increases quadratically with the size of the system, most of these integrals represent classical interactions between disjoint charge distributions. To discuss the classical and nonclassical interactions, we first rewrite the two-electron integrals (9.12.3) in terms of the error function (9.8.22). Using (9.8.24), we obtain

$$g_{abcd} = \operatorname{erf}(\sqrt{\alpha} R_{PQ}) \frac{S_{ab} S_{cd}}{R_{PQ}} \quad (9.12.5)$$

Next, introducing the complementary error function (9.8.27), we decompose the two-electron integral as

$$g_{abcd} = g_{abcd}^{\text{cls}} + g_{abcd}^{\text{non}} \quad (9.12.6)$$

where the *classical* and *nonclassical contributions* are given by

$$g_{abcd}^{\text{cls}} = \frac{S_{ab} S_{cd}}{R_{PQ}} \quad (9.12.7)$$

$$g_{abcd}^{\text{non}} = -\operatorname{erfc}(\sqrt{\alpha} R_{PQ}) \frac{S_{ab} S_{cd}}{R_{PQ}} \quad (9.12.8)$$

For small  $R_{PQ}$ , the classical and nonclassical contributions are both large, even when the integral  $g_{abcd}$  itself is small. Thus, as  $R_{PQ}$  tends to zero, the total integral represents a small difference

between a classical term and a nonclassical one, both of which tend to infinity. By contrast, for large  $R_{PQ}$ , the complementary error function in (9.12.8) vanishes according to (9.8.32) and the Coulomb interaction is dominated by the classical contribution (9.12.7). In large systems, therefore, most of the two-electron integrals will represent such purely classical interactions.

From the upper bound to the complementary error function (9.8.32), we find that the nonclassical contribution to the two-electron integrals is bounded by

$$|g_{abcd}^{\text{non}}| \leq S_{ab}S_{cd} \frac{\exp(-\alpha R_{PQ}^2)}{\sqrt{\pi\alpha R_{PQ}^2}} \quad (9.12.9)$$

and therefore decreases rapidly with increasing  $R_{PQ}$ . Indeed, comparing with the expression for the overlap integral (9.12.1), we find that the nonclassical Coulomb contribution decreases more rapidly with  $R_{PQ}$  than does the overlap integral with  $R_{AB}$ . We thus conclude that, for sufficiently large systems, the number of *nonclassical Coulomb integrals* (i.e. Coulomb integrals for which the nonclassical contribution is significant) should increase *linearly* with the size of the system.

In Figure 9.12, we have plotted the number of nonclassical two-electron integrals using a dashed line. Note that the crossover to linear scaling for the nonclassical Coulomb integrals occurs in the same region as the crossover to linear scaling for the overlap integrals and as the crossover to quadratic scaling for the classical two-electron integrals. The distribution of the significant nonclassical two-electron integrals is also illustrated in Figure 9.13, where these integrals are shaded in black and are seen to be located in a broad band along the matrix diagonal, unlike the classical integrals, which are distributed more evenly over the whole matrix.

To distinguish between the classical and nonclassical Coulomb integrals, it is useful to introduce the concept of the extent of a Gaussian distribution. For a target accuracy of  $10^{-k}$  in the evaluation, we introduce the *extent of a Gaussian distribution* of exponent  $p$  as [21]

$$r_p = p^{-1/2} \operatorname{erfc}^{-1}(10^{-k}) \quad (9.12.10)$$

where  $\operatorname{erfc}^{-1}(x)$  is the inverse of the complementary error function. We shall now demonstrate that two Gaussians separated by more than the sum of their extents

$$R_{PQ} > r_p + r_q \quad (9.12.11)$$

interact classically. Multiplying (9.12.11) by  $\sqrt{pq/(p+q)}$  and inserting the expressions for the Gaussian extents, we obtain

$$\sqrt{\frac{pq}{p+q}} R_{PQ} > \sqrt{\frac{pq}{p+q}} \left( \frac{1}{\sqrt{p}} + \frac{1}{\sqrt{q}} \right) \operatorname{erfc}^{-1}(10^{-k}) = \frac{\sqrt{p} + \sqrt{q}}{\sqrt{p+q}} \operatorname{erfc}^{-1}(10^{-k}) \quad (9.12.12)$$

which, by simple algebraic considerations, gives the inequality

$$\sqrt{\frac{pq}{p+q}} R_{PQ} > \operatorname{erfc}^{-1}(10^{-k}) \quad (9.12.13)$$

Recalling that  $\operatorname{erfc}(x)$  is a strictly decreasing function, we obtain

$$\operatorname{erfc} \left( \sqrt{\frac{pq}{p+q}} R_{PQ} \right) < 10^{-k} \quad (9.12.14)$$

Thus, when two Gaussian distributions are separated by more than the sum of their extents, the nonclassical contribution (9.12.8) will be negligible relative to the classical contribution (9.12.7) since

$$\frac{g_{abcd}^{\text{non}}}{g_{abcd}^{\text{cls}}} = -\text{erfc} \left( \sqrt{\frac{pq}{p+q}} R_{PQ} \right) \quad (9.12.15)$$

and the two-electron integral (9.12.5) may then be calculated classically. In practice, the requirement (9.12.14) is too strict, since it is the overall contribution of the nonclassical term (9.12.8) to, for example, the Hartree–Fock energy rather than its relative contribution to the two-electron integral that matters. Nevertheless, the extent of the Gaussian provides a useful test (9.12.11), easily applied to any pair of Gaussian distributions. We also note that, in our model example, the target accuracy is  $10^{-10}$  and the exponent of all distributions is equal to 2, giving an extent of  $3.2a_0$ . Therefore, as the system increases beyond twice the Gaussian extent of  $6.4a_0$ , some of the two-electron integrals should begin to represent purely classical interactions, as seen in Figure 9.12.

The different scaling behaviour of the classical and nonclassical two-electron integrals has important ramifications. Thus, whereas the nonclassical integrals must be evaluated by the standard techniques such the McMurchie–Davidson, Obara–Saika and Rys schemes, the classical integrals may be evaluated, to an accuracy of  $10^{-k}$ , more simply by the multipole method developed in Section 9.13. Moreover, to calculate the total Coulomb contribution to the Fock operator or to the energy in large systems, there is no need to evaluate the individual integrals explicitly. Rather, as discussed in Section 9.14, their contribution may be calculated much more efficiently by the fast multipole method, at a cost that scales only linearly with the size of the system.

To summarize, although the number of significant two-electron integrals scales quadratically with the size of the system, most of these integrals represent classical electrostatic interactions. These classical integrals may either be calculated individually by multipole expansions at a cost that scales quadratically with the size of the system (Section 9.13), or else their total contribution to, for example, the Hartree–Fock energy may be calculated collectively at a cost that scales only linearly (Section 9.14). The significant nonclassical two-electron integrals, by contrast, scale linearly with the size of the system and cannot be calculated by multipole expansions. *Mutatis mutandis*, the same considerations apply to the nuclear-attraction integrals – see Figure 9.12.

#### 9.12.4 THE SCHWARZ INEQUALITY

In Section 9.12.2, we established that, for sufficiently large systems, the number of significant two-electron integrals increases quadratically rather than quartically with the size of the system. For this result to be useful, however, we must develop some method according to which we may avoid the calculation of the small integrals. In the present subsection, we shall establish a useful upper bound to the two-electron integrals based on the Schwarz inequality.

The two-electron integrals can be viewed as a matrix with the electron distributions as row and column labels

$$g_{abcd} = \iint \frac{\Omega_{ab}(\mathbf{r}_1)\Omega_{cd}(\mathbf{r}_2)}{r_{12}} d\mathbf{r}_1 d\mathbf{r}_2 \quad (9.12.16)$$

Assuming that the orbitals are real, we shall demonstrate that this matrix is positive definite [22]. Let us consider the interaction between two electrons in the same distribution  $\rho(\mathbf{r})$ :

$$I[\rho] = \iint \frac{\rho(\mathbf{r}_1)\rho(\mathbf{r}_2)}{r_{12}} d\mathbf{r}_1 d\mathbf{r}_2 \quad (9.12.17)$$

Inserting the Fourier transform of the interaction operator

$$\frac{1}{r_{12}} = \frac{1}{2\pi^2} \int k^{-2} \exp[i\mathbf{k} \cdot (\mathbf{r}_1 - \mathbf{r}_2)] d\mathbf{k} \quad (9.12.18)$$

and carrying out the integration over the Cartesian coordinates, we obtain

$$I[\rho] = \frac{1}{2\pi^2} \int k^{-2} |\rho(\mathbf{k})|^2 d\mathbf{k} \quad (9.12.19)$$

where we have introduced the distributions

$$\rho(\mathbf{k}) = \int \exp(-i\mathbf{k} \cdot \mathbf{r}) \rho(\mathbf{r}) d\mathbf{r} \quad (9.12.20)$$

Since the integrand in (9.12.19) is always positive or zero, we obtain the inequality

$$I[\rho] > 0 \quad (9.12.21)$$

Moreover, expanding the charge distribution  $\rho(\mathbf{r})$  in (9.12.17) in a set of one-electron orbital distributions

$$\rho(\mathbf{r}) = \sum_{ab} c_{ab} \Omega_{ab}(\mathbf{r}) \quad (9.12.22)$$

we may write the inequality (9.12.21) in the form

$$\sum_{abcd} c_{ab} g_{abcd} c_{cd} > 0 \quad (9.12.23)$$

where the two-electron integrals are given by (9.12.16). Equation (9.12.23) constitutes the definition of a positive definite matrix. As a corollary, the diagonal elements are positive

$$g_{abab} > 0 \quad (9.12.24)$$

The two-electron integrals therefore satisfy the conditions for inner products, in a metric defined by  $r_{12}^{-1}$ . Application of the Schwarz inequality then yields [23]

$$|g_{abcd}| \leq \sqrt{g_{abab}} \sqrt{g_{cdcd}} \quad (9.12.25)$$

Thus, if we calculate the square root of all the diagonal integrals

$$G_{ab} = \sqrt{g_{abab}} \quad (9.12.26)$$

prior to the calculation of the full set of two-electron integrals, we can easily compute upper bounds to the individual integrals as these are generated. Integrals below a given threshold may then be identified in advance and their evaluation avoided. Note that the Schwarz inequality is optimal in the sense that it is exact for all diagonal elements. Also, from the discussion of the evaluation of two-electron integrals in the preceding sections of this chapter, we note that the diagonal integrals (9.12.26) may be calculated in a particularly efficient manner and in a closed form since, for such integrals, the argument to the Boys function  $\alpha R_{PQ}^2$  is always zero.

Let us consider the application of the Schwarz inequality to a two-electron integral of  $s$  orbitals (9.12.3). The integrals (9.12.26) are simply obtained from (9.12.3) as

$$G_{ab} = \left( \frac{2p}{\pi} \right)^{1/4} |S_{ab}| \quad (9.12.27)$$

since  $R_{PQ}$  is 0 and the Boys function becomes equal to 1. The Schwarz inequality (9.12.25) then gives the following upper bound to the two-electron integral (9.12.3):

$$|g_{abcd}| \leq \sqrt{\frac{2}{\pi}}(pq)^{1/4}|S_{ab}S_{cd}| \quad (9.12.28)$$

Note that this bound is independent of the separation between the distributions  $R_{PQ}$ . Since the integral decreases in magnitude with  $R_{PQ}$ , the Schwarz inequality provides a best estimate for small  $R_{PQ}$ . However, since  $R_{PQ}$  is usually considerably smaller than say  $100a_0$ , this overestimate does not reduce the usefulness of the Schwarz screening severely.

Assuming that  $R_{PQ}$  is zero, the Schwarz inequality (9.12.28) for the two-electron integral (9.12.3) may be expressed in the form

$$\sqrt{\frac{4\alpha}{\pi}}|S_{ab}S_{cd}| \leq \sqrt{\frac{2}{\pi}}(pq)^{1/4}|S_{ab}S_{cd}| \quad (9.12.29)$$

or equivalently

$$\frac{pq}{p+q} \leq \frac{1}{2}\sqrt{pq} \quad (9.12.30)$$

Thus, the Schwarz test provides a good upper bound when  $p$  and  $q$  are similar and a poorer one when they are different. As an illustration of the Schwarz screening, we note that, for the largest system with  $n = 16$  in Figure 9.12, 38.8% of the integrals passed the Schwarz screening. Of these integrals, nearly all (37.6%) turned out to be significant. Of course, since all exponents in this system are the same, it is particularly well suited to the Schwarz screening.

## 9.13 The multipole method for Coulomb integrals

In Section 9.12, we found that, in large molecular systems, most of the significant two-electron integrals represent classical electrostatic interactions between nonoverlapping charge distributions. Although these classical integrals may be evaluated in the same manner as the nonclassical ones, using one of the methods developed in the preceding sections such as the McMurchie–Davidson scheme, the Obara–Saika scheme and the Rys-quadrature scheme, it is usually much more efficient to evaluate these integrals by the *multipole method*, in which the integrals are evaluated by a multipole expansion of the Coulomb interaction [24,25]. In the present section, we discuss the evaluation of two-electron integrals by the multipole method.

### 9.13.1 THE MULTIPOLE METHOD FOR PRIMITIVE TWO-ELECTRON INTEGRALS

Let us consider the evaluation of the two-electron integral

$$g_{abcd} = \iint \frac{\Omega_{ab}(\mathbf{r}_1)\Omega_{cd}(\mathbf{r}_2)}{r_{12}} d\mathbf{r}_1 d\mathbf{r}_2 \quad (9.13.1)$$

where the two primitive Gaussian overlap distributions  $\Omega_{ab}(\mathbf{r}_1)$  and  $\Omega_{cd}(\mathbf{r}_2)$  are centred at  $\mathbf{P}$  and  $\mathbf{Q}$ . To set up a multipole expansion of this integral, we express the positions of the electrons relative to the centres of the overlap distributions as

$$\mathbf{r}_1 = \mathbf{r}_{1P} + \mathbf{P} \quad (9.13.2)$$

$$\mathbf{r}_2 = \mathbf{r}_{2Q} + \mathbf{Q} \quad (9.13.3)$$

and introduce the vectors

$$\Delta\mathbf{r}_{12} = \mathbf{r}_{1P} - \mathbf{r}_{2Q} \quad (9.13.4)$$

$$\mathbf{R}_{QP} = \mathbf{Q} - \mathbf{P} \quad (9.13.5)$$

We shall further assume that, in the regions where the integrand in (9.13.1) is nonnegligible, the following inequality holds:

$$\Delta r_{12} = |\Delta\mathbf{r}_{12}| < R_{QP} = |\mathbf{R}_{QP}| \quad (9.13.6)$$

For the purpose of evaluating the integral (9.13.1), we may then carry out a partial-wave expansion of the inverse interelectronic distance in accordance with (7.4.3):

$$\frac{1}{r_{12}} = \sum_{l=0}^{\infty} \frac{\Delta r_{12}^l}{R_{QP}^{l+1}} P_l(\cos \theta) \quad (9.13.7)$$

Here the  $P_l(\cos \theta)$  are the Legendre polynomials in  $\cos \theta$  introduced in Section 6.4.1 and  $\theta$  is the angle between  $\Delta\mathbf{r}_{12}$  and  $\mathbf{R}_{QP}$ :

$$\cos \theta = \frac{\Delta\mathbf{r}_{12} \cdot \mathbf{R}_{QP}}{\Delta r_{12} R_{QP}} \quad (9.13.8)$$

Since, for all  $\theta$ , the Legendre polynomials satisfy the inequality [9]

$$|P_l(\cos \theta)| \leq 1 \quad (9.13.9)$$

the convergence of the partial-wave expansion (9.13.7) follows directly from the assumption (9.13.6). In Section 9.13.2, we shall examine the convergence in more detail.

To develop the multipole expansion of the two-electron integral (9.13.1), we invoke the addition theorem for the spherical harmonics (7.3.3). In Racah's normalization of the spherical harmonics (6.4.10), the addition theorem takes the form

$$P_l(\cos \theta) = \sum_{m=-l}^l C_{lm}(\theta_{12}, \varphi_{12}) C_{lm}^*(\theta_{QP}, \varphi_{QP}) \quad (9.13.10)$$

where  $\theta_{12}$  and  $\varphi_{12}$  are the angular coordinates of  $\Delta\mathbf{r}_{12}$ , and  $\theta_{QP}$  and  $\varphi_{QP}$  are the corresponding coordinates of  $\mathbf{R}_{QP}$ . Inserting this expansion in (9.13.7), we obtain

$$\frac{1}{r_{12}} = \sum_{l=0}^{\infty} \sum_{m=-l}^l \Delta r_{12}^l C_{lm}(\theta_{12}, \varphi_{12}) R_{QP}^{-l-1} C_{lm}^*(\theta_{QP}, \varphi_{QP}) \quad (9.13.11)$$

At this point, it would be possible to express this expansion in terms of the solid harmonics (6.4.22)

$$C_{lm}(\mathbf{r}) = r^l C_{lm}(\theta, \varphi) \quad (9.13.12)$$

introduced in Section 6.4.2 to yield [24]

$$\frac{1}{r_{12}} = \sum_{l=0}^{\infty} \sum_{m=-l}^l \frac{C_{lm}(\Delta\mathbf{r}_{12}) C_{lm}^*(\mathbf{R}_{QP})}{R_{QP}^{2l+1}} \quad (9.13.13)$$

However, for our purposes, it turns out to be more convenient to work with the *scaled regular and irregular solid harmonics* [25]

$$R_{lm}(\mathbf{r}) = \frac{1}{\sqrt{(l-m)!(l+m)!}} r^l C_{lm}(\theta, \varphi) \quad (9.13.14)$$

$$I_{lm}(\mathbf{r}) = \sqrt{(l-m)!(l+m)!} r^{-l-1} C_{lm}(\theta, \varphi) \quad (9.13.15)$$

In terms of these functions, the partial-wave expansion of the inverse electronic separation (9.13.11) may be written compactly as

$$\frac{1}{r_{12}} = \sum_{l=0}^{\infty} \sum_{m=-l}^l R_{lm}(\Delta\mathbf{r}_{12}) I_{lm}^*(\mathbf{R}_{QP}) \quad (9.13.16)$$

We shall consider the recursive evaluation of the scaled regular and irregular solid harmonics (9.13.14) and (9.13.15) in Section 9.13.8. At present, we only note that these functions exhibit the same inversion and conjugation symmetries (6.4.17) and (6.4.18) as do the standard solid harmonics.

The next step in the derivation of the multipole expansion of the two-electron integrals is to separate the electronic coordinates according to (9.13.4). Invoking the *addition theorem for the regular solid harmonics* [24]

$$R_{lm}(\mathbf{u} + \mathbf{v}) = \sum_{j=0}^l \sum_{k=-j}^j R_{l-j, m-k}(\mathbf{u}) R_{jk}(\mathbf{v}) \quad (9.13.17)$$

we may write the expansion (9.13.16) in the following manner:

$$\begin{aligned} \frac{1}{r_{12}} &= \sum_{l=0}^{\infty} \sum_{m=-l}^l R_{lm}(\mathbf{r}_{1P} - \mathbf{r}_{2Q}) I_{lm}^*(\mathbf{R}_{QP}) \\ &= \sum_{l=0}^{\infty} \sum_{m=-l}^l \sum_{j=0}^l \sum_{k=-j}^j R_{l-j, m-k}(\mathbf{r}_{1P}) I_{lm}^*(\mathbf{R}_{QP}) R_{jk}(-\mathbf{r}_{2Q}) \\ &= \sum_{l=0}^{\infty} \sum_{m=-l}^l \sum_{j=0}^{\infty} \sum_{k=-j}^j (-1)^j R_{lm}(\mathbf{r}_{1P}) I_{l+j, m+k}^*(\mathbf{R}_{QP}) R_{jk}(\mathbf{r}_{2Q}) \end{aligned} \quad (9.13.18)$$

where, in the last expression, we have rearranged the dummy indices and used the inversion symmetry (6.4.17). For a proof of the addition theorem (9.13.17), we refer to standard textbooks on mathematical physics [26]. We note here that, in a normalization different from that of the scaled regular harmonics (9.13.14), the addition theorem assumes a more complicated form, involving a numerical factor that is different for each term in the expansion (9.13.17). Since the addition theorem of the regular solid harmonics will be used frequently in our discussion, the normalization (9.13.14) is adopted here.

Substituting the partial-wave expansion in the form (9.13.18) into (9.13.1), we arrive at the *bipolar multipole expansion* of the two-electron integral

$$g_{abcd} = \sum_{l=0}^{\infty} \sum_{m=-l}^l \sum_{j=0}^{\infty} \sum_{k=-j}^j q_{lm}^{ab}(\mathbf{P}) T_{lm, jk}(\mathbf{R}_{QP}) q_{jk}^{cd}(\mathbf{Q}) \quad (9.13.19)$$

where we have introduced the *multipole moments* of the charge distributions

$$q_{lm}^{ab}(\mathbf{P}) = \int \Omega_{ab}(\mathbf{r}) R_{lm}(\mathbf{r}_P) d\mathbf{r} \quad (9.13.20)$$

$$q_{jk}^{cd}(\mathbf{Q}) = \int \Omega_{cd}(\mathbf{r}) R_{jk}(\mathbf{r}_Q) d\mathbf{r} \quad (9.13.21)$$

and the elements of the *interaction matrix*

$$T_{lm,jk}(\mathbf{R}_{QP}) = (-1)^j I_{l+j,m+k}^*(\mathbf{R}_{QP}) \quad (9.13.22)$$

The term *bipolar* is used to describe this expansion since it involves two sets of multipole moments, with different origins. In matrix notation, the multipole expansion (9.13.19) may be written as

$$g_{abcd} = \mathbf{q}^{ab}(\mathbf{P})^T \mathbf{T}(\mathbf{R}_{QP}) \mathbf{q}^{cd}(\mathbf{Q}) \quad (9.13.23)$$

Here  $\mathbf{q}^{ab}(\mathbf{P})$  is a column vector of the multipole moments for the overlap distribution  $\Omega_{ab}$  with origin at  $\mathbf{P}$  and  $\mathbf{q}^{cd}(\mathbf{Q})$  is interpreted in a similar way. The elements of the multipole vectors  $\mathbf{q}$  are ordered as  $q_{00}, q_{1,-1}, q_{1,0}, q_{1,1}$ , and so on. Finally,  $\mathbf{T}(\mathbf{R}_{QP})$  is a square matrix containing the interaction moments for the vector  $\mathbf{R}_{QP}$ , its columns and rows ordered in the same manner as in the multipole vectors. More general expressions for bipolar multipole expansions can be derived, in which the interacting charge distributions are represented in local coordinate systems [24,27]. Such a formulation is important in the theory of intermolecular forces but unnecessarily complicated for our purposes since we employ a global coordinate system for all charges.

In the multipole expansion of the two-electron integral (9.13.23), the interaction tensor (9.13.22) depends only on the relative position of the origins about the charge distributions – all information about the charge distributions is contained in the multipole moments (9.13.20) and (9.13.21). As an illustration, consider the lowest-order expansion of the two-electron integrals. The moments of the charge distributions are given as

$$q_{00}^{ab}(\mathbf{P}) = \int \Omega_{ab}(\mathbf{r}) R_{00}(\mathbf{r}_P) d\mathbf{r} = \int \Omega_{ab}(\mathbf{r}) d\mathbf{r} = S_{ab} \quad (9.13.24)$$

$$q_{00}^{cd}(\mathbf{Q}) = \int \Omega_{cd}(\mathbf{r}) R_{00}(\mathbf{r}_Q) d\mathbf{r} = \int \Omega_{cd}(\mathbf{r}) d\mathbf{r} = S_{cd} \quad (9.13.25)$$

$$T_{00,00}(\mathbf{R}_{QP}) = R_{QP}^{-1} \quad (9.13.26)$$

and the integral becomes (see also Exercise 9.4)

$$g_{abcd} \approx \frac{S_{ab} S_{cd}}{R_{PQ}} \quad (9.13.27)$$

Note that, for spherical overlap distributions centred at  $\mathbf{P}$  and  $\mathbf{Q}$ , (9.13.24) and (9.13.25) are the only nonzero multipole moments and the monopole expansion (9.13.27) then represents an exact expression for the two-electron integral (assuming disjoint charge distributions) – see also the discussion in Section 9.12.3. In the same manner, the multipole expansion (9.13.19) terminates exactly after a finite number of terms whenever the charge distributions of the electrons are one-centre functions, whose centres are chosen as origins of the multipole expansions. In general, however, the bipolar multipole expansion does not terminate and the expansion is then truncated when the remainder is sufficiently small as discussed in Section 9.13.2.

In the multipole expansion of the two-electron integral (9.13.23), the complicated six-dimensional integration of the two-electron integral has been reduced to the much simpler three-dimensional integration of the one-electron multipoles (9.13.20) and (9.13.21). These one-electron integrals may be evaluated by, for example, the Obara–Saika technique of Section 9.3.2, whose recursive structure makes it well suited to the simultaneous generation of the full set of multipole moments needed in the multipole method. We also note that, for each electron, the number of such one-electron multipole-moment integrals to be evaluated is  $(L + 1)^2$ , where  $L$  is the order of the multipole expansion. Consequently, the cost of the contraction of the multipole vectors with the interaction matrix to form the final two-electron integral (9.13.19) scales as  $L^4$ .

### 9.13.2 CONVERGENCE OF THE MULTIPOLE EXPANSION

Let us consider the rate of convergence of the multipole expansion. Assuming that the partial-wave expansion in (9.13.7) has been carried out to order  $L$ , the error in the inverse interelectronic distance is given as

$$\delta_{12}^L = \sum_{l=L+1}^{\infty} \frac{\Delta r_{12}^l}{R_{QP}^{l+1}} P_l(\cos \theta) \leq \sum_{l=L+1}^{\infty} \frac{\Delta r_{12}^l}{R_{QP}^{l+1}} \quad (9.13.28)$$

Carrying out the summation, we obtain

$$\delta_{12}^L \leq \frac{1}{R_{QP} - \Delta r_{12}} \left( \frac{\Delta r_{12}}{R_{QP}} \right)^{L+1} \quad (9.13.29)$$

Clearly, for rapid convergence, the separation between the origins of the multipole expansions  $R_{QP}$  should be large relative to the size of the interacting charge distributions. We also note that, with each increment in the multipole expansion, the error is reduced by a constant factor. Indeed, using (9.13.29), it is possible to control the accuracy of the multipole expansion, although this simple estimate of the error is usually rather conservative. In practice, therefore, the achieved accuracy may be considerably higher than predicted by (9.13.29).

With regard to the convergence of the multipole expansion, it should be noted that two Gaussian distributions will always overlap to some extent, irrespective of their relative separation. The condition for convergence (9.13.6) is therefore, strictly speaking, never satisfied over the whole region of integration. In other words, the multipole expansion constitutes an asymptotic rather than convergent expansion. However, provided the product of the two charge distributions is sufficiently small in the divergent regions, this will not create problems in practice since convergence will be achieved in the important regions before the divergent contributions of the weakly overlapping regions become larger than the allowed error in the integral.

### 9.13.3 THE MULTIPOLE METHOD FOR CONTRACTED TWO-ELECTRON INTEGRALS

In Section 9.13.1, we considered the evaluation of a primitive two-electron integral by a bipolar multipole expansion, with the origins of  $\mathbf{q}^{ab}(\mathbf{P})$  and  $\mathbf{q}^{cd}(\mathbf{Q})$  at the centres  $\mathbf{P}$  and  $\mathbf{Q}$  of the overlap distributions  $\Omega_{ab}(\mathbf{r}_1)$  and  $\Omega_{cd}(\mathbf{r}_2)$ . Let us now consider the evaluation of a two-electron integral over a *contracted* set of overlap distributions, which we write here in the form

$$g_{\alpha\beta\gamma\delta} = \sum_{abcd} d_{ab}^{\alpha\beta} d_{cd}^{\gamma\delta} g_{abcd} \quad (9.13.30)$$

Inserting the multipole expansion (9.13.23) in this expression, we obtain

$$g_{\alpha\beta\gamma\delta} = \sum_{abcd} d_{ab}^{\alpha\beta} d_{cd}^{\gamma\delta} \mathbf{q}^{ab} (\mathbf{P}^{ab})^T \mathbf{T}(\mathbf{R}_{QP}^{abcd}) \mathbf{q}^{cd} (\mathbf{Q}^{cd}) \quad (9.13.31)$$

where the notation  $\mathbf{P}^{ab}$  is used to remind us that  $\mathbf{P}$  is calculated from the positions  $\mathbf{A}$  and  $\mathbf{B}$  according to (9.2.13) and similarly for  $\mathbf{R}_{QP}^{abcd}$  and  $\mathbf{Q}^{cd}$ . Since in (9.13.31) the origins of the multipole expansions are different for each pair of primitive overlap distributions, we must carry out a separate expansion for each such pair, making this particular application of the multipole method for the contracted two-electron integral rather expensive.

For contracted integrals, a more attractive approach is to introduce a single, shared origin  $\bar{\mathbf{P}}$  for the overlap distributions of the first electron and likewise a common origin  $\bar{\mathbf{Q}}$  for the distributions of the second electron. The two-electron integral (9.13.31) then takes the form

$$g_{\alpha\beta\gamma\delta} = \sum_{abcd} d_{ab}^{\alpha\beta} d_{cd}^{\gamma\delta} \mathbf{q}^{ab} (\bar{\mathbf{P}})^T \mathbf{T}(\mathbf{R}_{\bar{Q}\bar{P}}) \mathbf{q}^{cd} (\bar{\mathbf{Q}}) \quad (9.13.32)$$

Carrying out the summations, we now obtain the compact expression

$$g_{\alpha\beta\gamma\delta} = \mathbf{q}^{\alpha\beta} (\bar{\mathbf{P}})^T \mathbf{T}(\mathbf{R}_{\bar{Q}\bar{P}}) \mathbf{q}^{\gamma\delta} (\bar{\mathbf{Q}}) \quad (9.13.33)$$

where the multipole moments of the first electron are given by

$$q_{lm}^{\alpha\beta} (\bar{\mathbf{P}}) = \sum_{ab} d_{ab}^{\alpha\beta} \int \Omega_{ab}(\mathbf{r}) R_{lm}(\mathbf{r}_{\bar{P}}) d\mathbf{r} \quad (9.13.34)$$

and similarly for the second electron. This procedure is clearly superior to (9.13.31), reducing the quadruple summation over primitive functions to double summations (9.13.34) and requiring the formation of only a single bipolar multipole expansion (9.13.33).

More generally, we may calculate two-electron integrals over arbitrary linear combinations of primitive overlap distributions (representing, for example, the charge distribution of a large part of a molecular system) in the same manner, obtaining the multipole moments by an obvious extension of (9.13.34). We note, however, that this procedure will work only if the multipole expansion for the combined overlap distributions converges – that is, if the resulting combined overlap distributions are sufficiently far removed from each other for the partial-wave expansion to converge.

#### 9.13.4 TRANSLATION OF MULTIPOLE MOMENTS

An obvious strategy for calculating the multipole moments (9.13.34) would be first to set up the contracted charge distribution

$$\Omega_{\alpha\beta}(\mathbf{r}) = \sum_{ab} d_{ab}^{\alpha\beta} \Omega_{ab}(\mathbf{r}) \quad (9.13.35)$$

and then to evaluate the multipole moments

$$q_{lm}^{\alpha\beta} (\bar{\mathbf{P}}) = \int \Omega_{\alpha\beta}(\mathbf{r}) R_{lm}(\mathbf{r}_{\bar{P}}) d\mathbf{r} \quad (9.13.36)$$

by some chosen integration scheme. For distributions such as those present in a contracted two-electron integral, the integration may be carried out exactly, using some modification of the

Obara–Saika or McMurchie–Davidson schemes. For more general charge distributions, representing, for example, a large part of a molecular system, it may be better to carry out the integration numerically, using Gaussian quadrature or some other numerical scheme.

Let us now consider an alternative procedure for the evaluation of the contracted multipole moments (9.13.36). First, we calculate – for each primitive overlap distribution contributing to the two-electron integral – local multipole moments of the type (9.13.20), each with origin at the centre of the primitive overlap distribution:

$$q_{lm}^{ab}(\mathbf{P}) = \int \Omega_{ab}(\mathbf{r}) R_{lm}(\mathbf{r}_P) d\mathbf{r} \quad (9.13.37)$$

Next, we translate the origins  $\mathbf{P}$  of these local expansions to the common origin  $\bar{\mathbf{P}}$  employed for the evaluation of the two-electron integral (9.13.32). Invoking the addition theorem for the regular solid harmonics (9.13.17), we obtain

$$\begin{aligned} q_{lm}^{ab}(\bar{\mathbf{P}}) &= \int \Omega_{ab}(\mathbf{r}) R_{lm}(\mathbf{r}_P - \mathbf{R}_{\bar{\mathbf{P}}}) d\mathbf{r} \\ &= \sum_{j=0}^l \sum_{k=-j}^j R_{l-j, m-k}(-\mathbf{R}_{\bar{\mathbf{P}}}) \int \Omega_{ab}(\mathbf{r}) R_{jk}(\mathbf{r}_P) d\mathbf{r} \end{aligned} \quad (9.13.38)$$

Introducing the notation

$$W_{lm, jk}(\mathbf{R}_{\bar{\mathbf{P}}}) = R_{l-j, m-k}(-\mathbf{R}_{\bar{\mathbf{P}}}) \quad (9.13.39)$$

we may write the transformation (9.13.38) as

$$q_{lm}^{ab}(\bar{\mathbf{P}}) = \sum_{j=0}^l \sum_{k=-j}^j W_{lm, jk}(\mathbf{R}_{\bar{\mathbf{P}}}) q_{jk}^{ab}(\mathbf{P}) \quad (9.13.40)$$

In matrix notation, the shift of origin from  $\mathbf{P}$  to  $\bar{\mathbf{P}}$  for the full set of multipole moments may be expressed compactly as a linear transformation

$$\mathbf{q}^{ab}(\bar{\mathbf{P}}) = \mathbf{W}(\mathbf{R}_{\bar{\mathbf{P}}}) \mathbf{q}^{ab}(\mathbf{P}) \quad (9.13.41)$$

where  $\mathbf{W}(\mathbf{R}_{\bar{\mathbf{P}}})$  is the *translation matrix*. Using this expression, we may calculate the integral (9.13.23) from

$$g_{abcd} = \mathbf{q}^{ab}(\mathbf{P})^T \mathbf{W}(\mathbf{R}_{\bar{\mathbf{P}}})^T \mathbf{T}(\mathbf{R}_{\bar{\mathbf{Q}}\bar{\mathbf{P}}}) \mathbf{W}(\mathbf{R}_{\bar{\mathbf{Q}}\bar{\mathbf{Q}}}) \mathbf{q}^{cd}(\mathbf{Q}) \quad (9.13.42)$$

Such translations of the origins of the multipole expansions will prove particularly useful in the development of the multipole method for the calculation of Coulomb interactions in large systems, where each multipole moment contributes to a large number of Coulomb interactions with different origins; see Section 9.14.

By inspection of (9.13.39), we see that the translation matrix  $\mathbf{W}$  is a lower triangular matrix with unit diagonal elements. This structure implies that the monopole moment at  $\mathbf{P}$  makes contributions to all multipoles at  $\bar{\mathbf{P}}$ , that the dipole moment at  $\mathbf{P}$  makes contributions to the dipole and all higher moments at  $\bar{\mathbf{P}}$ , and so on. In particular, we note that a charge distribution that is represented exactly by a finite number of multipoles centred at  $\mathbf{P}$ , will require an infinite expansion at a different position  $\bar{\mathbf{P}}$  for an exact evaluation.

### 9.13.5 REAL MULTIPOLE MOMENTS

A disadvantage of the multipole method presented so far is that it is expressed in terms of complex multipole moments and interaction tensors. Since the Coulomb interactions are real, it is more natural (and, it turns out, more efficient) to express the expansions in terms of real moments and interaction tensors. In the remainder of this section, we shall see how the transformation to real expressions may be accomplished.

We begin by decomposing the complex regular and irregular solid harmonics as

$$R_{lm}(\mathbf{r}) = R_{lm}^c(\mathbf{r}) + iR_{lm}^s(\mathbf{r}) \quad (9.13.43)$$

$$I_{lm}(\mathbf{r}) = I_{lm}^c(\mathbf{r}) + iI_{lm}^s(\mathbf{r}) \quad (9.13.44)$$

where  $R_{lm}^c(\mathbf{r})$  and  $R_{lm}^s(\mathbf{r})$  are the real (cosine) and imaginary (sine) parts of  $R_{lm}(\mathbf{r})$ :

$$R_{lm}^c(\mathbf{r}) = \frac{R_{lm}(\mathbf{r}) + R_{lm}^*(\mathbf{r})}{2} \quad (9.13.45)$$

$$R_{lm}^s(\mathbf{r}) = \frac{R_{lm}(\mathbf{r}) - R_{lm}^*(\mathbf{r})}{2i} \quad (9.13.46)$$

Note that the real and imaginary components are defined for negative as well as positive indices  $m$ . Using (9.13.14), (6.4.22) and (6.4.18), we find that the real regular solid harmonics satisfy the following symmetry properties:

$$R_{l,-m}^c(\mathbf{r}) = (-1)^m R_{lm}^c(\mathbf{r}) \quad (9.13.47)$$

$$R_{l,-m}^s(\mathbf{r}) = -(-1)^m R_{lm}^s(\mathbf{r}) \quad (9.13.48)$$

The irregular solid harmonics satisfy analogous relations.

It should be realized that the real regular solid harmonics  $R_{lm}^c(\mathbf{r})$  and  $R_{lm}^s(\mathbf{r})$  introduced here differ from the real solid harmonics  $S_{lm}(\mathbf{r})$  of Section 6.4.2. Thus, whereas the real functions in Section 6.4.2 were obtained by a unitary transformation of the complex ones (in Racah's normalization), the transformation in (9.13.45) and (9.13.46) is not unitary. It is adopted here since it leads to simpler expressions for the multipole expansions.

It is often convenient to employ a common notation for the cosine and sine components of the solid harmonics. In such cases, we shall indicate real components by the use of Greek letters, adopting the following convention to distinguish between the cosine and sine components

$$R_{l\mu}(\mathbf{r}) = \begin{cases} R_{l\mu}^c(\mathbf{r}) & \mu \geq 0 \\ R_{l\mu}^s(\mathbf{r}) & \mu < 0 \end{cases} \quad (9.13.49)$$

However, it should be understood that  $R_{lm}^c(\mathbf{r})$  and  $R_{lm}^s(\mathbf{r})$  are both defined for positive and negative indices  $m$ , obeying the relationships (9.13.47) and (9.13.48).

Having defined the real regular solid harmonics, we now go on to consider the associated multipole moments. The complex multipole moments may be written as

$$q_{lm}(\mathbf{P}) = q_{lm}^c(\mathbf{P}) + iq_{lm}^s(\mathbf{P}) \quad (9.13.50)$$

where  $q_{lm}^c(\mathbf{P})$  and  $q_{lm}^s(\mathbf{P})$  are the real multipole moments, generated by integration over the appropriate charge distribution multiplied by the real regular solid harmonics:

$$q_{lm}^c(\mathbf{P}) = \int \rho(\mathbf{r}) R_{lm}^c(\mathbf{r}_P) d\mathbf{r} \quad (9.13.51)$$

$$q_{lm}^s(\mathbf{P}) = \int \rho(\mathbf{r}) R_{lm}^s(\mathbf{r}_P) d\mathbf{r} \quad (9.13.52)$$

As for the real solid harmonics in (9.13.49), we shall use the common notation  $q_{l\mu}(\mathbf{P})$  for the cosine and sine components of the complex multipole moments  $q_{lm}(\mathbf{P})$ .

### 9.13.6 THE REAL TRANSLATION MATRIX

To obtain an expression for the real translation matrix, we begin by writing (9.13.40) as

$$q_{lm}(\bar{\mathbf{P}}) = \sum_{j=0}^l \sum_{k=-j}^j W_{lm,jk}(\mathbf{R}_{\bar{\mathbf{P}}\mathbf{P}}) q_{jk}(\mathbf{P}) = \sum_{j=0}^l \sum_{k=-j}^j R_{l-j,m-k}(-\mathbf{R}_{\bar{\mathbf{P}}\mathbf{P}}) q_{jk}(\mathbf{P}) \quad (9.13.53)$$

Inserting (9.13.43) and (9.13.50) and treating the cosine and sine components separately, we obtain

$$q_{lm}^c(\bar{\mathbf{P}}) = \sum_{jk} R_{l-j,m-k}^c(-\mathbf{R}_{\bar{\mathbf{P}}\mathbf{P}}) q_{jk}^c(\mathbf{P}) - \sum_{jk} R_{l-j,m-k}^s(-\mathbf{R}_{\bar{\mathbf{P}}\mathbf{P}}) q_{jk}^s(\mathbf{P}) \quad (9.13.54)$$

$$q_{lm}^s(\bar{\mathbf{P}}) = \sum_{jk} R_{l-j,m-k}^c(-\mathbf{R}_{\bar{\mathbf{P}}\mathbf{P}}) q_{jk}^s(\mathbf{P}) + \sum_{jk} R_{l-j,m-k}^s(-\mathbf{R}_{\bar{\mathbf{P}}\mathbf{P}}) q_{jk}^c(\mathbf{P}) \quad (9.13.55)$$

where the summation ranges are the same as in (9.13.53). These expressions are now manipulated as illustrated here for one of the contributions to the first term in (9.13.54) (omitting arguments):

$$A_j^{cc} = \sum_k R_{l-j,m-k}^c q_{jk}^c \quad (9.13.56)$$

Considering positive and negative  $k$  separately and invoking (9.13.47), we obtain

$$\begin{aligned} A_j^{cc} &= \sum_{k \geq 0} R_{l-j,m-k}^c q_{jk}^c + \sum_{k < 0} R_{l-j,m-k}^c q_{jk}^c \\ &= \sum_{k \geq 0} R_{l-j,m-k}^c q_{jk}^c + \sum_{k > 0} R_{l-j,m+k}^c q_{j,-k}^c \\ &= \sum_{k \geq 0} R_{l-j,m-k}^c q_{jk}^c + \sum_{k > 0} (-1)^k R_{l-j,m+k}^c q_{jk}^c \\ &= \sum_{k \geq 0} \left(\frac{1}{2}\right)^{\delta_{k0}} [R_{l-j,m-k}^c + (-1)^k R_{l-j,m+k}^c] q_{jk}^c \end{aligned} \quad (9.13.57)$$

Similar manipulations may be carried out for the other terms in (9.13.54) and (9.13.55) as well. Introducing the matrix elements

$$W_{lm,jk}^{cc}(\mathbf{R}_{\bar{\mathbf{P}}\mathbf{P}}) = \left(\frac{1}{2}\right)^{\delta_{k0}} [R_{l-j,m-k}^c(-\mathbf{R}_{\bar{\mathbf{P}}\mathbf{P}}) + (-1)^k R_{l-j,m+k}^c(-\mathbf{R}_{\bar{\mathbf{P}}\mathbf{P}})] \quad (9.13.58)$$

$$W_{lm,jk}^{cs}(\mathbf{R}_{\bar{\mathbf{P}}\mathbf{P}}) = -R_{l-j,m-k}^s(-\mathbf{R}_{\bar{\mathbf{P}}\mathbf{P}}) + (-1)^k R_{l-j,m+k}^s(-\mathbf{R}_{\bar{\mathbf{P}}\mathbf{P}}) \quad (9.13.59)$$

$$W_{lm,jk}^{sc}(\mathbf{R}_{\bar{\mathbf{P}}\mathbf{P}}) = \left(\frac{1}{2}\right)^{\delta_{k0}} [R_{l-j,m-k}^s(-\mathbf{R}_{\bar{\mathbf{P}}\mathbf{P}}) + (-1)^k R_{l-j,m+k}^s(-\mathbf{R}_{\bar{\mathbf{P}}\mathbf{P}})] \quad (9.13.60)$$

$$W_{lm,jk}^{ss}(\mathbf{R}_{\bar{\mathbf{P}}\mathbf{P}}) = R_{l-j,m-k}^c(-\mathbf{R}_{\bar{\mathbf{P}}\mathbf{P}}) - (-1)^k R_{l-j,m+k}^c(-\mathbf{R}_{\bar{\mathbf{P}}\mathbf{P}}) \quad (9.13.61)$$

we may now write the transformations (9.13.54) and (9.13.55) as

$$q_{lm}^c(\bar{\mathbf{P}}) = \sum_{j,k \geq 0} W_{lm,jk}^{cc}(\mathbf{R}_{\bar{\mathbf{P}}\mathbf{P}}) q_{jk}^c(\mathbf{P}) + \sum_{j,k > 0} W_{lm,jk}^{cs}(\mathbf{R}_{\bar{\mathbf{P}}\mathbf{P}}) q_{jk}^s(\mathbf{P}) \quad (9.13.62)$$

$$q_{lm}^s(\bar{\mathbf{P}}) = \sum_{j,k \geq 0} W_{lm,jk}^{sc}(\mathbf{R}_{\bar{\mathbf{P}}\mathbf{P}}) q_{jk}^c(\mathbf{P}) + \sum_{j,k > 0} W_{lm,jk}^{ss}(\mathbf{R}_{\bar{\mathbf{P}}\mathbf{P}}) q_{jk}^s(\mathbf{P}) \quad (9.13.63)$$

where the summation ranges have been reduced by one-half.

As is easily verified, the elements (9.13.58)–(9.13.61) have the same symmetries with respect to sign changes of  $m$  and  $k$  as do the cosine and sine components of the regular solid harmonics (9.13.47) and (9.13.48), for example

$$W_{lm,jk}^{sc} = -(-1)^m W_{l\bar{m},jk}^{sc} = (-1)^k W_{lm,\bar{j}\bar{k}}^{sc} \quad (9.13.64)$$

where, to avoid ambiguity, we have used the notation  $\bar{m} = -m$ . We may therefore carry out each of the summations in (9.13.62) and (9.13.63) over positive or negative indices, with no changes in the expressions. Associating positive and negative indices with the cosine and sine components as in (9.13.49), we may write the transformation of the real multipole moments compactly as

$$q_{l\mu}(\bar{\mathbf{P}}) = \sum_{j=0}^l \sum_{\kappa=-j}^j W_{l\mu,j\kappa}(\mathbf{R}_{\bar{\mathbf{P}}\mathbf{P}}) q_{jk}(\mathbf{P}) \quad (9.13.65)$$

or, in matrix notation,

$$\mathbf{q}(\bar{\mathbf{P}}) = \mathbf{W}(\mathbf{R}_{\bar{\mathbf{P}}\mathbf{P}}) \mathbf{q}(\mathbf{P}) \quad (9.13.66)$$

Obviously, this matrix representation has the same form as in the complex case, with identical summation ranges. Since the real multipole moments and translation-matrix elements have one instead of two components as in the complex counterpart to (9.13.66), the real formulation is more compact.

### 9.13.7 THE REAL INTERACTION MATRIX

Let us finally consider the real expression for the interaction matrix. We proceed in the same manner as for the translation matrix, beginning with (9.13.19), which we write as

$$\begin{aligned} g_{abcd} &= \sum_{lm} \sum_{jk} q_{lm}(\mathbf{P}) T_{lm,jk}(\mathbf{R}_{\mathbf{Q}\mathbf{P}}) q_{jk}(\mathbf{Q}) \\ &= \sum_{lm} \sum_{jk} (-1)^j q_{lm}(\mathbf{P}) I_{l+j,m+k}^*(\mathbf{R}_{\mathbf{Q}\mathbf{P}}) q_{jk}(\mathbf{Q}) \end{aligned} \quad (9.13.67)$$

To obtain the real interaction matrix, we substitute in this expression the two-term expansions of the multipole moments (9.13.50) and of the irregular harmonics (9.13.44) in real components. This substitution gives eight distinct terms, one of which is given as (omitting arguments)

$$g_{abcd}^{ccc} = \sum_{lm} \sum_{jk} (-1)^j q_{lm}^c I_{l+j,m+k}^c q_{jk}^c \quad (9.13.68)$$

Expanding in positive and negative components, we obtain

$$\begin{aligned}
 g_{abcd}^{ccc} &= \sum_{lm} \sum_{\substack{j \\ k \geq 0}} (-1)^j \left(\frac{1}{2}\right)^{\delta_{k0}} q_{lm}^c (I_{l+j,m+k}^c q_{jk}^c + I_{l+j,m-k}^c q_{j,-k}^c) \\
 &= \sum_{lm} \sum_{\substack{j \\ k \geq 0}} (-1)^j \left(\frac{1}{2}\right)^{\delta_{k0}} q_{lm}^c (I_{l+j,m+k}^c + (-1)^k I_{l+j,m-k}^c) q_{jk}^c \\
 &= 2 \sum_{\substack{l \\ m \geq 0}} \sum_{\substack{j \\ k \geq 0}} (-1)^j \left(\frac{1}{2}\right)^{\delta_{k0} + \delta_{m0}} q_{lm}^c (I_{l+j,m+k}^c + (-1)^k I_{l+j,m-k}^c) q_{jk}^c
 \end{aligned} \quad (9.13.69)$$

Treating the remaining seven terms that arise from (9.13.67) in the same manner, we find that the four imaginary terms vanish and that the full expansion (9.13.67) may be written as

$$\begin{aligned}
 g_{abcd} &= \sum_{\substack{l,m \geq 0 \\ j,k \geq 0}} q_{lm}^c(\mathbf{P}) T_{lm,jk}^{cc}(\mathbf{R}_{QP}) q_{jk}^c(\mathbf{Q}) + \sum_{\substack{l,m \geq 0 \\ j,k \geq 0}} q_{lm}^c(\mathbf{P}) T_{lm,jk}^{cs}(\mathbf{R}_{QP}) q_{jk}^s(\mathbf{Q}) \\
 &\quad + \sum_{\substack{l,m \geq 0 \\ j,k \geq 0}} q_{lm}^s(\mathbf{P}) T_{lm,jk}^{sc}(\mathbf{R}_{QP}) q_{jk}^c(\mathbf{Q}) + \sum_{\substack{l,m \geq 0 \\ j,k \geq 0}} q_{lm}^s(\mathbf{P}) T_{lm,jk}^{ss}(\mathbf{R}_{QP}) q_{jk}^s(\mathbf{Q})
 \end{aligned} \quad (9.13.70)$$

in terms of the following real components of the interaction matrix

$$T_{lm,jk}^{cc}(\mathbf{R}_{QP}) = (-1)^j \left(\frac{1}{2}\right)^{\delta_{m0} + \delta_{k0}} 2[I_{l+j,m+k}^c(\mathbf{R}_{QP}) + (-1)^k I_{l+j,m-k}^c(\mathbf{R}_{QP})] \quad (9.13.71)$$

$$T_{lm,jk}^{cs}(\mathbf{R}_{QP}) = (-1)^j \left(\frac{1}{2}\right)^{\delta_{m0} + \delta_{k0}} 2[I_{l+j,m+k}^s(\mathbf{R}_{QP}) - (-1)^k I_{l+j,m-k}^s(\mathbf{R}_{QP})] \quad (9.13.72)$$

$$T_{lm,jk}^{sc}(\mathbf{R}_{QP}) = (-1)^j \left(\frac{1}{2}\right)^{\delta_{m0} + \delta_{k0}} 2[I_{l+j,m+k}^s(\mathbf{R}_{QP}) + (-1)^k I_{l+j,m-k}^s(\mathbf{R}_{QP})] \quad (9.13.73)$$

$$T_{lm,jk}^{ss}(\mathbf{R}_{QP}) = (-1)^j \left(\frac{1}{2}\right)^{\delta_{m0} + \delta_{k0}} 2[-I_{l+j,m+k}^c(\mathbf{R}_{QP}) + (-1)^k I_{l+j,m-k}^c(\mathbf{R}_{QP})] \quad (9.13.74)$$

The indices  $m$  and  $k$  of the interaction matrix (9.13.71)–(9.13.74) obey the same symmetries as the indices of the translation matrix; see (9.13.64). Recognizing that  $q_{l0}^s$  is zero since  $q_{l0}$  is real, we may, by the convention (9.13.49), write the interaction (9.13.70) in exactly the same manner as in the complex case (9.13.67):

$$g_{abcd} = \sum_{l\mu} \sum_{jk} q_{l\mu}(\mathbf{P}) T_{l\mu,jk}(\mathbf{R}_{QP}) q_{jk}(\mathbf{Q}) \quad (9.13.75)$$

The real formulation is more economical since each term involves only real numbers. Also, we shall see that simple recurrence relations may be set up for the evaluation of the regular and irregular solid harmonics, making the generation of the interaction and translation matrices a straightforward matter.

### 9.13.8 EVALUATION OF THE SCALED SOLID HARMONICS

Let us consider the evaluation of the scaled real solid harmonics defined in (9.13.43) and (9.13.44). We first note that the real regular solid harmonics are related to the standard functions of Section 6.4 as

$$R_{l,|m|}^c(\mathbf{r}) = \frac{(-1)^m}{\sqrt{(2 - \delta_{m0})(l - m)!(l + m)!}} S_{l,|m|}(\mathbf{r}) \quad (9.13.76)$$

$$R_{l,|m|}^s(\mathbf{r}) = \frac{(1 - \delta_{m0})(-1)^m}{\sqrt{2(l-m)!(l+m)!}} S_{l,-|m|}(\mathbf{r}) \quad (9.13.77)$$

Using these relations, it is trivial to set up an explicit expression for their evaluation analogous to (6.4.47) for  $S_{lm}(\mathbf{r})$ . The recurrence relations may be obtained from (6.4.55), (6.4.56) and (6.4.69). Taking into account the different normalizations (9.13.76) and (9.13.77) and also the symmetry relations (9.13.47) and (9.13.48), we obtain after some algebra the following set of recurrence relations for the scaled regular solid harmonics:

$$R_{00}^c = 1 \quad (9.13.78)$$

$$R_{00}^s = 0 \quad (9.13.79)$$

$$R_{l+1,l+1}^c = -\frac{xR_{ll}^c - yR_{ll}^s}{2l+2} \quad (9.13.80)$$

$$R_{l+1,l+1}^s = -\frac{yR_{ll}^c + xR_{ll}^s}{2l+2} \quad (9.13.81)$$

$$R_{l+1,m}^{c/s} = \frac{(2l+1)zR_{lm}^{c/s} - r^2 R_{l-1,m}^{c/s}}{(l+m+1)(l-m+1)}, \quad 0 \leq m < l \quad (9.13.82)$$

In the last recurrence, the use of  $R_{lm}^{c/s}(\mathbf{r})$  indicates that the relation is valid for both  $R_{lm}^c(\mathbf{r})$  and  $R_{lm}^s(\mathbf{r})$ . We note that the recurrence relations for the scaled functions  $R_{lm}(\mathbf{r})$  are slightly simpler than those for their unscaled counterparts (6.4.70)–(6.4.73).

Let us now consider the scaled irregular solid harmonics, related to the unscaled real solid harmonics by

$$I_{l,|m|}^c(\mathbf{r}) = (-1)^m \sqrt{\frac{(l-m)!(l+m)!}{2 - \delta_{m0}}} \frac{S_{l,|m|}(\mathbf{r})}{r^{2l+1}} \quad (9.13.83)$$

$$I_{l,|m|}^s(\mathbf{r}) = (-1)^m (1 - \delta_{m0}) \sqrt{\frac{(l-m)!(l+m)!}{2}} \frac{S_{l,-|m|}(\mathbf{r})}{r^{2l+1}} \quad (9.13.84)$$

Again, it is trivial to set up an explicit expression for their evaluation, analogous to (6.4.47) for  $S_{lm}(\mathbf{r})$ . The recurrence relations are obtained as for the regular harmonics, including  $r^{-2l-1}$  in the scaling factor. After some algebra, we arrive at the following recurrence relations for the real irregular solid harmonics:

$$I_{00}^c = \frac{1}{r} \quad (9.13.85)$$

$$I_{00}^s = 0 \quad (9.13.86)$$

$$I_{l+1,l+1}^c = -(2l+1) \frac{xI_{ll}^c - yI_{ll}^s}{r^2} \quad (9.13.87)$$

$$I_{l+1,l+1}^s = -(2l+1) \frac{yI_{ll}^c + xI_{ll}^s}{r^2} \quad (9.13.88)$$

$$I_{l+1,m}^{c/s} = \frac{(2l+1)zI_{lm}^{c/s} - (l^2 - m^2)I_{l-1,m}^{c/s}}{r^2}, \quad 0 \leq m < l \quad (9.13.89)$$

Using relations (9.13.78)–(9.13.82) and (9.13.85)–(9.13.89), the solid harmonics required for the evaluation of the bipolar multipole expansions may be easily generated.

## 9.14 The multipole method for large systems

The multipole method discussed in Section 9.13 may be applied not only to the evaluation of two-electron integrals, but more generally to the evaluation of Coulomb interactions in any system. For example, applied to the evaluation of the Coulomb potential in Hartree–Fock theory, it can be developed to a highly efficient scheme that requires an amount of work that increases only linearly with the size of the molecular system [25].

In the present section, we shall discuss the application of the multipole method to the evaluation of Coulomb interactions in large systems, with special emphasis on aspects related to the linear scaling of the evaluation with the size of the system [25,28,29]. To simplify the presentation, we shall in Sections 9.14.1–9.14.3 assume that the system consists of a set of point charges contained in an equilateral cubic box. The modifications needed to treat Gaussian charge distributions in a molecular system are considered in Section 9.14.4.

### 9.14.1 THE NAIVE MULTIPOLE METHOD

The direct evaluation of the Coulomb interactions in a system containing point-charge particles involves the explicit calculation of all pairwise interactions according to Coulomb's law:

$$U = \sum_{i>j} \frac{Z_i Z_j}{R_{ij}} \quad (9.14.1)$$

For a large number  $N$  of particles, this procedure becomes unnecessarily expensive since, for a given required accuracy, there is no need to calculate all interactions exactly. A better approach is to apply the multipole method, where the long-range interactions are calculated approximately by multipole expansions, leaving only the short-range interactions to be treated explicitly.

To apply the multipole method, we divide the system into a set of *cubic boxes*, all of the same size. For each box A in the system, we set up a multipole expansion  $\mathbf{q}_A$  of its charge distribution, with the origin at the centre of the box. For all pairs of boxes A and B that are sufficiently far away from each other, the interaction between their charge distributions may then be evaluated as a multipole expansion (9.13.75)

$$U_{AB} = \mathbf{q}_A^T \mathbf{T}_{AB} \mathbf{q}_B \quad (9.14.2)$$

where  $\mathbf{T}_{AB}$  is the interaction matrix for the two boxes

$$\mathbf{T}_{AB} = \mathbf{T}(\mathbf{R}_{BA}) \quad (9.14.3)$$

The remaining interactions are evaluated explicitly according to (9.14.1), summing only over those pairs whose interactions cannot be treated by multipole expansions (9.14.2).

Let us consider which interactions can be calculated by multipole expansions. From the discussion in Section 9.13.1, we recall that the interaction between two charge distributions may be calculated by a multipole expansion if, for all particles in the two systems, the following inequality condition is satisfied

$$|\mathbf{a} - \mathbf{b}| < |\mathbf{R}| \quad (9.14.4)$$

where  $\mathbf{a}$  and  $\mathbf{b}$  are the position vectors of the particles relative to the origins of the bipolar multipole expansion and  $\mathbf{R}$  the vector connecting these origins – see (9.13.6). This condition is equivalent to the requirement that the charges in the two systems may be enclosed by two spheres that do

not intersect – see Figure 9.14. It is noteworthy that, for a multipole expansion to converge, it is not sufficient that the two interacting distributions do not overlap.

Let us consider how this condition can be met in our application of the multipole method to the partitioned system. In the system, two boxes that share a boundary point are said to be *nearest neighbours*, otherwise they are said to be *well separated*. Since nearest neighbours cannot be enclosed by nonintersecting spheres, their interactions cannot be calculated by a multipole expansion. By contrast, a pair of well-separated boxes can always be enclosed by two nonintersecting spheres and their interactions may therefore be obtained from a bipolar expansion with origins at the box centres. In Figure 9.15, the nearest neighbours of box C are shaded light grey and the well-separated boxes dark grey.

Let us now consider the evaluation of the interaction of a particle  $i$  located in box C with the other particles in the system. There are two distinct contributions to this interaction: the *near-field*

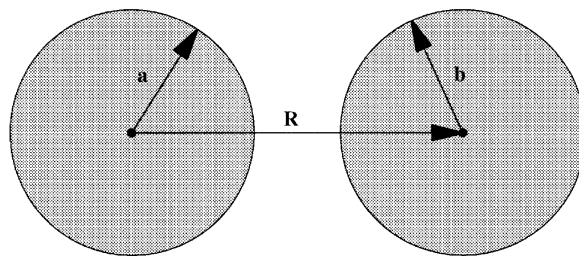


**Fig. 9.14.** The condition for convergence of the bipolar multipole expansion. The condition  $|\mathbf{a} - \mathbf{b}| < |\mathbf{R}|$  implies that the two systems are enclosed in spheres that do not intersect.

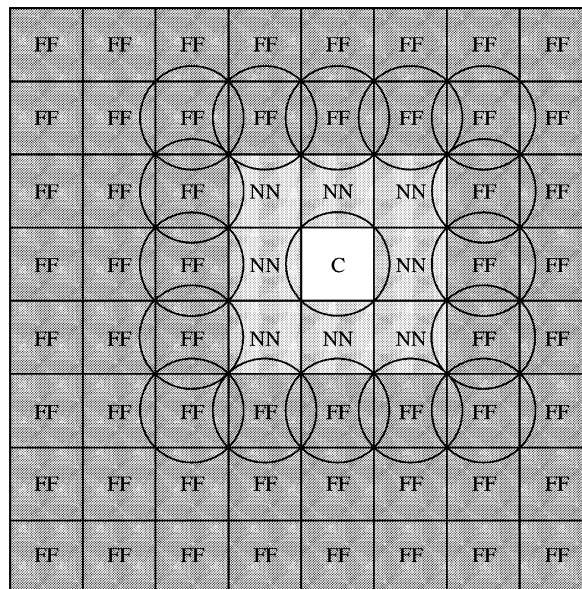


**Fig. 9.15.** A partitioned two-dimensional system. The nearest neighbours (NN) to C are shaded light grey and the FF boxes dark grey.

(*NF*) contribution from the particles located in C and its nearest neighbours, and the *far-field (FF)* contribution from the particles in the boxes that are well separated from C:

$$U_i = U_i^{\text{NF}} + U_i^{\text{FF}} \quad (9.14.5)$$

The NF interactions are obtained directly, by summing over all particles located in the *NF boxes* (defined as C and its nearest neighbours):

$$U_i^{\text{NF}} = \sum_{\substack{j \in \text{NF} \\ j \neq i}} Z_i Z_j R_{ij}^{-1} \quad (9.14.6)$$

The FF interactions, on the other hand, are obtained by calculating multipole expansions with the *FF boxes* (the well-separated boxes) in the following manner:

$$U_i^{\text{FF}} = \sum_{A \in \text{FF}} \mathbf{q}_{iC}^T \mathbf{T}_{CA} \mathbf{q}_A \quad (9.14.7)$$

Here  $\mathbf{q}_{iC}$  contains the multipole moments of particle  $i$  with the origin at the centre of box C and  $\mathbf{q}_A$  is the multipole expansion of all particles in box A:

$$\mathbf{q}_A = \sum_{i \in A} \mathbf{q}_{iA} \quad (9.14.8)$$

The order of the multipole expansion is adjusted so that the required accuracy is obtained. If a sufficiently large number of particles is contained in each box, this approach is considerably faster than the direct evaluation of all interactions according to (9.14.1) since (9.14.7) involves a summation over boxes whereas (9.14.1) sums over particles.

It is possible to carry out the calculation of the FF interactions more efficiently than indicated by (9.14.7). First, we set up the *FF field vector* at the center of box C:

$$\mathbf{V}_C^{\text{FF}} = \sum_{A \in \text{FF}} \mathbf{T}_{CA} \mathbf{q}_A \quad (9.14.9)$$

Next, we calculate the interaction with particle  $i$  by contracting this field vector with the multipoles of particle  $i$ :

$$U_i^{\text{FF}} = \mathbf{q}_{iC}^T \mathbf{V}_C^{\text{FF}} \quad (9.14.10)$$

The advantage of this scheme is that we may use the same field vector  $\mathbf{V}_C^{\text{FF}}$  for all particles in box C. Even simpler, the total interaction with all particles in C may be obtained by contracting the field vector (9.14.9) with the multipoles for all particles in C:

$$U_C^{\text{FF}} = \mathbf{q}_C^T \mathbf{V}_C^{\text{FF}} \quad (9.14.11)$$

Finally, the interaction among all particles in the system is obtained by summing the interactions (9.14.5) for all particles.

Regarding computational cost of the multipole method, we note that the cost of the FF calculation increases *quadratically* with the size of the system since, for a given box, the number of FF boxes is proportional to the size of the system (assuming that the size of the boxes is kept constant in order to maintain the same accuracy in the calculation). By contrast, the cost of the NF calculation increases only *linearly* with the size of the system since, for a given box, the number of NF

boxes is always 27 (9 in a two-dimensional system) – irrespective of the size of the system. In short, the cost of the *naive multipole method* described in this subsection increases quadratically with the size of the system. Still, provided that each box contains a sufficiently large number of particles, this method should perform considerably better than the explicit evaluation of the Coulomb interactions.

### 9.14.2 THE TWO-LEVEL MULTIPOLE METHOD

From Section 9.13.2, we recall that the multipole expansion may be regarded as an expansion in  $r/R$ , where  $r$  is the radius of the two spheres containing the interacting boxes and  $R$  the distance between the centres of the boxes. For a fixed order of the multipole expansions  $L$ , the long-range multipole interactions are therefore calculated to an accuracy higher than the short-range multipole interactions. One way to avoid this waste of accuracy would be to calculate distant interactions using lower-order multipole expansions. However, even though this approach improves the situation somewhat, it does not change it fundamentally – the cost of the calculation still scales quadratically with the size of the system since, for each interacting pair, we must retain at least one term in the expansion. A better solution to this problem is to group the small boxes into larger ones and to calculate the long-range interactions in terms of these larger boxes. By increasing the box size and keeping the ratio  $r/R$  approximately constant, we should be able to maintain a uniform accuracy in the evaluation of the short- and long-range interactions.

Let us consider the system of Section 9.14.1 at two levels of subdivision. At level 2, the system has been subdivided twice; at level 3, we have carried out three such subdivisions. These levels of subdivision are illustrated in Figure 9.16 for a two-dimensional system. Our strategy is now to calculate the long-range interactions at the coarse level and the short-range interactions at the fine level. For this purpose, it is useful to introduce some notation.

To describe the relationships between boxes at different levels, we introduce the terms *parent* and *child*. The cells obtained by subdividing a given cell are the *children* of this *parent*. Each parent thus contains eight children (four in a two-dimensional system) and each child has a single

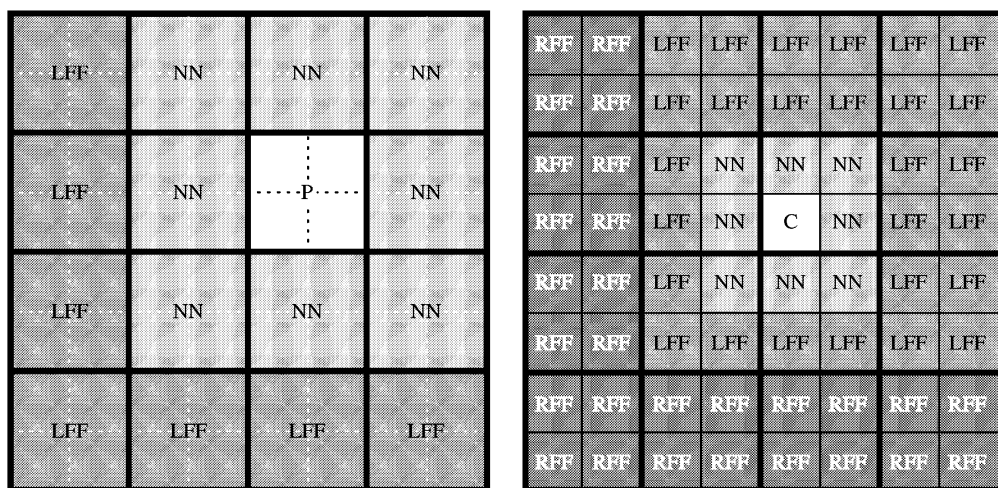


**Fig. 9.16.** The hierarchy of boxes in a two-dimensional system. The level-2 system to the left has been subdivided twice; the level-3 system to the right has been subdivided three times.

parent. To describe the relationships between boxes at the same level, we retain the terms *nearest neighbour* and *well separated* of Section 9.14.1, as well as the concepts of NF and FF boxes. However, we shall now need to distinguish between two types of FF boxes: The *local FF (LFF) boxes* are those FF boxes that are the children of the nearest neighbours of C's parent P; the remaining FF boxes are called the *remote FF (RFF) boxes*. The RFF boxes are the children of the parent's FF boxes.

Let us now consider the evaluation of the Coulomb interactions of the particles in C with the remaining particles in the system. The interaction of particle  $i$  may be calculated as

$$U_i = U_i^{\text{NF}} + \sum_{A \in \text{LFF}} \mathbf{q}_{iC}^T \mathbf{T}_{CA} \mathbf{q}_A + \sum_{B \in \text{RFF}} \mathbf{q}_{iC}^T \mathbf{T}_{CB} \mathbf{q}_B \quad (9.14.12)$$

where the first term represents the NF interactions (9.14.6) and the second and third terms the LFF and RFF interactions, respectively, expressed as bipolar expansions at the centres of C and its FF boxes. Carrying out partial summations, we first evaluate the FF vectors at the centres of C and its parent P:

$$\mathbf{V}_C^{\text{LFF}} = \sum_{A \in \text{LFF}} \mathbf{T}_{CA} \mathbf{q}_A \quad (9.14.13)$$

$$\mathbf{V}_P^{\text{RFF}} = \sum_{B \in \text{RFF}} \mathbf{T}_{PB} \mathbf{q}_B \quad (9.14.14)$$

Using the translation relation (9.13.41) in the form

$$\mathbf{q}_{iP} = \mathbf{W}_{PC} \mathbf{q}_{iC} \quad (9.14.15)$$

the interaction (9.14.12) may be expressed compactly as

$$U_i = U_i^{\text{NF}} + \mathbf{q}_{iC}^T (\mathbf{V}_C^{\text{LFF}} + \mathbf{W}_{PC}^T \mathbf{V}_P^{\text{RFF}}) \quad (9.14.16)$$

Note that the field vector  $\mathbf{V}_C^{\text{LFF}}$  is used by all particles located in box C and that  $\mathbf{V}_P^{\text{RFF}}$  is shared by all children of P, reducing the cost of evaluating the full set of interactions  $U_i$  in the system. As we shall see in Section 9.14.3, when generalized to many levels of subdivision, the two-level strategy developed here leads to a scheme according to which the Coulomb interactions may, for a given fixed accuracy, be evaluated at a cost that increases only linearly with the size of the system.

### 9.14.3 THE FAST MULTIPOLE METHOD

As a generalization of the technique discussed in Section 9.14.2, we now introduce a *hierarchy of boxes* in the interacting system. At the highest level 0, the whole system is contained in a single box. Next, at level 1, the system is subdivided into eight equal-size equilateral cubic boxes. A further subdivision produces a system containing 64 boxes at level 2, and so on. This process is continued until, at the lowest level, each box contains only a small number of particles (10–100).

To calculate the number of levels and boxes in such a hierarchy, let us assume that the total number  $N$  of particles is equal to some power of 8 and that the smallest boxes each contain a single particle. At level  $l$ , there are  $8^l$  boxes and the deepest level in the hierarchy is given by

$$S = \log_8 N \quad (9.14.17)$$

Consequently, the total number of boxes in the hierarchy is given as

$$\sum_{l=0}^{\log_8 N} 8^l = \frac{8N - 1}{7} \quad (9.14.18)$$

We note that the number of boxes in the hierarchy increases *linearly* with the number of particles and that nearly 90% of the boxes are located at the deepest level. In practice, the number of particles is not always equal to some power of 8, and the smallest boxes contain more than a single particle. Thus, for a system consisting of a million uniformly distributed particles,  $S = 5$  gives a system in which about 30 particles are contained in each of the smallest boxes.

Having introduced this hierarchy of boxes, we may now calculate the Coulomb interactions in the system by a clever generalization of the two-level scheme of Section 9.14.2 – *the fast multipole method (FMM)* [28,29]:

1. Evaluate the multipole expansions for all particles  $\mathbf{q}_{iA}$  and all boxes  $\mathbf{q}_A$  at the deepest level:

$$\mathbf{q}_A = \sum_{i \in A} \mathbf{q}_{iA} = \sum_{i \in A} \mathbf{W}_{Ai} \mathbf{q}_i \quad (9.14.19)$$

Since each particle belongs to a single box A, the cost of this step increases linearly with the size of the system.

2. Generate multipole expansions for all boxes at higher levels. For each parent box P, there is one contribution from each of its eight children:

$$\mathbf{q}_P = \sum_{C \in P} \mathbf{W}_{PC} \mathbf{q}_C \quad (9.14.20)$$

Since the number of parent boxes is proportional to  $N$ , the cost of this step increases linearly with the size of the system. At this stage, we have generated a multipole expansion for each box B at all levels in the system.

3. For each box B in the system, calculate the field vector from its  $6^3 - 3^3 = 189$  LFF boxes:

$$\mathbf{V}_B^{\text{LFF}} = \sum_{F \in \text{LFF}(B)} \mathbf{T}_{BF} \mathbf{q}_F \quad (9.14.21)$$

When constructing the field vector, we have not included the NF and RFF boxes – the NF interactions are treated at deeper levels and the RFF interactions at higher levels. Since the number of boxes B in (9.14.21) is proportional to  $N$  and since there are always 189 terms in the sum, the cost of this step scales linearly with the size of the system.

4. For each box B in the hierarchy, calculate  $\mathbf{V}_B^{\text{FF}}$ , representing the field generated by *all* FF boxes – the remote ones as well as the local ones. At levels 0 and 1, there are no well separated boxes and therefore no FF. At level 2, each box T has a local FF but no remote FF:

$$\mathbf{V}_T^{\text{FF}} = \mathbf{V}_T^{\text{LFF}} \quad (9.14.22)$$

At all deeper levels, there is a remote as well as a local contribution to the FF, the RFF of a given box C corresponding (by definition) to the total FF of its parent P:

$$\mathbf{V}_C^{\text{FF}} = \mathbf{V}_C^{\text{LFF}} + \mathbf{V}_C^{\text{RFF}} = \mathbf{V}_C^{\text{LFF}} + \mathbf{W}_{PC}^T \mathbf{V}_P^{\text{FF}} \quad (9.14.23)$$

In short, each box receives an RFF from its parent, which is added to its own LFF; at the next level, the  $\mathbf{V}_C^{\text{FF}}$  is transferred to its eight children. The process ends when it reaches the deepest level. At this point, we have generated, for each box A at the deepest level, the vector  $\mathbf{V}_A^{\text{FF}}$ , which represents the total field generated by all well-separated boxes in the system. Again, since the amount of work is the same for each box and independent of the size of the system, the cost of this step scales linearly with the size of the system.

5. For each particle in the system, we now calculate its interaction with all well-separated particles:

$$U_i^{\text{FF}} = \mathbf{q}_{iA}^T \mathbf{V}_A^{\text{FF}} \quad (9.14.24)$$

This step involves a constant amount of work for each particle and the cost is again proportional to the number of particles in the system.

6. At this point, it remains only to add the NF contributions to the interactions, summing over all NF particles (including those contained in box A itself)

$$U_i = \sum_{\substack{j \in \text{NF}(A) \\ j \neq i}} Z_i Z_j R_{ij}^{-1} + U_i^{\text{FF}} \quad (9.14.25)$$

Since there are 27 such boxes for each particle in the system, the cost scales linearly with the size of the system.

7. If needed, the total Coulomb interaction energy of the system is obtained as

$$U = \frac{1}{2} \sum_i U_i \quad (9.14.26)$$

where the factor of one-half arises since each pairwise interaction is included twice.

Following these basic steps, it is possible to calculate the interactions of all particles in a system in a manner that scales linearly with the size of the system.

Clearly, the accuracy and efficiency of the FMM depend on the order of the multipole expansion  $L$  and the number of subdivisions  $S$  (i.e. the number of particles in the smallest boxes). The number of subdivisions (and therefore the size of the boxes) is usually chosen such that the smallest boxes contain 10–100 particles. The order of the multipole expansion is then adjusted such that the required accuracy is achieved.

However, the performance of the FMM may also be affected by adjusting the size of the NF. Let us introduce the *NF width parameter*  $\Omega$ , which represents the number of NF boxes that separates a given box in the system from its FF boxes. In our discussion, we have included in the NF only the nearest neighbours – that is, we have used  $\Omega = 1$ . Often, a better performance is achieved with  $\Omega = 2$ , including in the NF also the second nearest neighbours, thus reducing the  $r/R$  ratio. For a given accuracy, the order of the multipole expansion may then be reduced, improving the overall efficiency of the calculation – provided that the increased cost of the NF interactions does not offset the reduced cost of the FF interactions. In practice, it is usually best to use a small width parameter  $\Omega$  for low accuracy and large  $\Omega$  for high accuracy.

#### 9.14.4 THE CONTINUOUS FAST MULTIPOLE METHOD

The FMM described in Section 9.14.3 was developed for point charges. For systems of continuous charge distributions such as Gaussians, the FMM cannot be applied directly since such distributions

may interact nonclassically. Also, in a given system, the distributions may vary considerably in size, making the separation into NF and FF interactions more difficult than for point charges. In the present subsection, we describe the *continuous fast multipole method (CFMM)*, which is a generalization of the FMM to systems of continuous charge distributions.

In generalizing the FMM to continuous distributions, we must accomplish two objectives. First, we must ensure that only classical interactions are included in the FF calculations. Second, to reduce as much as possible the number of classical interactions that are evaluated explicitly (i.e. as NF interactions), we must introduce a flexible system for determining the FF region. In the CFMM [21,30], these objectives are achieved by introducing, at each level, a range of NF width parameters

$$\Omega_n = 2n, \quad n = 1, 2, \dots \quad (9.14.27)$$

and by associating with each  $\Omega_n$  a separate *branch* of boxes and distributions. (The reason for restricting the  $\Omega_n$  to even numbers will become clear shortly.) At a given level in the hierarchy, the branches define the NF regions assigned to their boxes. Thus, the first branch has the smallest width parameter  $\Omega_1$  (indicating that each box in each direction is separated from its FF by only two boxes) and is used by the most compact distributions. For more diffuse charge distributions, branches of larger  $\Omega_n$  are used in order to increase the width of the NF region.

At the deepest level of the hierarchy, each Gaussian distribution is assigned to a branch and a box, based on its extent and position. Let the size of the boxes at level  $l$  be given by

$$A_l = \left(\frac{1}{2}\right)^l A_0 \quad (9.14.28)$$

where  $A_0$  is the largest box in the hierarchy. A Gaussian distribution of exponent  $p$  and extent (9.12.10)

$$r_p = p^{-1/2} \operatorname{erfc}^{-1}(10^{-k}) \quad (9.14.29)$$

is then assigned to the  $n$ th branch, whose width parameter is given by

$$\Omega_n = \max \left( \Omega_1, 2 \left\lceil \frac{r_p}{A_l} \right\rceil \right) \quad (9.14.30)$$

where  $\lceil i \rceil$  is the smallest integer greater than or equal to  $i$ . Note that  $2\lceil r_p/A_l \rceil$  is the smallest number of boxes needed to ensure classical interactions between two Gaussians of extent  $r_p$ . It thus follows that, in a given branch, the distributions inside two boxes interact classically if they are separated by  $\Omega_n$  or more boxes. Also, two boxes in different branches (at the same level) interact classically when separated by  $\Omega_{mn}$  or more boxes, where  $\Omega_{mn}$  is the average of the NF width parameters of the two branches:

$$\Omega_{mn} = \frac{\Omega_m + \Omega_n}{2} \quad (9.14.31)$$

Since  $\Omega_m$  and  $\Omega_n$  are even numbers,  $\Omega_{mn}$  is an integer. Having thus sorted the Gaussian distributions at the deepest level into boxes and branches based on their position and extent, we are now ready to discuss the CFMM evaluation of Coulomb interactions for continuous charge distributions.

In describing the application of the CFMM, we shall refer to the steps of the FMM procedure of Section 9.14.3. Unlike the FMM, where all particles in the same box are treated collectively, the CFMM treats collectively all distributions that belong to the same box and branch. In step 1, we form multipole expansions by integrating over the Gaussian distributions in all boxes in all branches at the deepest level, using the techniques of Section 9.13. This step differs from that of the FMM only in that the summations are replaced by integrations. Next, in step 2, we generate multipole expansions

in all boxes at the higher levels. In translating the expansions to the higher levels, we note that two boxes in different branches may have the same parent since, in some cases, the NF width parameter (9.14.30) is reduced by one-half (rounded up to the nearest even integer) as  $l$  is reduced by 1. This parent sharing by boxes in different branches improves the efficiency of the CFMM by reducing the number of multipole expansions that must be calculated at higher levels.

Having created the multipole expansions, we proceed to step 3 and generate, for each box in all branches, the LFF field vector  $\mathbf{V}_B^{\text{LFF}}$  (9.14.21), noting that there are now contributions from all branches at the same level, with the separation into LFF and RFF boxes governed by the  $\Omega_n$  parameter of each branch. No interactions are counted twice if, for each box, we include in the LFF all boxes not included in its parent's FF. Next, in step 4, we traverse the hierarchy downwards, generating at each level the field vectors  $\mathbf{V}_B^{\text{FF}}$  by adding the RFF contributions from the parents according to (9.14.23). At the end of this process, we have generated, for each box in each branch at the deepest level, a vector that represents the total field from all FF boxes in the system. Using this vector we calculate, in step 5, for each distribution at the deepest level, its interaction with all FF boxes. Finally, we add the NF contributions for each distribution in step 6, replacing the FMM summation by integration.

It should be understood that the CFMM differs from the FMM in that the work required for the evaluation of the Coulomb interactions depends critically on the extent of the Gaussians. Thus, in the limit where all Gaussians extend over the whole system, there are no FF interactions and the CFMM reduces to the standard nonclassical integration, whose cost scales quartically with the size of the system. Linear scaling of the CFMM is achieved only when the system extends significantly beyond the largest Gaussian extent of the system – in general, the cost of the CFMM is intermediate between that of the explicit Gaussian integration and that of the point-charge FMM.

## References

- [1] S. F. Boys, *Proc. Roy. Soc. A* **200**, 542 (1950).
- [2] R. McWeeny, *Nature* **166**, 21 (1950).
- [3] H. Taketa, S. Huzinaga and K. O-ohata, *J. Phys. Soc. Jpn* **21**, 2313 (1966).
- [4] T. Helgaker and P. R. Taylor, in D. R. Yarkony (ed.), *Modern Electronic Structure Theory*, World Scientific, 1995, p. 725.
- [5] S. Obara and A. Saika, *J. Chem. Phys.* **84**, 3963 (1986); *J. Chem. Phys.* **89**, 1540 (1988).
- [6] L. E. McMurchie and E. R. Davidson, *J. Comput. Phys.* **26**, 218 (1978).
- [7] T. Živković and Z. B. Maksić, *J. Chem. Phys.* **49**, 3083 (1968).
- [8] W. H. Press, S. A. Teukolsky, W. T. Vetterling and B. P. Flannery, *Numerical Recipes*, Cambridge University Press, 1986.
- [9] M. Abramowitz and I. A. Stegun, *Handbook of Mathematical Functions*, Dover, 1965.
- [10] M. Dupuis, J. Rys and H. F. King, *J. Chem. Phys.* **65**, 111 (1976).
- [11] I. Shavitt, *Meth. Comput. Phys.* **2**, 1 (1963).
- [12] P. M. W. Gill, *Adv. Quantum Chem.* **25**, 141 (1994).
- [13] P. M. W. Gill, M. Head-Gordon and J. A. Pople, *Int. J. Quantum Chem.* **S23**, 269 (1989); P. M. W. Gill, M. Head-Gordon and J. A. Pople, *J. Phys. Chem.* **94**, 5564 (1990); P. M. W. Gill and J. A. Pople, *Int. J. Quantum Chem.* **40**, 753 (1991).
- [14] T. P. Hamilton and H. F. Schaefer III, *Chem. Phys.* **150**, 163 (1991).
- [15] R. Lindh, U. Ryu and B. Liu, *J. Chem. Phys.* **95**, 5889 (1991).
- [16] M. Head-Gordon and J. A. Pople, *J. Chem. Phys.* **89**, 5777 (1988).
- [17] H. F. King and M. Dupuis, *J. Comput. Phys.* **21**, 144 (1976).
- [18] V. R. Saunders, in G. H. F. Diercksen and S. Wilson (eds.), *Methods in Computational Molecular Physics*, Reidel, 1983, p. 1.
- [19] J. Rys, M. Dupuis and H. F. King, *J. Comput. Chem.* **4**, 154 (1983).

- [20] D. L. Strout and G. E. Scuseria, *J. Chem. Phys.* **102**, 8448 (1995).
- [21] C. A. White, B. G. Johnson, P. M. W. Gill and M. Head-Gordon, *Chem. Phys. Lett.* **230**, 8 (1994).
- [22] C. C. J. Roothaan, *Rev. Mod. Phys.* **23**, 69 (1951).
- [23] M. Häser and R. Ahlrichs, *J. Comput. Chem.* **10**, 104 (1989).
- [24] A. J. Stone, *The Theory of Intermolecular Forces*, Clarendon, 1996.
- [25] C. A. White and M. Head-Gordon, *J. Chem. Phys.* **101**, 6593 (1994).
- [26] D. M. Brink and G. R. Satchler, *Angular Momentum*, 2nd edn, Clarendon Press, 1968.
- [27] C. Hättig and B. A. Hess, *Mol. Phys.* **81**, 813 (1994); C. Hättig, *Chem. Phys. Lett.* **260**, 341 (1996).
- [28] L. Greengard and V. I. Rokhlin, *J. Comput. Phys.* **73**, 325 (1987); L. Greengard, *Science* **265**, 909 (1994).
- [29] H.-Q. Ding, N. Karasawa and W. A. Goddard III, *Chem. Phys. Lett.* **196**, 6 (1992); *J. Chem. Phys.* **97**, 4309 (1992).
- [30] C. A. White, B. G. Johnson, P. M. W. Gill and M. Head-Gordon, *Chem. Phys. Lett.* **253**, 268 (1996).

## Further reading

- P. M. W. Gill, Molecular integrals over Gaussian basis functions, *Adv. Quantum Chem.* **25**, 141 (1994).
- L. Greengard, Fast algorithms for classical physics, *Science* **265**, 909 (1994).
- T. Helgaker and P. R. Taylor, Gaussian basis sets and molecular integrals, in D. R. Yarkony (ed.), *Modern Electronic Structure Theory*, World Scientific, 1995, p. 725.
- R. Lindh, Integrals of electron repulsion, in P. v. R. Schleyer, N. L. Allinger, T. Clark, J. Gasteiger, P. A. Kollman, H. F. Schaefer III and P. R. Schreiner (eds), *Encyclopedia of Computational Chemistry*, Vol. 2, Wiley, 1998, p. 1337.
- V. R. Saunders, An introduction to molecular integral evaluation, in G. H. F. Diercksen, B. T. Sutcliffe and A. Veillard (eds), *Computational Techniques in Quantum Chemistry and Molecular Physics*, Reidel, 1974, p. 347.
- V. R. Saunders, Molecular integrals for Gaussian type functions, in G. H. F. Diercksen and S. Wilson (eds), *Methods in Computational Molecular Physics*, Reidel, 1983, p. 1.
- I. Shavitt, The history and evolution of Gaussian basis sets, *Isr. J. Chem.* **33**, 357 (1993).
- A. J. Stone, *The Theory of Intermolecular Forces*, Clarendon, 1996.
- M. C. Strain, G. E. Scuseria and M. J. Frisch, Achieving linear scaling for the electronic quantum Coulomb problem, *Science*, **271**, 51 (1996).

## Exercises

### EXERCISE 9.1

The self-overlap integral of a Cartesian Gaussian

$$G_{ijk} = x_A^i y_A^j z_A^k \exp(-ar_A^2) \quad (9E.1.1)$$

is given by

$$\langle G_{ijk}|G_{ijk} \rangle = \frac{(2i-1)!!(2j-1)!!(2k-1)!!}{(4a)^{i+j+k}} \left(\frac{\pi}{2a}\right)^{3/2} \quad (9E.1.2)$$

where the double factorial is defined in (6.5.10).

1. Using the McMurchie–Davidson scheme, verify that the general expression (9E.1.2) holds for the special cases  $\langle p_x|p_x \rangle$  and  $\langle d_{x^2}|d_{x^2} \rangle$ .
2. Show that the one-centre even-order multipole  $s$  integrals are given by

$$\langle s|x_A^n|s \rangle = (n-1)!!(4a)^{-n/2} \left(\frac{\pi}{2a}\right)^{3/2}, \quad n = 0, 2, 4, \dots \quad (9E.1.3)$$

Why do the one-centre multipole integrals vanish for odd  $n$ ?

3. For  $n = 2$ , verify the expression

$$\langle s|(-i\partial/\partial x)^n|s\rangle = (n-1)!!a^{n/2} \left(\frac{\pi}{2a}\right)^{3/2}, \quad n = 0, 2, 4, \dots \quad (9E.1.4)$$

### EXERCISE 9.2

Consider the ground-state hydrogen and helium atoms in a basis of a single Gaussian with exponent  $a$ :

$$G_{1s} = \exp(-ar^2) \quad (9E.2.1)$$

1. Show that the overlap and kinetic-energy integrals are given by

$$S_{1s1s}(a) = \left(\frac{\pi}{2a}\right)^{3/2} \quad (9E.2.2)$$

$$T_{1s1s}(a) = \frac{3a}{2} \left(\frac{\pi}{2a}\right)^{3/2} \quad (9E.2.3)$$

and that the Coulomb integrals are given by

$$C_{1s1s}(Z, a) = -ZV_{1s1s}(a) = -Z\frac{\pi}{a} \quad (9E.2.4)$$

$$g_{1s1s1s1s}(a) = \frac{1}{4} \left(\frac{\pi}{a}\right)^{5/2} \quad (9E.2.5)$$

where  $Z$  is the nuclear charge.

2. Show that the energy expressions for the hydrogen and helium atoms in the basis of a single Gaussian with exponent  $a$  are given by

$$E_H(a) = \frac{3a}{2} - 2\sqrt{\frac{2a}{\pi}} \quad (9E.2.6)$$

$$E_{He}(a) = 3a + (2 - 8\sqrt{2})\sqrt{\frac{a}{\pi}} \quad (9E.2.7)$$

3. Optimize the energies by means of the variation principle and show that we obtain for the hydrogen atom

$$a_H^* = \frac{8}{9\pi} = 0.2829 \quad (9E.2.8)$$

$$E_H(a_H^*) = -\frac{4}{3\pi} = -0.4244 \quad (9E.2.9)$$

and for the helium atom

$$a_{He}^* = \frac{33 - 8\sqrt{2}}{9\pi} = 0.7670 \quad (9E.2.10)$$

$$E_{He}(a_{He}^*) = \frac{8\sqrt{2} - 33}{3\pi} = -2.3010 \quad (9E.2.11)$$

How do these results compare with the exact ground-state energies of the hydrogen and helium atoms?

4. For an atom, the virial theorem of Section 4.2.7 states that the kinetic and total energies are related by

$$E_{\text{kin}} = -E_{\text{tot}} \quad (9E.2.12)$$

Determine the Gaussian exponent for the hydrogen atom from the virial theorem. How does the result obtained in this way compare with that obtained from the variation principle?

### EXERCISE 9.3

Prove the recurrence relations for the Boys function (9.8.13) and (9.8.14). Why is the upward recursion numerically unstable for small arguments?

### EXERCISE 9.4

Show that, for a sufficiently large separation between the overlap distributions, the two-electron integral (9.9.33) reduces to the simple expression

$$g_{abcd} = \frac{S_{ab}S_{cd}}{R_{PQ}} \quad (9E.4.1)$$

where  $S_{ab}$  is the overlap integral. This is the first term in the multipole expansion of the two-electron integral (9.13.27).

### EXERCISE 9.5

Show that the expression for the two-electron repulsion integral (9.9.33) reduces to the one-electron potential integral (9.9.32) when the second charge distribution represents a unit point charge.

## Solutions

### SOLUTION 9.1

1. According to (9E.1.2), the self-overlap integrals are given by

$$\langle p_x | p_x \rangle = \frac{1}{2p} \left( \frac{\pi}{p} \right)^{3/2} \quad (9S.1.1)$$

$$\langle d_{x^2} | d_{x^2} \rangle = \frac{3}{(2p)^2} \left( \frac{\pi}{p} \right)^{3/2} \quad (9S.1.2)$$

where

$$p = 2a \quad (9S.1.3)$$

According to (9.5.41), these integrals may, in the McMurchie–Davidson scheme, be written in the form

$$\langle p_x | p_x \rangle = E_0^{11} E_0^{00} E_0^{00} \left( \frac{\pi}{p} \right)^{3/2} \quad (9S.1.4)$$

$$\langle d_{x^2} | d_{x^2} \rangle = E_0^{22} E_0^{00} E_0^{00} \left( \frac{\pi}{p} \right)^{3/2} \quad (9S.1.5)$$

where, for a one-centre integral, the Hermite-to-Cartesian expansion coefficients for the three Cartesian directions are the same. We also note that, for a one-centre integral, the Hermite recurrence relations (9.5.6)–(9.5.8) may be written in the simplified form

$$E_0^{00} = 1 \quad (9S.1.6)$$

$$E_t^{i+1,j} = E_t^{i,j+1} = \frac{1}{2p} E_{t-1}^{ij} + (t+1) E_{t+1}^{ij} \quad (9S.1.7)$$

since

$$K_{ab}^x = K_{ab}^y = K_{ab}^z = 1 \quad (9S.1.8)$$

$$X_{PA} = Y_{PA} = Z_{PA} = 0 \quad (9S.1.9)$$

We now obtain the following expansion coefficients

$$E_0^{11} = E_1^{01} = \frac{1}{2p} E_0^{00} = \frac{1}{2p} \quad (9S.1.10)$$

$$E_0^{22} = E_1^{12} = \frac{1}{2p} E_0^{11} + 2E_2^{11} = \frac{1}{2p} E_1^{01} + 2 \frac{1}{2p} E_1^{01} = \frac{3}{2p} E_1^{01} \quad (9S.1.11)$$

$$= 3 \left( \frac{1}{2p} \right)^2 E_0^{00} = 3 \left( \frac{1}{2p} \right)^2$$

which, combined with (9S.1.4) and (9S.1.5), yield (9S.1.1) and (9S.1.2) directly.

2. The left-hand side of (9E.1.3) is easily written as

$$\langle s | x_A^n | s \rangle = \langle G_{n/2,0,0} | G_{n/2,0,0} \rangle \quad (9S.1.12)$$

The relation (9E.1.3) now follows directly from (9E.1.2). For odd  $n$ , these integrals vanish as the integrand is then antisymmetric about the origin.

3. We use partial integration to obtain

$$\langle s | (-i\partial/\partial x)^2 | s \rangle = \left\langle \frac{\partial s}{\partial x} \left| \frac{\partial s}{\partial x} \right. \right\rangle = 4a^2 \langle p_x | p_x \rangle \quad (9S.1.13)$$

from which (9E.1.4) follows for  $n = 2$  by application of (9E.1.2).

## SOLUTION 9.2

1. The overlap and kinetic-energy integrals (9E.2.2) and (9E.2.3) follow directly from the results in Exercise 9.1, in particular from (9E.1.2) and (9E.1.4). For the evaluation of (9E.2.4) and (9E.2.5), we note that, for  $s$  orbitals, (9.9.32) and (9.9.33) reduce to

$$V_{1s1s} = \frac{2\pi}{2a} E_{000} R_{000}(2a, 0) = \frac{\pi}{a} F_0(0) = \frac{\pi}{a} \quad (9S.2.1)$$

$$g_{1s1s1s1s} = \frac{2\pi^{5/2}}{(2a)^2 \sqrt{2a+2a}} E_{000} E_{000} R_{000}(a, 0) = \frac{1}{4} \left( \frac{\pi}{a} \right)^{5/2} \quad (9S.2.2)$$

where we have used (9.2.15) and (9.9.27) to obtain  $E_{000} = 1$ . To simplify the Hermite integrals, we have used (9.9.9) and (9.8.6). Note that, for one-centre functions, the Coulomb integrals may be expressed in a closed analytical form.

2. The energies are given by the expressions

$$E_H(a) = \frac{T_{1s1s} + C_{1s1s}(1)}{S_{1s1s}} = \frac{3a}{2} - 2\sqrt{\frac{2a}{\pi}} \quad (9S.2.3)$$

$$E_{He}(a) = 2\frac{T_{1s1s} + C_{1s1s}(2)}{S_{1s1s}} + \frac{g_{1s1s1s1s}}{S_{1s1s}^2} = 3a + (2 - 8\sqrt{2})\sqrt{\frac{a}{\pi}} \quad (9S.2.4)$$

by substitution of (9E.2.2)–(9E.2.5).

3. Differentiating (9E.2.6) and (9E.2.7) with respect to  $a$  and setting the results equal to zero, we obtain

$$\frac{3}{2} - \sqrt{\frac{2}{a_H^* \pi}} = 0 \quad (9S.2.5)$$

$$3 + (1 - 4\sqrt{2})\sqrt{\frac{1}{a_{He}^* \pi}} = 0 \quad (9S.2.6)$$

which have the solutions (9E.2.8) and (9E.2.10). Inserting these solutions into the energy expressions, we obtain (9E.2.9) and (9E.2.11). The calculated hydrogen energy is 15% higher than the true energy of  $-\frac{1}{2} E_h$  and the calculated helium energy is 21% higher than the true energy of  $-2.903724 E_h$ .

4. From the virial theorem (9E.2.12), we obtain the condition

$$2T_{1s1s} = -C_{1s1s} \quad (9S.2.7)$$

which, upon substitution of (9E.2.3) and (9E.2.4), yields the same solution as the variation principle.

### SOLUTION 9.3

The Boys function is defined as

$$F_n(x) = \int_0^1 \exp(-xt^2) t^{2n} dt \quad (9S.3.1)$$

Writing the integrand as  $uv'$  with

$$u = \exp(-xt^2) \quad (9S.3.2)$$

$$v' = t^{2n} \quad (9S.3.3)$$

we obtain by partial integration

$$F_n(x) = \frac{2x}{2n+1} \int_0^1 \exp(-xt^2) t^{2n+2} dt + \left[ \exp(-xt^2) \frac{t^{2n+1}}{2n+1} \right]_0^1 \quad (9S.3.4)$$

and consequently

$$F_n(x) = \frac{2x}{2n+1} F_{n+1}(x) + \frac{\exp(-x)}{2n+1} \quad (9S.3.5)$$

which may be rearranged to give the recurrence relations (9.8.13) and (9.8.14). The upward recursion is numerically unstable since, for small  $x$ ,

$$(2n + 1)F_n(x) \approx \exp(-x) \approx 1 \quad (9S.3.6)$$

where we have used (9.8.6).

#### SOLUTION 9.4

For large separations

$$R_{PQ} \gg 0 \quad (9S.4.1)$$

we may write the zero-order Boys function as

$$F_0(\alpha R_{PQ}^2) = \sqrt{\frac{\pi}{4\alpha}} \frac{1}{R_{PQ}} \quad (9S.4.2)$$

where we have used (9.8.9). We may now write the Hermite integrals in (9.9.33) in the form

$$R_{t+\tau, u+v, v+\phi} = \left( \frac{\partial}{\partial P_x} \right)^{t+\tau} \left( \frac{\partial}{\partial P_y} \right)^{u+v} \left( \frac{\partial}{\partial P_z} \right)^{v+\phi} \sqrt{\frac{\pi}{4\alpha}} \frac{1}{R_{PQ}} \quad (9S.4.3)$$

where we have used (9.9.9) and (9S.4.2). From (9S.4.3), we note that

$$R_{000} \gg R_{t+\tau, u+v, v+\phi} \quad (9S.4.4)$$

which means that the two-electron integrals (9.9.33) may be written in the simple form

$$g_{abcd} = \frac{2\pi^{5/2}}{pq\sqrt{p+q}} E_{000}^{ab} E_{000}^{cd} \sqrt{\frac{\pi}{4\alpha}} \frac{1}{R_{PQ}} \quad (9S.4.5)$$

where we have neglected higher-order terms. Using (9.7.22), (9S.4.5) may now be rearranged to give

$$g_{abcd} = \left( \frac{\pi}{p} \right)^{3/2} E_{000}^{ab} \left( \frac{\pi}{q} \right)^{3/2} E_{000}^{cd} \frac{1}{R_{PQ}} = \frac{S_{ab} S_{cd}}{R_{PQ}} \quad (9S.4.6)$$

where we have also used (9.5.41) for the overlap integrals.

#### SOLUTION 9.5

When the second overlap distribution corresponds to a one-centre  $1s$  charge distribution, the two-electron integrals in (9.9.33) may be written as

$$g_{abss} = \frac{2\pi^{5/2}}{pq\sqrt{p+q}} \sum_{tuv} E_{tuv}^{ab} R_{tuv} \left( \frac{pq}{p+q}, \mathbf{R}_{PQ} \right) \quad (9S.5.1)$$

Normalizing the second charge contribution to unity, we obtain

$$G_{ab}(q) = \left( \frac{q}{\pi} \right)^{3/2} \frac{2\pi^{5/2}}{pq\sqrt{p+q}} \sum_{tuv} E_{tuv}^{ab} R_{tuv} \left( \frac{pq}{p+q}, \mathbf{R}_{PQ} \right) \quad (9S.5.2)$$

In the limit as  $q$  tends to infinity, this integral becomes

$$\lim_{q \rightarrow \infty} G_{ab}(q) = \frac{2\pi}{p} \sum_{tuv} E_{tuv}^{ab} R_{tuv}(p, \mathbf{R}_{PQ}) \quad (9S.5.3)$$

which is equivalent to the expression for the Coulomb-potential integral (9.9.32).